Escuela de Modelación y Métodos Numéricos
Modelación & Simulación de Materiales

21-24 JUNIO 2016

Multiscale homogenization methods for the numerical analysis of composite materials

Xavier Martinez

Sergio Oller – Fermín Otero

UNIVERSITAT POLITÈCNICA DE CATALUNYA BARCELONATECH

CIMNE International Center for Numerical Methods in Engineering

PLCd

Presentation of the Institution

UPC and CIMNE

and the Research Group

CIMNE Composites – PLCd Group

Location

BARCELONA

Polytechnic University of Catalonia

Although its main campus is located in Barcelona, it has also campuses in four other cities close to Barcelona.

The UPC was founded in 1965 when several architectural and engineering schools where gathered together. Some of them existed from mid XIX century.

In 1990 the Faculty of Nautical Studies joins the UPC. It is the oldest nautical school in Spain as it was founded in 1769.

International Center for Numerical Methods in Engineering

CIMNE is a research center associated to the UPC. It was founded in 1987 as a partnership between the regional government and the UPC.

The aim of CIMNE is the development of numerical methods and computational techniques for advancing knowledge and technology in engineering in applied sciences.

It has more than 200 research scientists working in several disciplines. It has 8 branches and more than 30 classrooms spread around the globe.

International Center for Numerical Methods in Engineering

The research areas that are covered by CIMNE can be summarized in the following:

Bio-Medical Engineering Area

- Biomechanics Group

Computational and Information Technologies Area

- Information and Communication Technology Group
- Large-scale Scientific Computing Group
- Mathematical and Computational Modelling Group
- Pre and Post-Processing

Transport Area

- Aerospace Engineering Group
- Naval and Marine Engineering Group

Civil and Mechanical Engineering Area

- Fluid Mechanics Group
- Geomechanics Group
- Industrial Forming Processes Group
- Structural Mechanics Group

Energy and Environment Area

- Building, Energy and Environmental Group
- Nature Group
- Risk Analysis Group

CIMNE Composites – PLCd Group

CIMNE Composites or PLCd group is composed by the following people:


Dr. Sergio Oller Martínez


Dr. Xavier Martínez


M.Sc. Fermin Otero


MSc. Lucia Gratiela Barbu


M.Sc. Ester Comellas


M. Sc. Joel Jurado


Dr. Cuauhtemoc Escudero


M.Sc. Stefano Zaghi


M. Sc. Vicent Alemany Marí

+ The Salta (Argentina) team:
  - Dr. Bibiana Luccioni
  - Dr. Facundo Bellomo
  - Dr. Rita Rango

CIMNE Composites – PLCd Group

Some of the research lines in which the group has worked or is working are:

Constitutive modelling of biological tissues

Constitutive equations describe the macroscopic behavior resulting from the internal constitution of a material. They represent, through a mathematical model, the real behavior of a material. However ...

MORE

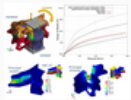

Inverse methods for the determination of material parameters using optimization techniques

A common difficulty encountered when modelling biological tissues is determining the correct material parameters for the constitutive models used to represent their behaviour. Unlike inert tissues, b ...

MORE

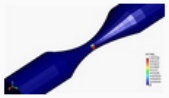

Numerical Simulation of Fatigue

The fatigue phenomenon is defined more generally in the ASTM E1823 standard as: "the process of permanent, progressive and localized structural change which occurs to a material point subjected to st ...

MORE

Inflatable Structures

This research line is linked with a project developed for West Virginia University. This project consisted in the numerical simulation of an inflatable structure designed to stop a high pressure flui ...

MORE

CIMNE Composites – PLCd Group

Some of the research lines in which the group has worked or is working are:

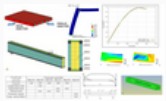

Phenomenological homogenization methods

Since the classical mixing theory was developed many extension or modification to complete this one have been done. A relevant modification was introducing of serial-parallel concept which gave as re ...

MORE

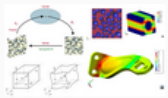

Multi-scale homogenization methods

In a multi-scale homogenization procedure the modelling problem of heterogeneous or composite materials is divided into two or more scales. Originally the method was formulated in terms of asymptotic ...

MORE

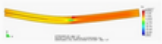

Delamination of composites

Delamination can be probably considered the most common failure mode of composite laminates. In it, the loss of adherence between the different layers of the composite leads to a reduction of the sec ...

MORE

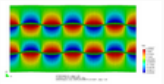

Fiber buckling of composite laminates

The failure criteria of long fiber composites subjected to compressive forces can be due to two main reasons, fiber buckling and/or composite delamination. A special formulation has been developed to ...

MORE

A more detailed description of these research lines can be obtained from www.cimne.com/PLCd

All the developments are implemented in an in-house FEM code: PLCd

Xavier Martinez

- Civil Engineer by the Polytechnic University of Catalonia (2001)
- Researcher at CIMNE since 2004
- Professor at the UPC since 2009
  - Teaching at the Faculty of Nautical and Naval Studies (FNB)
  - Teaching at the Civil Engineering School
  - Vice-Dean of academic affairs at the FNB
- Member of the board committee of the Spanish Association of Composite Materials (AEMAC) since 2015

Mail: x.martinez@upc.edu

Webpage: https://web.cimne.upc.edu/users/xmartinez/

Course Outline

Course Outline

1. Introduction to Multiscale Methods
    1.1. Need for multiscale methods
    1.2. Some examples of multiscale procedures

2. First Order Computational Homogenization (FOCH)
    2.1. Basic Principles
    2.2. Formulation
    2.3. Implementation
    2.4. Numerical examples

Course Outline

3. Enhanced First Order Computational Homogenization (EFOCH)
    - 3.1. Formulation
    - 3.2. Implementation
    - 3.3. Numerical examples – Comparison FOCH vs. EFOCH
    - 3.4. Discussion

4. Non-Linear Analyses Using Multiscale Methods
    - 4.1. Different approaches to conduct non-linear analyses
    - 4.2. Proposal of a Non-Linear Strategy (NLS + SFS)
    - 4.3. Mesh objectivity – Fracture length
    - 4.4. Numerical implementation
    - 4.5. Numerical Examples

1. Introduction to Multiscale Methods

NEED FOR MULTISCALE METHODS

Structural Analysis:

The incorporation of computational tools in structural analysis has allowed improving the complexity of engineering structures.

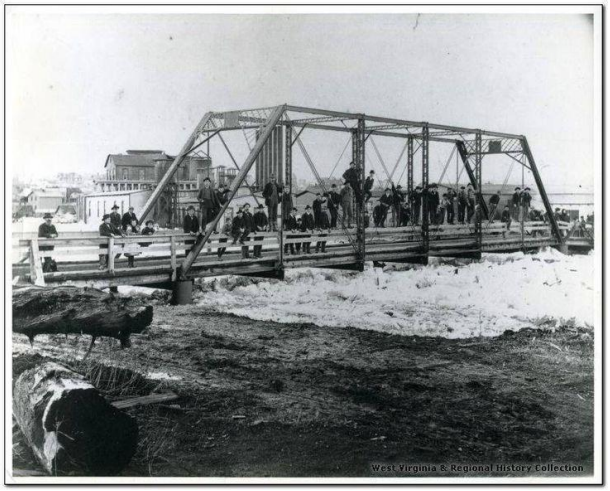

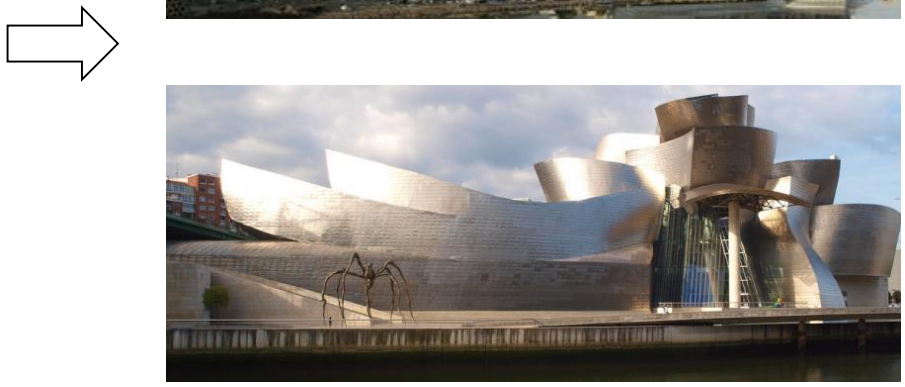

Materials in structural analysis

Not only the structure has become more complex, but the materials are better known and can be modelled more precisely.

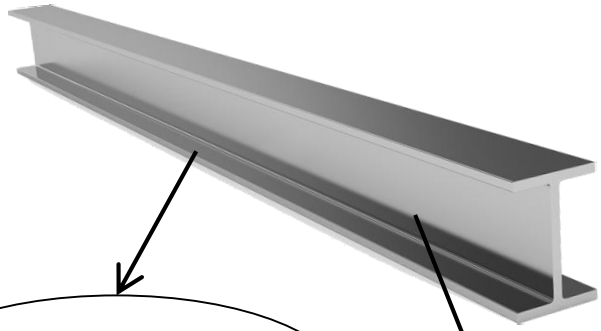

Elastic analysis:
E, ν

Plastic analysis

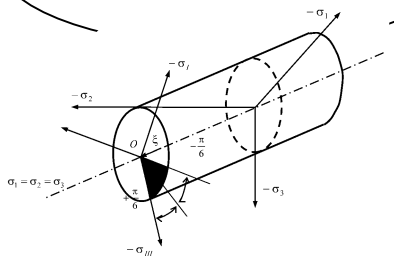

Non-linear
laminate models

Materials in structural analysis

However, the complexity of the internal structures of nowadays composites makes necessary to improve the analysis tools, in order to characterize properly the composite performance.

This is specially important when the analysis wants to be conducted in the non-linear range.

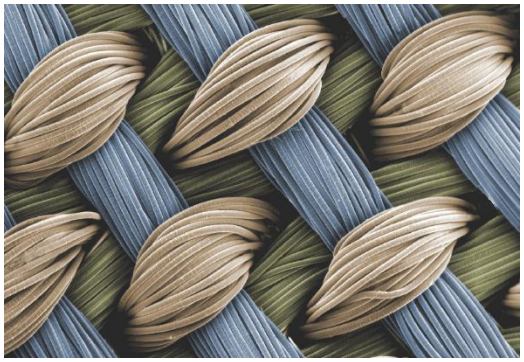

I-Chien Liao *et al.* (2013)

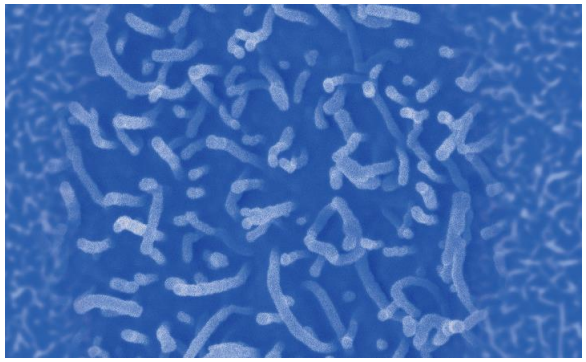

Hayashida, K. and Tanaka, H. (2012)

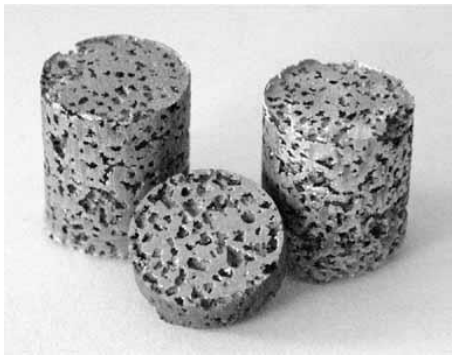

Michailidis *et al.* (2012)

Basic analysis of composite materials

In most cases, composite materials are analyzed as an elastic material with orthotropic properties inherited from its constituents (or given by the manufacturer).

Failure is obtained with a comparison criterion such as: maximum strain, maximum stress, Tsai-Hill, **Tsai-Wu**, etc.

$$f_1(\sigma_1) + f_2(\sigma_2) + f_{11}(\sigma_1)^2 + f_{22}(\sigma_2)^2 + 2f_{12}(\sigma_1\sigma_2) + f_3(\tau_{12})^2 = 1$$

$$f_1 = \frac{1}{F_{1t}} - \frac{1}{F_{1c}} \qquad f_2 = \frac{2}{F_{2t}} - \frac{2}{F_{2c}} \qquad f_{12} = -\frac{1}{2F_{1t}^2}$$

$$f_{11} = \frac{1}{F_{1t}F_{1c}} \qquad f_{22} = \frac{1}{F_{2t}F_{2c}} \qquad f_3 = \frac{1}{F_{12}^2}$$

These approaches does not allow knowing the non-linear performance of the composite. Neither the analysis of complex composite micro-structures.

FEM elements for composite analyses

These models can be applied to solid materials, and can be also applied to shell elements using a lamination theory.

In solid elements, different strategies have been developed to characterize some failure modes. In example, for delamination, a quite extended procedure is the using a zero thickness decohesion element:

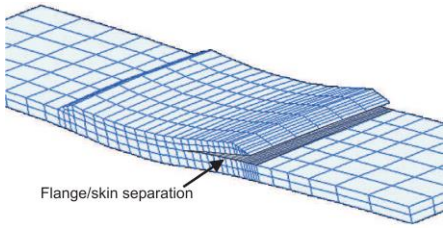

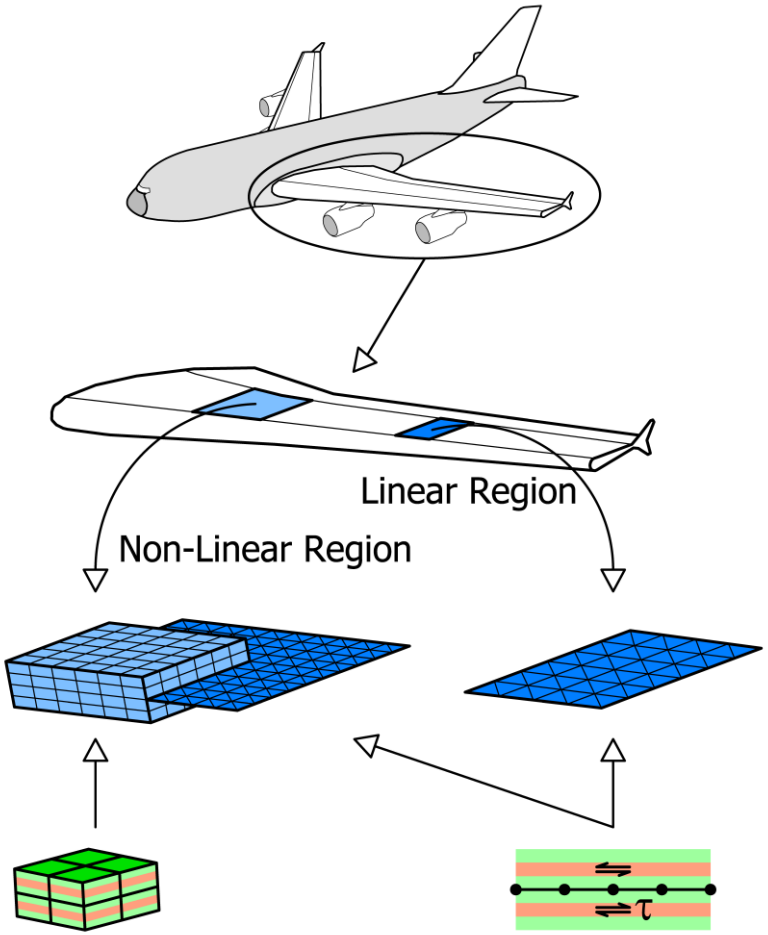

Required approach to analyze composite materials

There are also specific models to capture some failure modes, such as matrix transversal cracking, fiber buckling, etc.

However, in order to have an accurate prediction of the composite performance, it is necessary to treat it according to what it is: a **micro-structure with different components interacting between them.**

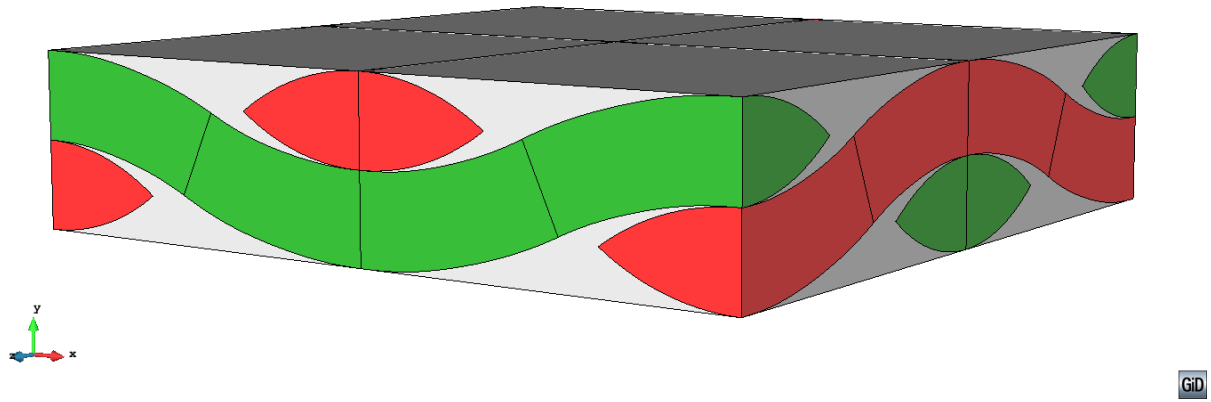

This can be done with a multiscale procedure

Multiscale methods – A possible solution

A multiscale method consist on obtaining the material performance of the macro-structure from a micro-model of the material.

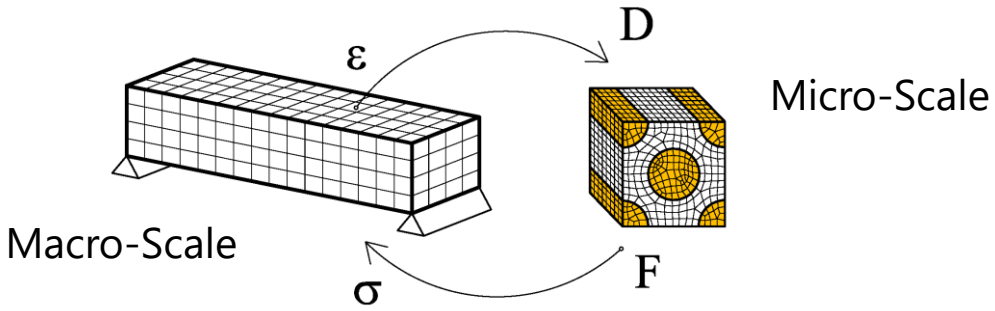

Coupling disciplines

With a multiscale approach we are not only coupling “scales”, but also disciplines.

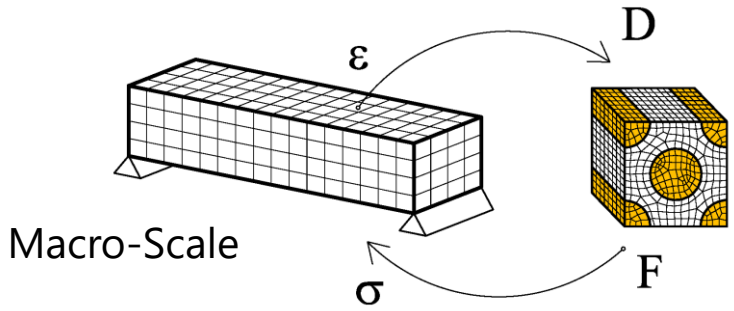

Macro-Scale

Micro-Scale

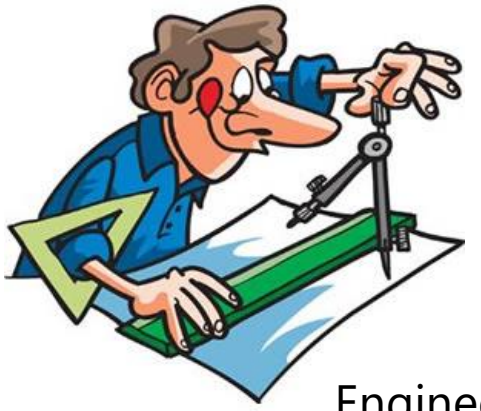

Engineering

Material Science

Coupling disciplines

The community that works on multiscale analysis can focus in many different aspects:

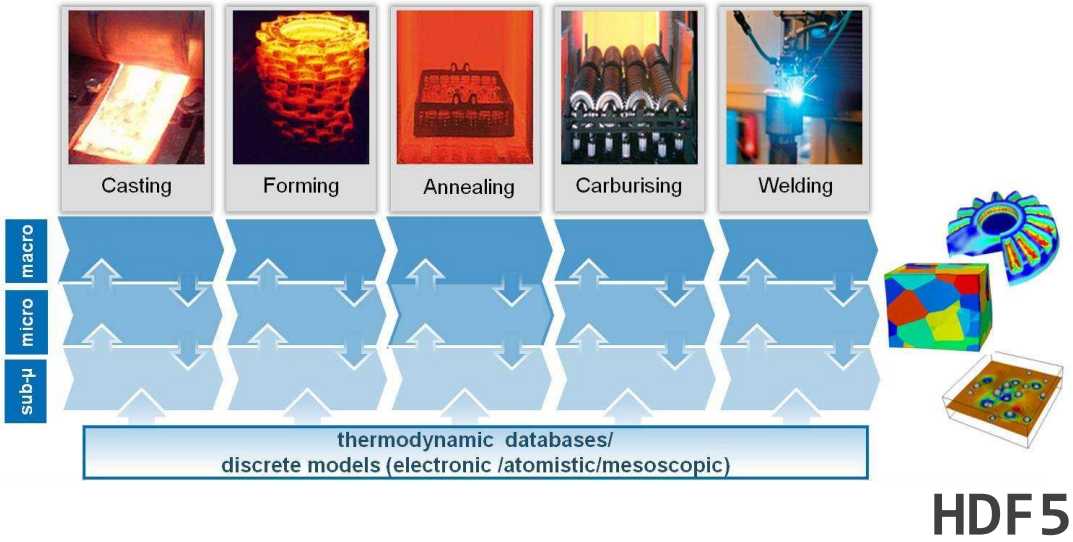

Integrated Computational Materials Engineering expert group

Objective of current course

Among the different aspects that can be considered in multiscale analyses, this course is focused in one of them.

SOME EXAMPLES OF MULSTICALE PROCEDURES

In the following will be described some multiscale procedures with the aim of providing a better understanding on how these methods work, as well as giving a hint of different existing approaches.

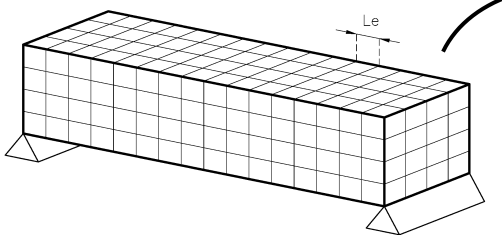

Material Model

Models based on continuum mechanics

- Constitutive equations

6. Serial/Parallel mixing theory

Models based on homogenization procedures:

1. Effective medium approximation
2. Asymptotic homogenization theory
3. Periodic microstructure model
4. Numerical homogenization
5. Homogenization using Lagrange Multipliers

1. Effective medium approximation

The effective medium approximation was initially studied by Eshelby, who analyzed the performance of an homogeneous medium with an internal ellipsoidal inclusion.

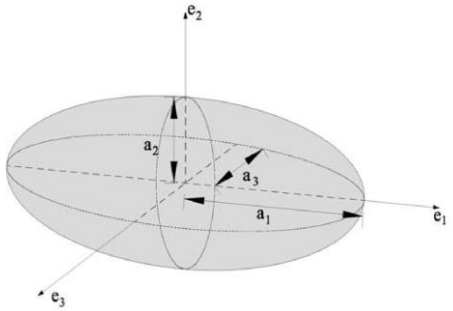

The solution obtained by Eshelby provided the stresses and strains in the medium.

This solution can be, and is, used to represent different composite materials, such as materials with ellipsoidal or elliptical cracks.

2. Asymptotic homogenization theory

This theory was initially proposed by Sanchez-Palencia in 1987 and can be considered the mathematical basis for most of the multiscale approaches proposed afterwards.

The two scales that are used to solve the problem are related through a parameter δ that takes into account the difference of magnitude between both scales.

Defining x as macroscopic quantity and $y = x/\delta$, a microscopic quantity, the two-scale process introduced in the partial differential equations of the problem produces equations in x, y, and in both variables.

Normally, the equations in y are solvable if the microscopic structure is periodic.

3. Periodic microstructure model

This model was developed by Luciano and Barbero in 1995.

The model is written to analyze the following composite:

- Long fiber reinforced matrices
- Fibers with circular cross section
- Rectangular, equally-spaced distribution of fibers in the composite (a_2 and a_3 are constant in the composite, and $a_2 = a_3$)
- Fibers oriented in x direction

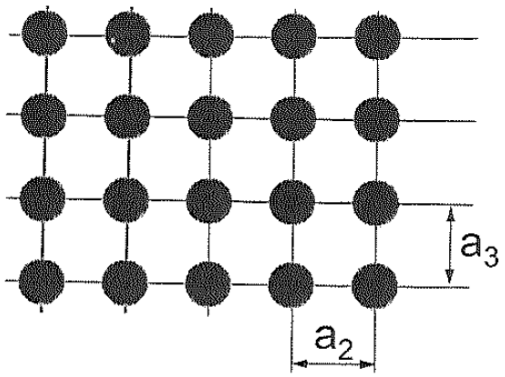

3. Periodic microstructure model

If previous assumptions are fulfilled, the stiffness tensor of the composite can be obtained with the following parameters

$$C^*_{11} = \lambda_m + 2\,\mu_m - \frac{V_f}{D}\left[\frac{S_3^2}{\mu_m^2} - \frac{2S_6S_3}{\mu_m^2 g} - \frac{aS_3}{\mu_m c} + \frac{S_6^2 - S_7^2}{\mu_m^2 g^2} + \frac{aS_6 + bS_7}{\mu_m gc} + \frac{a^2 - b^2}{4\,c^2}\right]$$

$$C^*_{12} = \lambda_m + \frac{V_f}{D} b\left[\frac{S_3}{2c\mu_m} - \frac{S_6 - S_7}{2c\mu_m g} - \frac{a+b}{4\,c^2}\right]$$

$$C^*_{23} = \lambda_m + \frac{V_f}{D}\left[\frac{aS_7}{2\,\mu_m gc} - \frac{ba + b^2}{4\,c^2}\right]$$

$$C^*_{22} = \lambda_m + 2\,\mu_m - \frac{V_f}{D}\left[-\frac{aS_3}{2\,\mu_m c} + \frac{aS_6}{2\,\mu_m gc} + \frac{a^2 - b^2}{4\,c^2}\right]$$

$$C^*_{44} = \mu_m - V_f\left[-\frac{2\,S_3}{\mu_m} + (\mu_m - \mu_f)^{-1} + \frac{4\,S_7}{\mu_m(2 - 2\nu_m)}\right]^{-1}$$

$$C^*_{66} = \mu_m - V_f\left[-\frac{S_3}{\mu_m} + (\mu_m - \mu_f)^{-1}\right]^{-1}$$

Note: The above notation assumes that the stress and strain tensors have the following order: (x_{11}, x_{22}, x_{33}, x_{23}, x_{13}, x_{12})

3. Periodic microstructure model

The parameters that appear in previous equations are:

$$D = \frac{a S_3^2}{2\,\mu_m^2 c} - \frac{a S_6 S_3}{\mu_m^2 g c} + \frac{a(S_6^2 - S_7^2)}{2\mu_m^2 g^2 c} + \\ + \frac{S_3(b^2 - a^2)}{2\,\mu_m\, c^2} + \frac{S_6(a^2 - b^2) + S_7(ab + b^2)}{2\,\mu_m g c^2} + \frac{(a^3 - 2b^3 - 3\,ab^2)}{8\,c^3}$$

$$a = \mu_f - \mu_m - 2\,\mu_f\,\nu_m + 2\,\mu_m\,\nu_f$$
$$b = -\mu_m\,\nu_m + \mu_f\,\nu_f + 2\,\mu_m\,\nu_m\,\nu_f - 2\,\mu_1\,\nu_m\,\nu_f$$
$$c = (\mu_m - \mu_f)(\mu_f - \mu_m + \mu_f\,\nu_f - \mu_m\,\nu_m + 2\,\mu_m\,\nu_f - 2\,\mu_f\,\nu_m + \\ + 2\,\mu_m\,\nu_m\,\nu_f - 2\,\mu_f\,\nu_m\,\nu_f)$$
$$g = (2 - 2\nu_m)$$

$$S_3 = 0.49247 - 0.47603 V_f - 0.02748 V_f^2$$
$$S_6 = 0.36844 - 0.14944 V_f - 0.27152 V_f^2$$
$$S_7 = 0.12346 - 0.32035 V_f + 0.23517 V_f^2$$

Equations equivalent to those shown can be obtained if a_2 and a_3 distances, defining the distribution of fibers in the composite, are not equal.

3. Periodic microstructure model

The described model is valid under the following assumptions:

- Perfect elastic materials
- Perfect bonding between fiber and matrix
- The material is in a small strain regime

4. Numerical Homogenization

After previous approach, which was solved analytically, Barbero proposed a numerical homogenization in which the composite parameters where obtained from a finite element model of a Representative Volume Element.

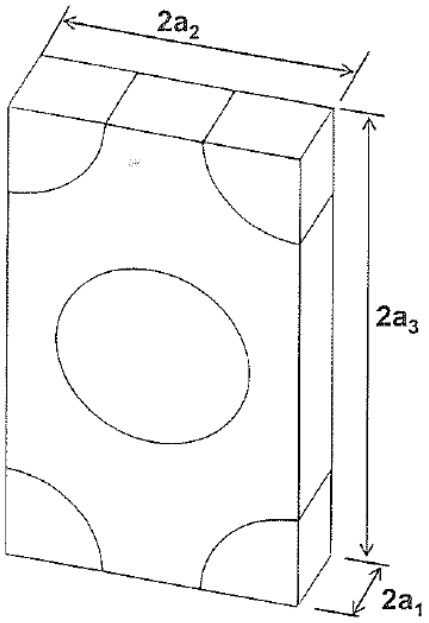

The stiffness tensor of the composite is obtained by applying different strain tensors on the RVE

$$u_i(a_1, x_2, x_3) - u_i(-a_1, x_2, x_3) = 2a_1\varepsilon^0_{i1} \qquad \begin{matrix} -a_2 \le x_2 \le a_2 \\ -a_3 \le x_3 \le a_3 \end{matrix}$$

$$u_i(x_1, a_2, x_3) - u_i(x_1, -a_2, x_3) = 2a_2\varepsilon^0_{i2} \qquad \begin{matrix} -a_1 \le x_1 \le a_1 \\ -a_3 \le x_3 \le a_3 \end{matrix}$$

$$u_i(x_1, x_2, a_3) - u_i(x_1, x_2, -a_3) = 2a_3\varepsilon^0_{i3} \qquad \begin{matrix} -a_1 \le x_1 \le a_1 \\ -a_2 \le x_2 \le a_2 \end{matrix}$$

$$C_{\alpha\beta} = \overline{\sigma}_\alpha = \frac{1}{V}\int_V \sigma_\alpha(x_1, x_2, x_3)\ dV \quad \text{with } \epsilon^0_\beta = 1$$

4. Numerical Homogenization

In example, to obtain the first column of the stiffness tensor:

$$\epsilon_1^o = 1 \qquad \epsilon_2^o = \epsilon_3^o = \gamma_4^o = \gamma_5^o = \gamma_6^o = 0$$

$$\begin{aligned} u_1(+a_1, x_2, x_3) - u_1(-a_1, x_2, x_3) &= 2a_1 \\ u_2(+a_1, x_2, x_3) - u_2(-a_1, x_2, x_3) &= 0 \\ u_3(+a_1, x_2, x_3) - u_3(-a_1, x_2, x_3) &= 0 \end{aligned} \qquad \begin{aligned} -a_2 \le x_2 \le a_2 \\ -a_3 \le x_3 \le a_3 \end{aligned}$$

$$u_i(x_1, +a_2, x_3) - u_i(x_1, -a_2, x_3) = 0 \qquad \begin{aligned} -a_1 \le x_1 \le a_1 \\ -a_3 \le x_3 \le a_3 \end{aligned}$$

$$u_i(x_1, x_2, +a_3) - u_i(x_1, x_2, -a_3) = 0 \qquad \begin{aligned} -a_1 \le x_1 \le a_1 \\ -a_2 \le x_2 \le a_2 \end{aligned}$$

$$C_{\alpha 1} = \overline{\sigma}_\alpha = \frac{1}{V} \int_V \sigma_\alpha(x_1, x_2, x_3)\ dV$$

The considerations made on the periodic microstructure model are still valid: elasticity, perfect bonding between materials and small strains

5. Homogenization using Lagrange Multipliers

This model was initially proposed by Zalamea, Oller in 2001.

It consists in obtaining the material performance by solving a finite element model of a representative volume element.

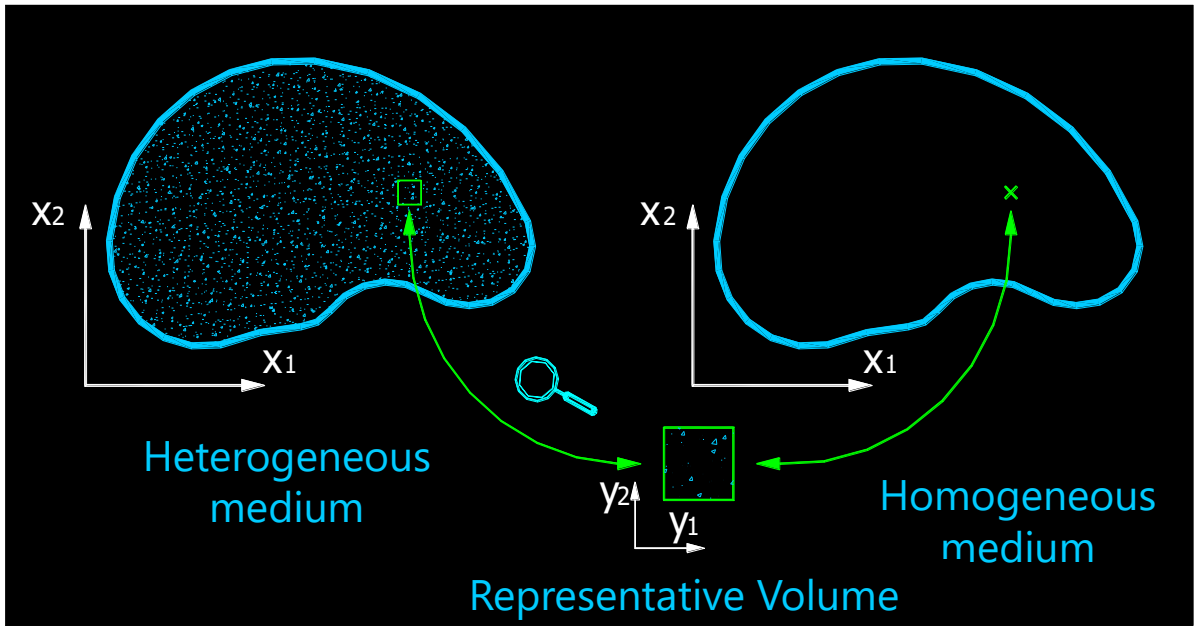

5. Homogenization using Lagrange Multipliers

The representative volume element is defined by cells. These have to be defined respecting the periodicity of the base material. To have the cell perfectly defined, it is necessary to define also the periodicity vectors.

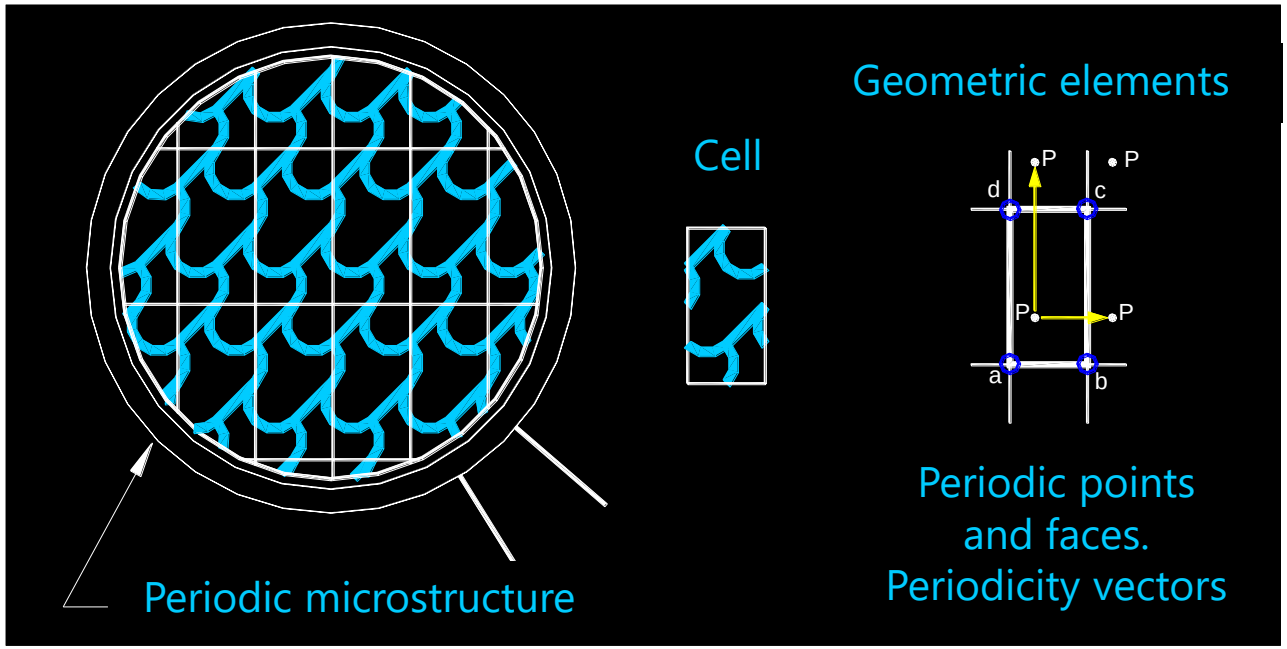

5. Homogenization using Lagrange Multipliers

The periodicity elements will vary depending on the cell defined as Representative Volume Element.

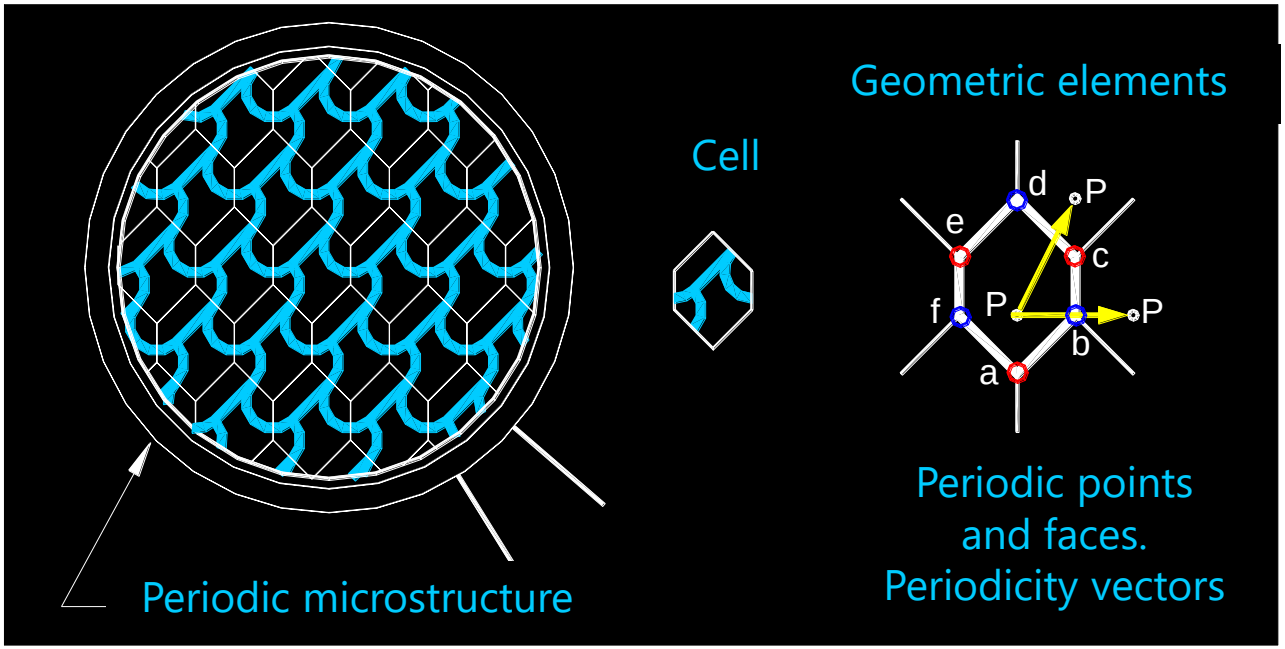

5. Homogenization using Lagrange Multipliers

The deformation obtained in the macro-model is transferred to the micro-model using the average theory.

It is important to remark that the micro-model deformation does not only modify the geometry of the RVE but also the periodicity vectors

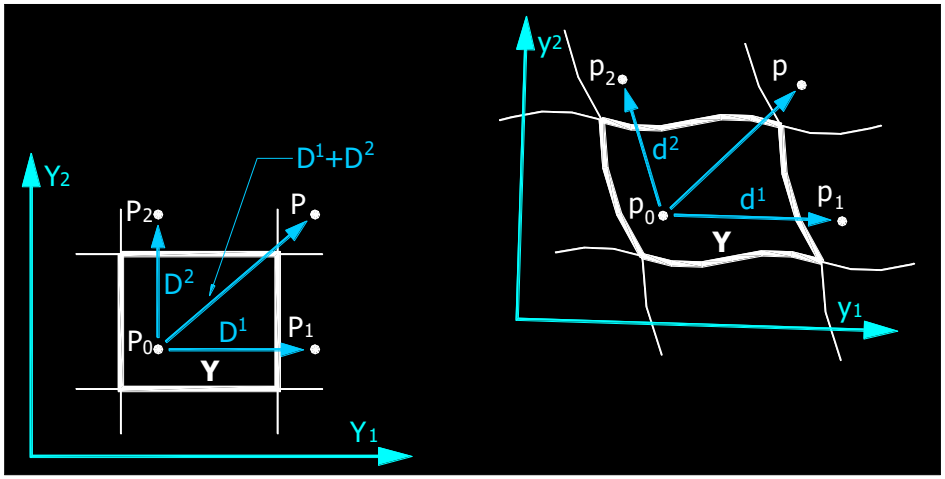

5. Homogenization using Lagrange Multipliers

The use of Lagrange Multipliers to force the periodicity at the RVE increases the computational cost and the complexity of the system.

On the other hand, it allows defining periodicity vectors. With these, the same RVE can be used to characterize different composites.

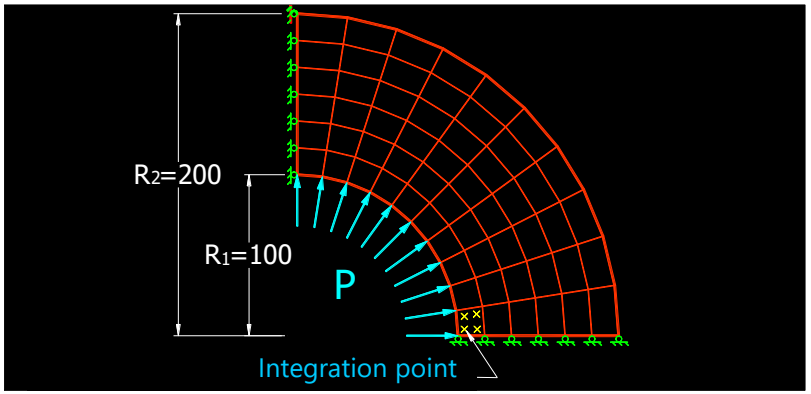

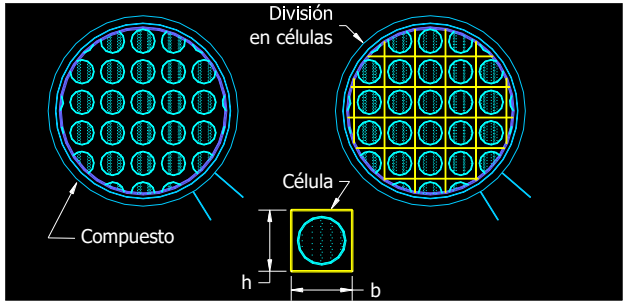

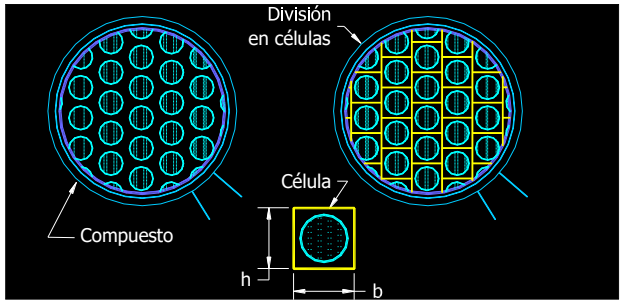

5. Homogenization using Lagrange Multipliers

The results obtained for the simulations previously presented are:

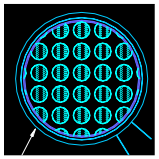

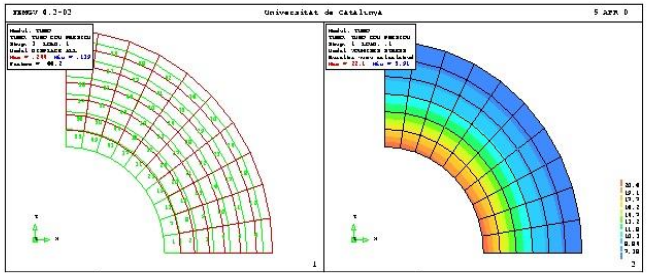

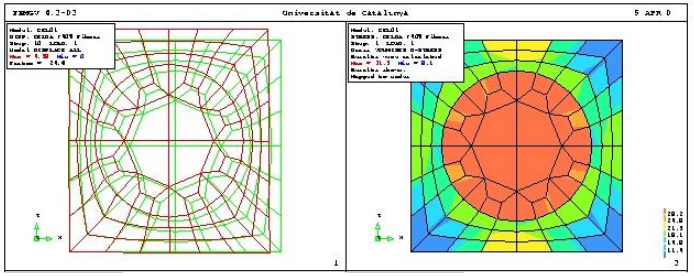

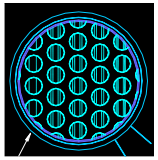

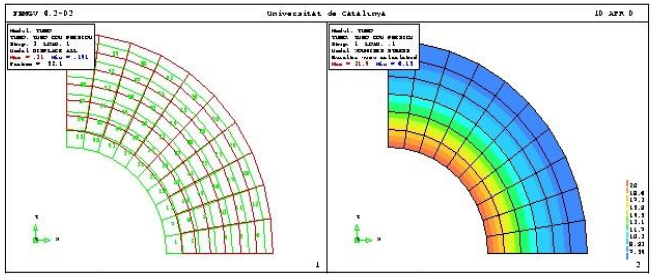

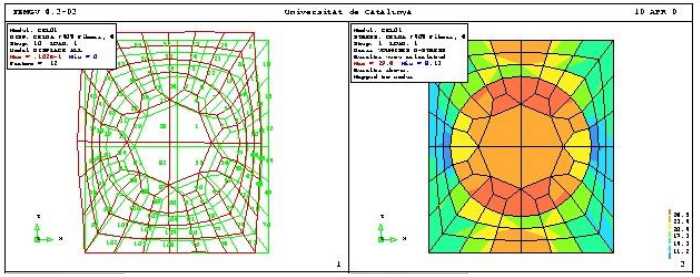

5. Homogenization using Lagrange Multipliers

Besides the additional complexity provided by the use of Lagrange Multipliers to solve the RVE problem, the major drawback of this homogenization procedure was:

It was proposed in 2001!

Computational capabilities were substantially smaller than today.

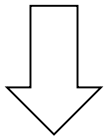

The analyses that could be performed were only academic

In example:

Previous case consisted in a macro model with 60 linear 2D elements and a micro model with 108 linear 2D elements.

The problem was solved with a parallel process with 4 processors and required 1h15min to be solved

6. Serial-parallel mixing theory

This last example differs from the others, as it does not defines an specific model to characterize a given composite geometry, but instead provides the mechanical response of the composite by defining specific relations between the constitutive equations of its components.

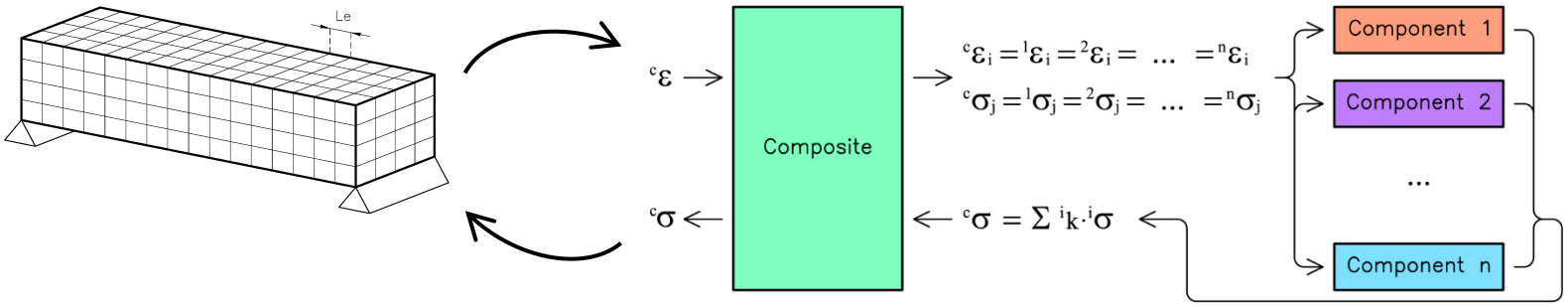

The serial-parallel mixing theory (SP RoM) can be understood as a phenomenological homogenization or a constitutive equation manager.

6. Serial-parallel mixing theory

In order to understand the performance of the serial/parallel mixing theory we will analyze a basic material:

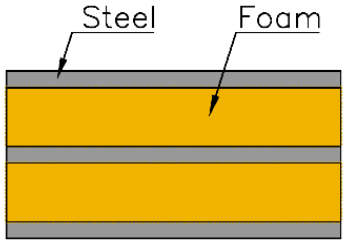

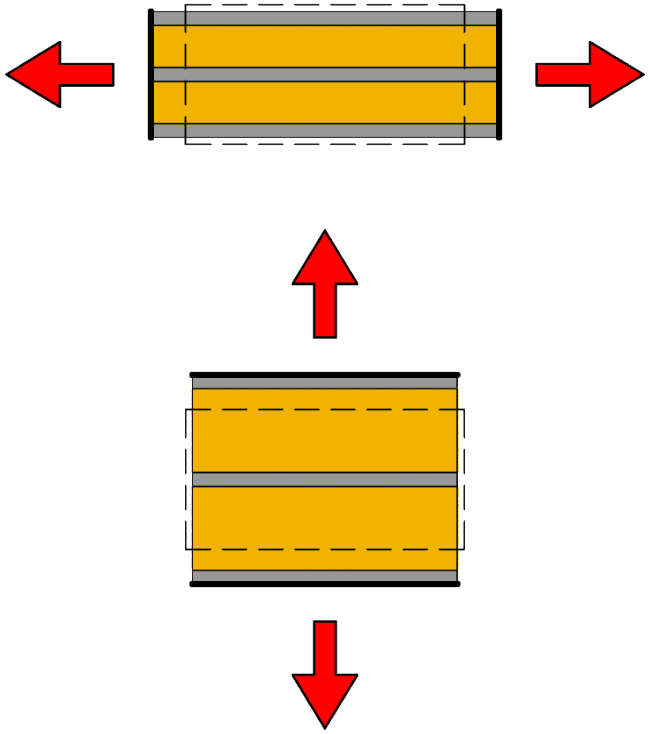

Parallel behavior

$\varepsilon_1 = \varepsilon_2 = \ldots = \varepsilon_n$

Serial behavior

$\sigma_1 = \sigma_2 = \ldots = \sigma_n$

6. Serial-parallel mixing theory

The serial/parallel mixing theory states that:

1. All components have the same strains in parallel direction
2. All components have the same stress in serial direction
3. All components participate in the composite material proportionally to their volumetric participation

This is:

Parallel direction

$$\begin{cases} {}^{c}\varepsilon_P = {}^{m}\varepsilon_P = {}^{f}\varepsilon_P \\ {}^{c}\sigma_P = {}^{m}k\,{}^{m}\sigma_P + {}^{f}k\,{}^{f}\sigma_P \end{cases}$$

Serial direction

$$\begin{cases} {}^{c}\varepsilon_S = {}^{m}k\,{}^{m}\varepsilon_S + {}^{f}k\,{}^{f}\varepsilon_S \\ {}^{c}\sigma_S = {}^{m}\sigma_S = {}^{f}\sigma_S \end{cases}$$

6. Serial-parallel mixing theory

Application of the SP RoM formulation to laminate materials:

Laminates simulated with solid elements:

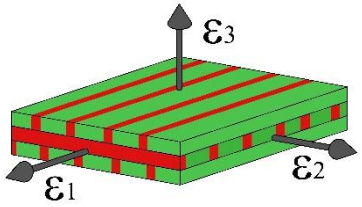

1) Apply parallel RoM at layer level $^{c}\varepsilon = {}^{L1}\varepsilon = \ldots = {}^{Ln}\varepsilon$

2) Apply SP RoM for each layer $^{Li}\varepsilon \rightarrow {}^{Li}\sigma$

3) Obtain stresses with parallel RoM $^{c}\sigma = \sum {}^{Li}k \, {}^{Li}\sigma$

Laminates simulated with shell elements:

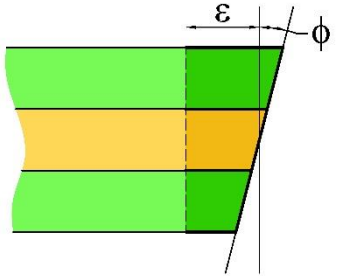

1) $$\begin{Bmatrix} {}^{Li}\varepsilon_x \\ {}^{Li}\varepsilon_y \\ {}^{Li}\gamma_{xy} \end{Bmatrix} = \begin{Bmatrix} \varepsilon_x^0 \\ \varepsilon_y^0 \\ \gamma_{xy}^0 \end{Bmatrix} + z \begin{Bmatrix} \kappa_x \\ \kappa_y \\ \kappa_{xy} \end{Bmatrix}$$

2) SP RoM

$^{Li}\varepsilon \rightarrow {}^{Li}\sigma$

6. Serial-parallel mixing theory

Parallel Load:

Stress-strain graph
in the load direction

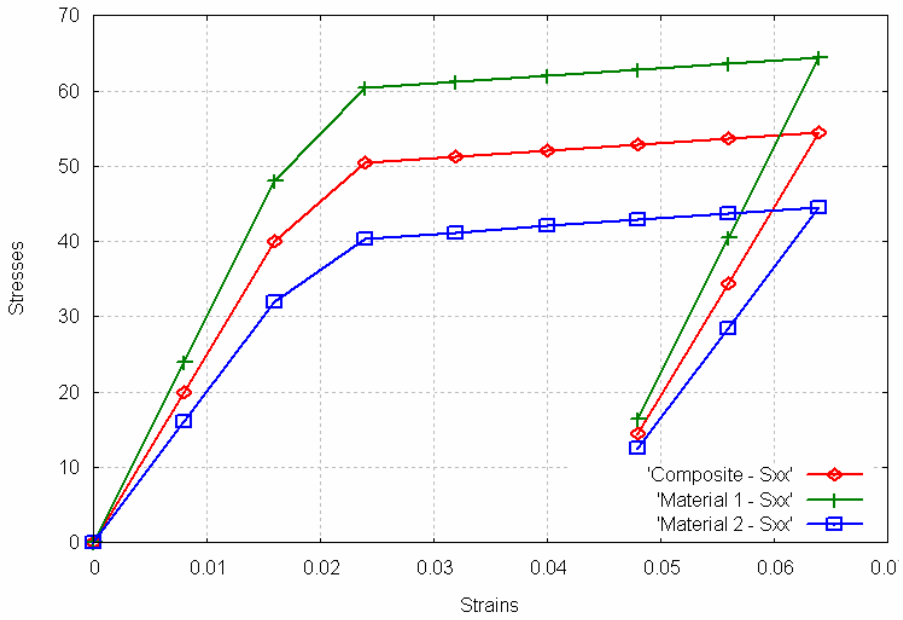

ISO-STRAIN Behaviour

Stress-strain graph
perpendicular to the load direction

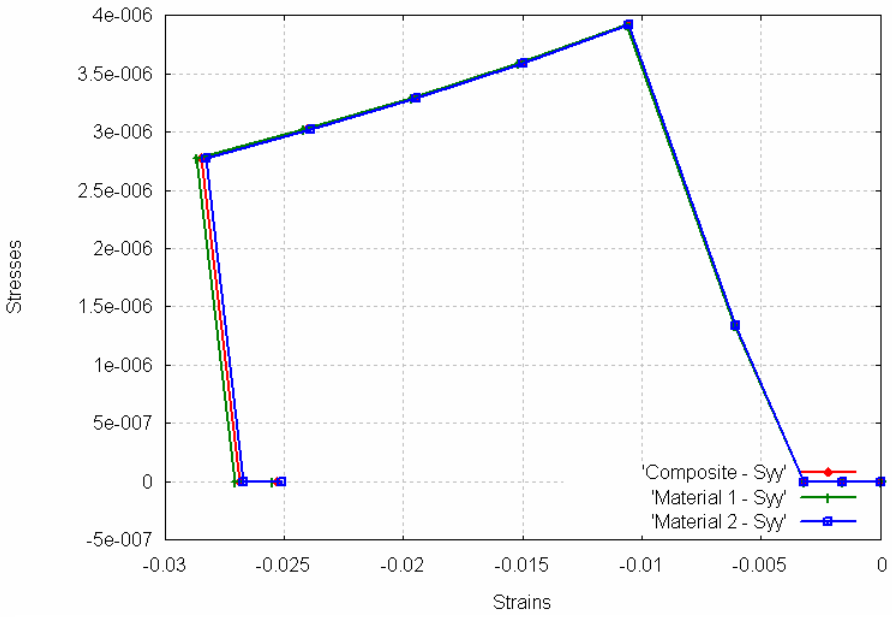

ISO-STRESS Behaviour

6. Serial-parallel mixing theory

Serial Load:

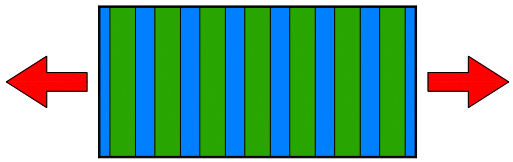

Stress-strain graph
in the load direction

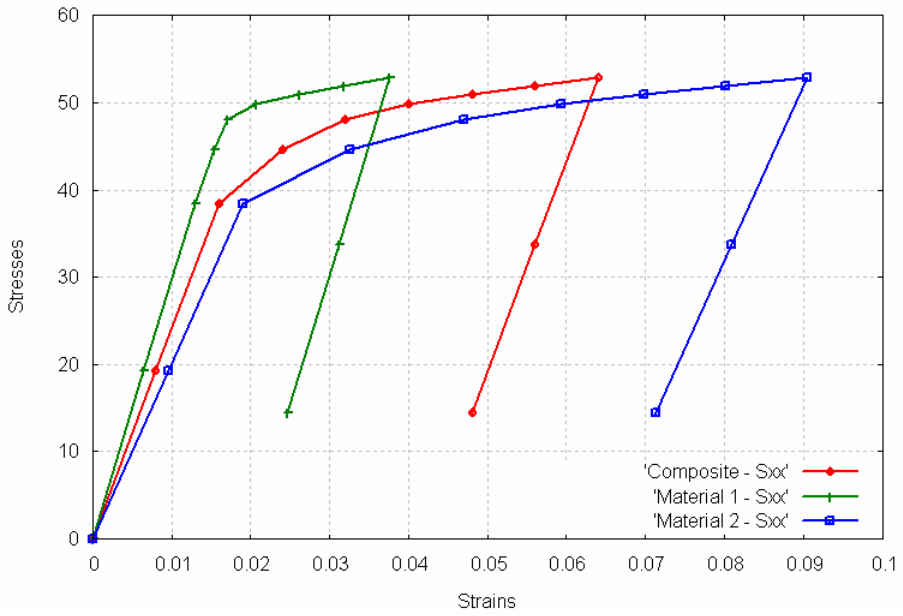

ISO-STRESS Behaviour

Stress-strain graph
perpendicular to the load direction

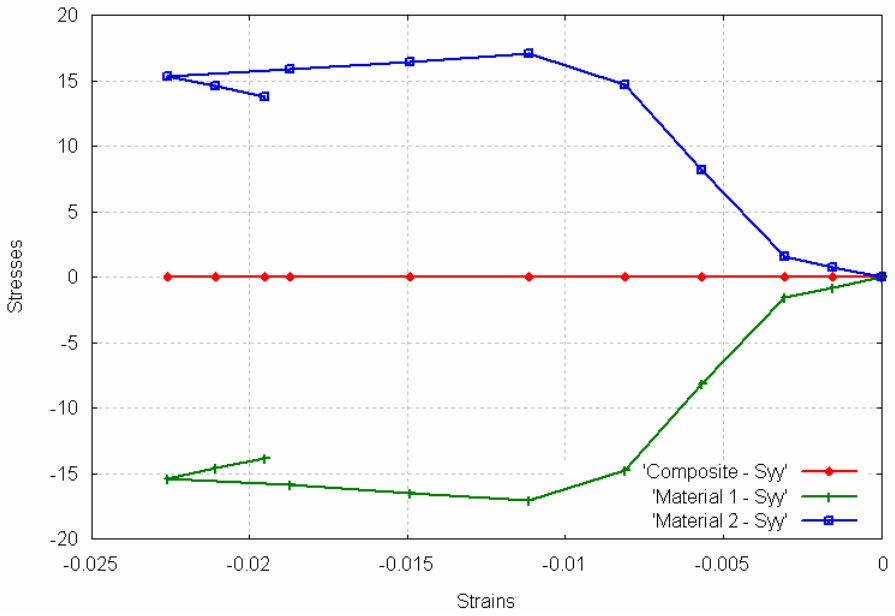

ISO-STRAIN Behaviour

6. Serial-parallel mixing theory

Numerical example. Delamination of composites

One of the most common failure modes of composite laminates is delamination. The SP RoM is capable of predicting this failure mode naturally.

Example: Ply drop-off test

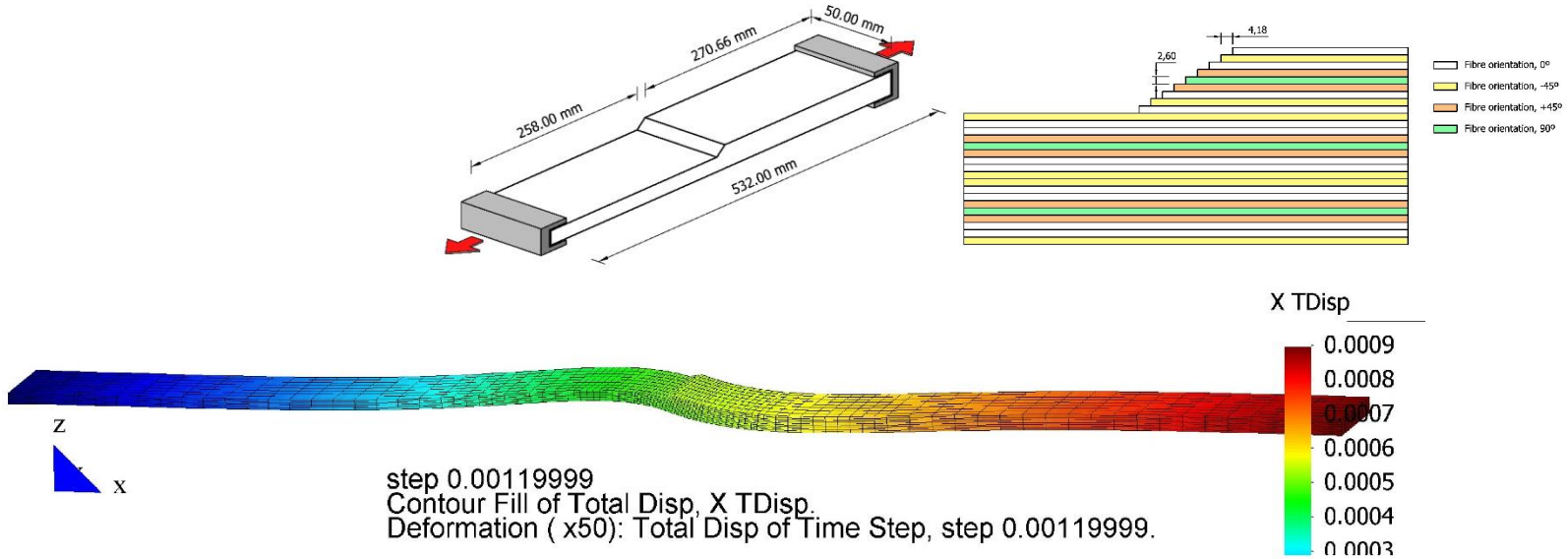

6. Serial-parallel mixing theory

Failure mode of the ply drop-off test:

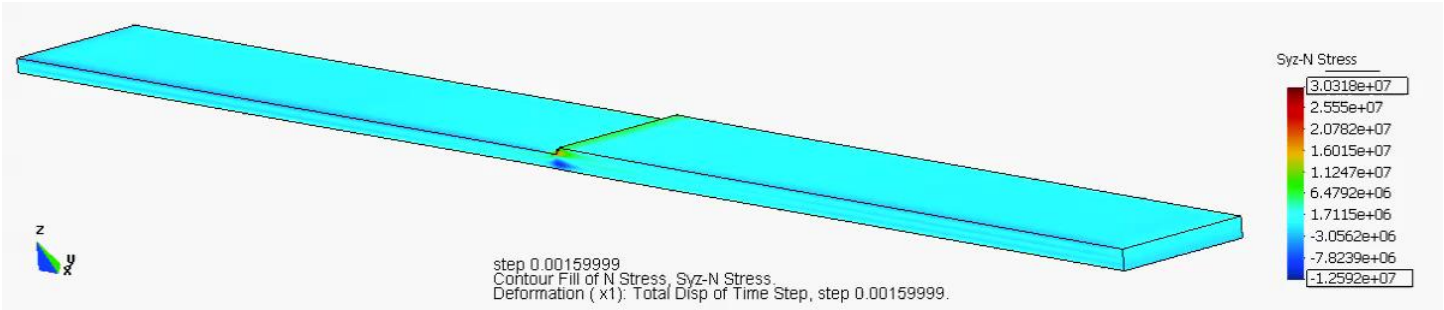

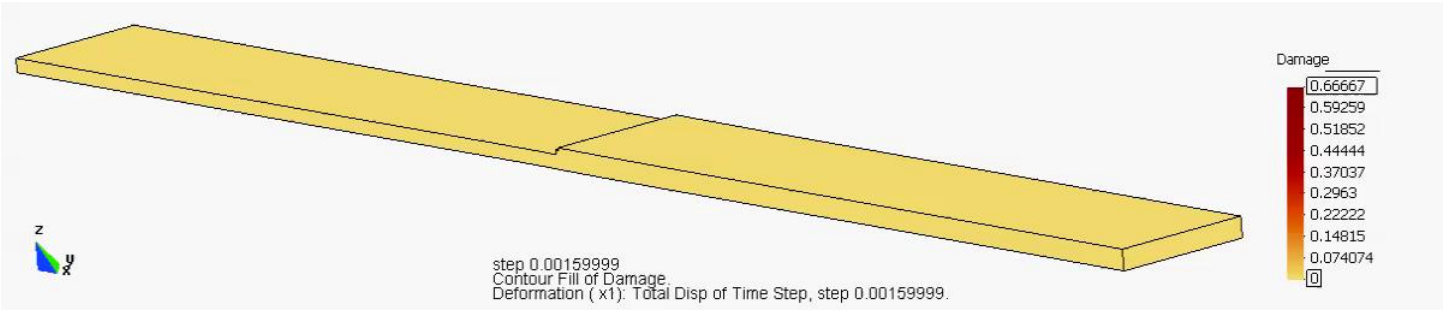

SUMMARY

- As materials have increased their complexity, advanced numerical approaches are also required for a correct characterization.

- Multiscale procedures are the perfect framework to increase, as much as wanted, the complexity of the model used to define the composite.

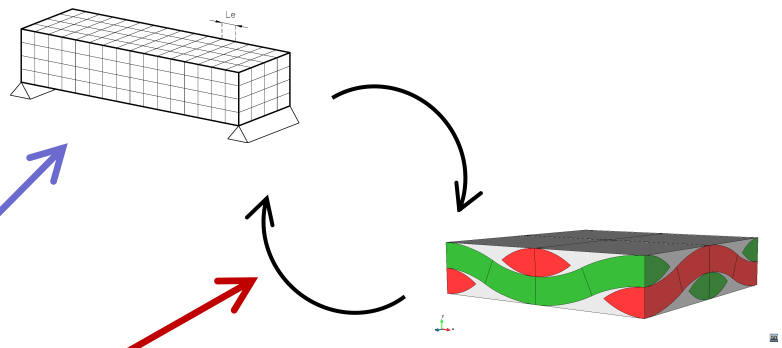

- Our interest lays in the information exchange between the two scales. The procedure chosen must allow:

  - Solve engineering problems
  - An accurate material characterization. So all the possibilities of nowadays composites can be taken into account.

2. First Order Computational Homogenization

First Order Computational Homogenization

2. First Order Computational Homogenization (FOCH)
    - 2.1. Basic Principles
    - 2.2. Formulation
    - 2.3. Implementation
    - 2.4. Numerical examples

BASIC PRINCIPLES – Multiscale procedures

A multiscale procedure consists on solving a numerical model, in which the response of some of its components is obtained from a numerical model found in a lower scale.

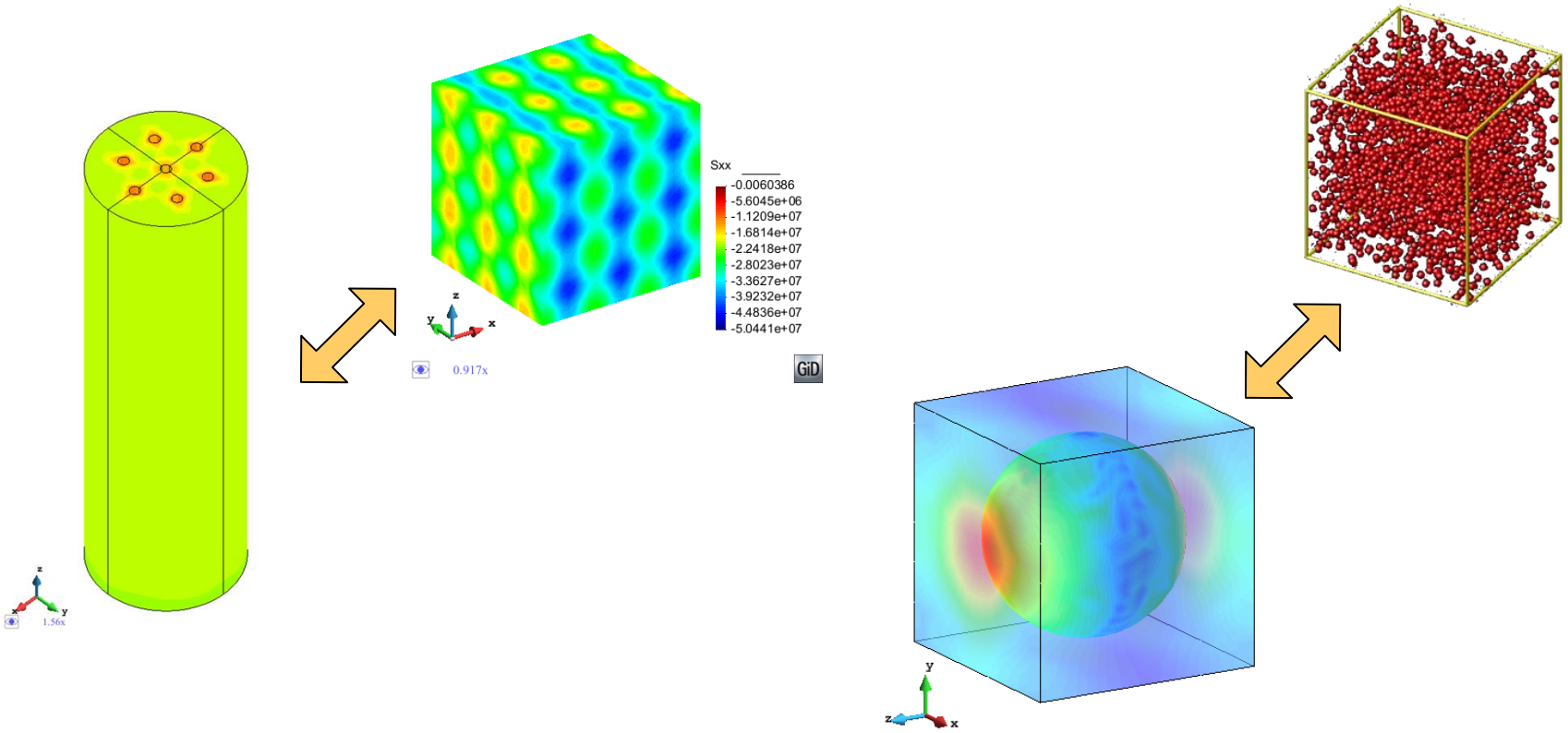

Multiscale procedures in mechanical problems

If this is applied to the solution of structural mechanical problems, the multiscale procedure consists on:

Transfer the deformation gradient tensor $\boldsymbol{\varepsilon_M}$ to the micro-scale, where is solved a boundary value problem (BVP) over a representative volume element (RVE). The macroscopic stress tensor $\boldsymbol{\sigma_M}$ and tangent stiffness matrix $\mathbf{C_{hom}}$ can be obtained from this scale. (Geers et al. 2010)

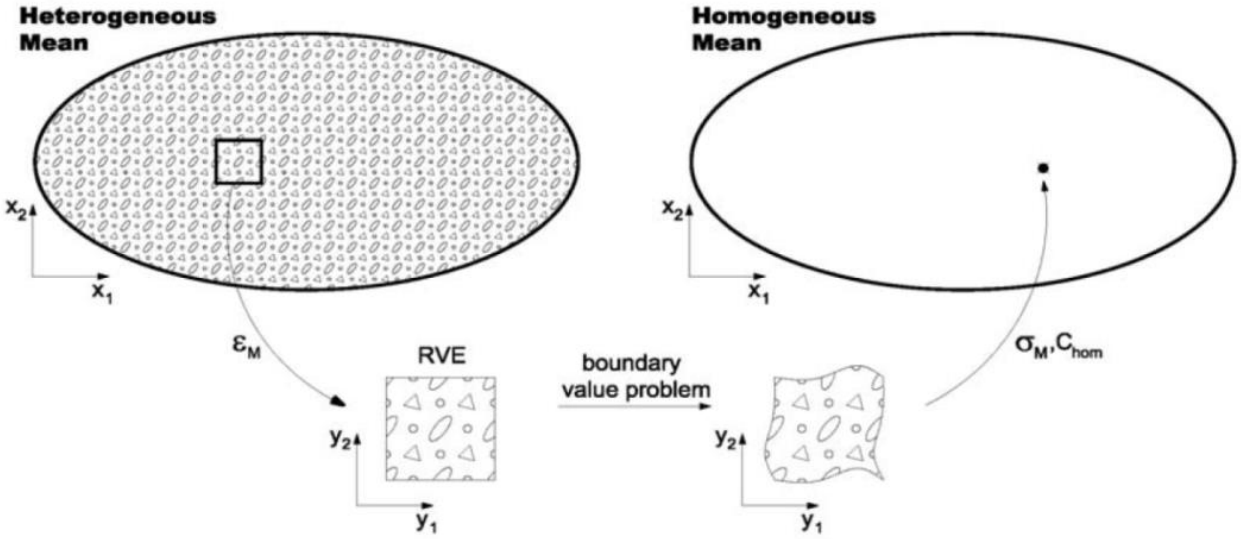

Conditions to apply a multiscale procedure

In order to apply a multiscale procedure there are two conditions that must be fulfilled:

1. Periodicity of the RVE

2. Scale separation

   Lm <<< Le

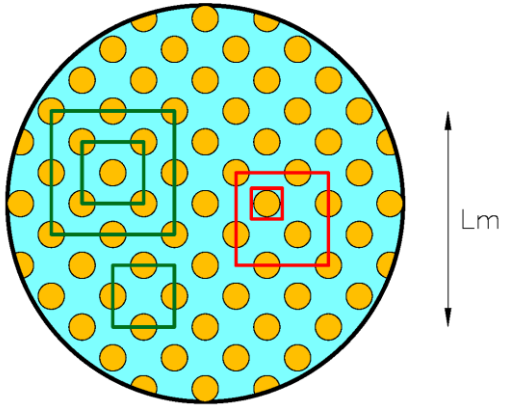

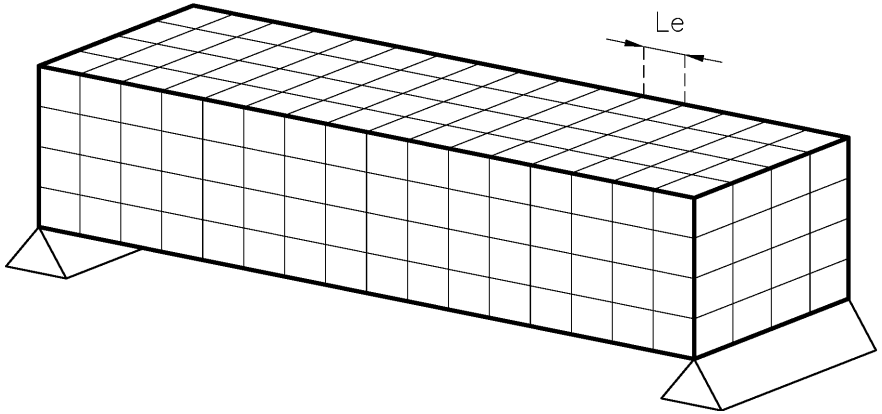

There are several studies concerning the most representative size of the RVE, such as:

S.M. Mirkhalaf, F.M. Andrade Pires, Ricardo Simoes: *Determination of the size of the Representative Volume Element (RVE) for the simulation of heterogeneous polymers at finite strains*. Finite Elements in Analysis and Design (119), 2016

FORMULATION – Macro displacement

The displacement field in the macro scale can be computed as:

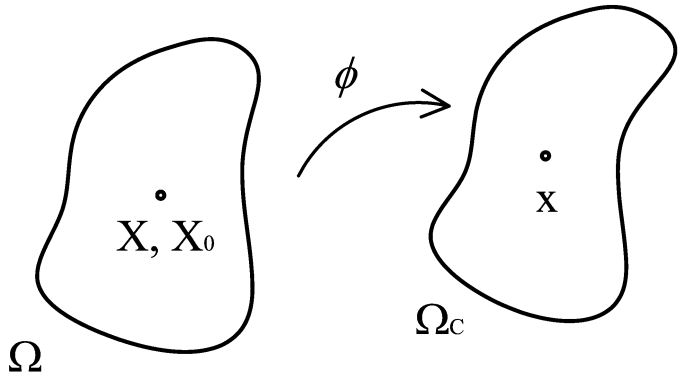

Macro scale displacement:

Continuum: $d\mathrm{x} = \mathrm{F} \cdot d\mathrm{X}$

Taylor's exp.: $\triangle \mathbf{x} = \mathbf{F}\left(\mathbf{X}_o\right) \cdot \triangle \mathbf{X} + \frac{1}{2}\mathbf{G}\left(\mathbf{X}_o\right) : \triangle \mathbf{X} \otimes \triangle \mathbf{X} + \mathcal{O}\left(\triangle \mathbf{X}_o^3\right)$

with

F = Deformation gradient tensor $\mathrm{F} = \frac{\partial \phi}{\partial \mathrm{X}}$

G = Gradient of the deformation gradient tensor $\mathrm{G} = \nabla \mathrm{F} = \frac{\partial}{\partial \mathrm{X}}\left(\frac{\partial \phi}{\partial \mathrm{X}}\right)$

Micro Displacement

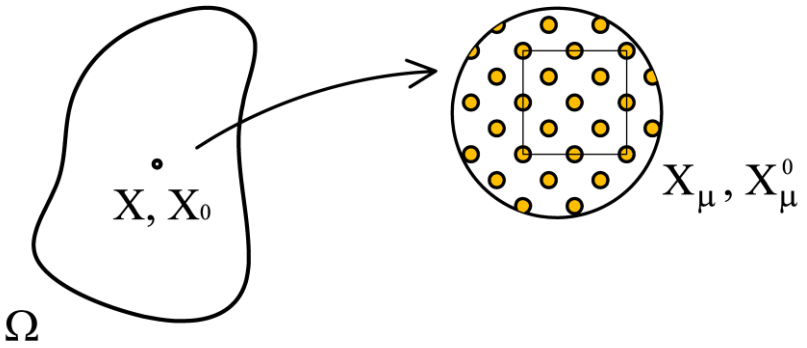

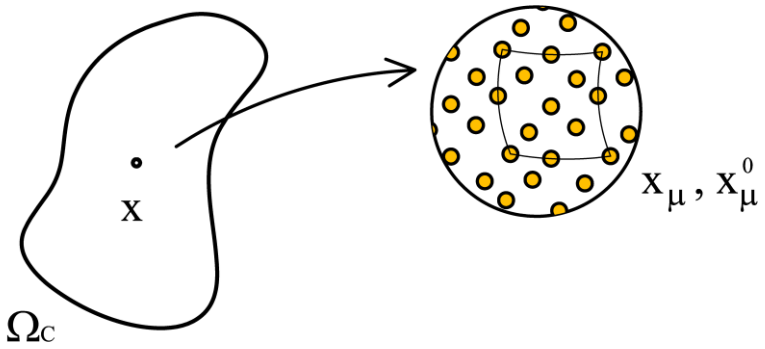

The displacement field in the micro scale is a combination of the displacements provided by the macro structure and a micro fluctuation:

$$\mathbf{x}_\mu\left(\mathbf{X}_o,\mathbf{X}_\mu\right)\cong\mathbf{x}_\mu^o+\mathbf{F}\left(\mathbf{X}_o\right)\cdot\triangle\mathbf{X}_\mu+\mathbf{w}\left(\mathbf{X}_\mu\right)$$

$$\triangle\mathbf{X}_\mu=\mathbf{X}_\mu-\mathbf{X}_\mu^o$$

$$\triangle\mathbf{x}=\mathbf{F}\left(\mathbf{X}_o\right)\cdot\triangle\mathbf{X}+\frac{1}{2}\mathbf{G}\left(\mathbf{X}_o\right):\triangle\mathbf{X}\otimes\triangle\mathbf{X}+\mathcal{O}\left(\triangle\mathbf{X}_o^3\right)$$

This is a FIRST ORDER HOMOGENIZATION because it only considers the first term of the macro displacement field.

Micro Displacement

To simplify the symbolic manipulation and for symmetry purposes, it is convenient to set the origin of the RVE's coordinate system as:

$$\mathbf{X}_{\mu}^{o} = 0 \qquad and \qquad \mathbf{x}_{\mu}^{o} = 0$$

Therefore,

$$\mathbf{x}_{\mu}\left(\mathbf{X}_{o}, \mathbf{X}_{\mu}\right) \cong \mathbf{F}\left(\mathbf{X}_{o}\right) \cdot \mathbf{X}_{\mu} + \mathbf{w}\left(\mathbf{X}_{\mu}\right)$$

And the displacement field of the RVE can be written as:

$$\mathbf{u}_{\mu} = \mathbf{x}_{\mu} - \mathbf{X}_{\mu}$$

$$\mathbf{u}_{\mu}\left(\mathbf{X}_{o}, \mathbf{X}_{\mu}\right) \cong \left[\mathbf{F}\left(\mathbf{X}_{o}\right) - \mathbf{I}\right] \cdot \mathbf{X}_{\mu} + \mathbf{w}\left(\mathbf{X}_{\mu}\right)$$

Boundary Conditions in the RVE

The first average theorem states that the volume average of the microstructural deformation gradient over the RVE must be equal to the macroscopic deformation gradient:

$$\mathbf{F}\left(\mathbf{X}_o\right) = \frac{1}{V_\mu}\int_{\Omega_\mu} \mathbf{F}_\mu\left(\mathbf{X}_o, \mathbf{X}_\mu\right)\ dV$$

The microstructural deformation gradient can be written as:

$$\mathbf{F}_\mu\left(\mathbf{X}_o, \mathbf{X}_\mu\right) = \nabla \mathbf{x}_\mu\left(\mathbf{X}_o, \mathbf{X}_\mu\right) \cong \mathbf{F}\left(\mathbf{X}_o\right) + \nabla \mathbf{w}\left(\mathbf{X}_\mu\right)$$

With some math, it is finally obtained:

$$\int_{\Omega_\mu} \nabla \mathbf{w}\left(\mathbf{X}_\mu\right)\ dV = \mathbf{0}$$

Boundary Conditions in the RVE

Applying the divergence theorem, the last expression becomes:

$$\int_{\partial\Omega_\mu} \mathbf{w}\left(\mathbf{X}_\mu\right) \otimes \mathbf{N}\; dA = \mathbf{0}$$

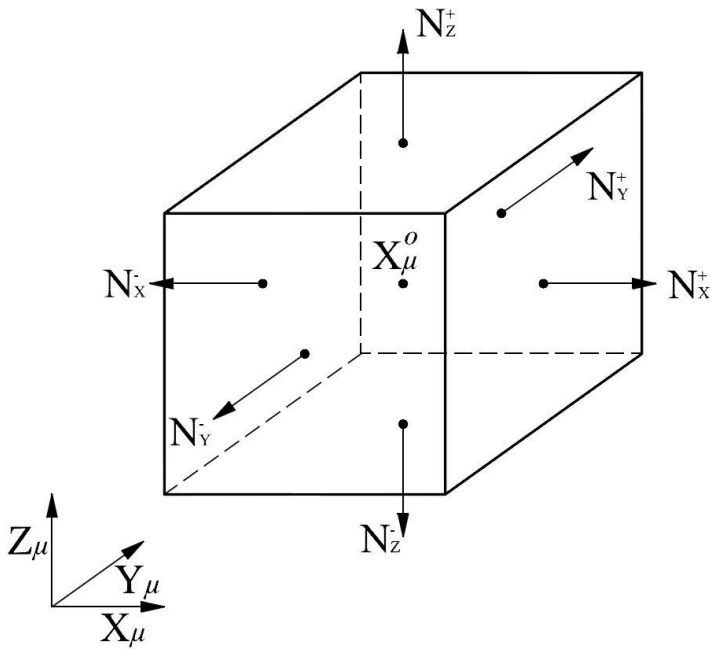

Which can be rewritten as:

$$\left(\int_{\mathbf{N}_X^+} \mathbf{w}\; dA_{yz} - \int_{\mathbf{N}_X^-} \mathbf{w}\; dA_{yz}\right) \otimes \mathbf{N}_X^+ + \left(\int_{\mathbf{N}_Y^+} \mathbf{w}\; dA_{xz} - \int_{\mathbf{N}_Y^-} \mathbf{w}\; dA_{xz}\right) \otimes \mathbf{N}_Y^+ + \left(\int_{\mathbf{N}_Z^+} \mathbf{w}\; dA_{xy} - \int_{\mathbf{N}_Z^-} \mathbf{w}\; dA_{xy}\right) \otimes \mathbf{N}_Z^+ = \mathbf{0}$$

Boundary Conditions in the RVE

There are several boundary conditions that can be applied to the RVE that fulfil the defined requirement:

- Taylor Model (zero fluctuations):

$$\mathbf{w},\ \text{sufficiently regular} \mid \mathbf{w}\left(\mathbf{X}_\mu\right) = \mathbf{0},\ \forall\, \mathbf{X}_\mu \in \Omega_\mu$$

- Linear boundary displacements (zero boundary fluctuations):

$$\mathbf{w},\ \text{sufficiently regular} \mid \mathbf{w}\left(\mathbf{X}_\mu\right) = \mathbf{0},\ \forall\, \mathbf{X}_\mu \in \partial\Omega_\mu$$

- Periodic boundary fluctuations:

$$\mathbf{w},\ \text{sufficiently regular} \mid \mathbf{w}\left(\mathbf{X}_\mu^+\right) = \mathbf{w}\left(\mathbf{X}_\mu^-\right),\ \forall\, pairs\ \left\{\mathbf{X}_\mu^+, \mathbf{X}_\mu^-\right\} \in \partial\Omega_\mu$$

- Minimal constrain:

  There is no specific restriction, besides the integral over the fluctuation field.

Macro and micro strain tensor

The macro strain tensor must be equal to the volume average of the micro strain tensor:

$$\mathbf{E}\left(\mathbf{X}_o\right) = \frac{1}{V_\mu}\int_{\Omega_\mu} \mathbf{E}_\mu\left(\mathbf{X}_o, \mathbf{X}_\mu\right)\ dV$$

And the micro strain tensor can be written as:

$$\mathbf{E}_\mu\left(\mathbf{X}_o, \mathbf{X}_\mu\right) = \mathbf{E}\left(\mathbf{X}_o\right) + \mathbf{E}_\mu^w\left(\mathbf{X}_\mu\right)$$

being $\mathbf{E}_\mu^w = \frac{1}{2}\left(\nabla\mathbf{w} + \left(\nabla\mathbf{w}\right)^T\right) = \nabla^s\mathbf{w}$

Hill-Mandel principle and RVE Equilibrium

The Hill-Mandel energy condition states that the virtual work of the point $\mathbf{X_0}$ must be equal to the volume average of the virtual work in the RVE for any kinematically admissible displacement field:

$$\mathbf{S} : \delta\mathbf{E}\left(\mathbf{X}_o\right) = \frac{1}{V_\mu}\int_{\Omega_\mu} \mathbf{S}_\mu : \delta\mathbf{E}_\mu \; dV$$

$$= \frac{1}{V_\mu}\int_{\Omega_\mu} \mathbf{S}_\mu \; dV : \delta\mathbf{E}\left(\mathbf{X}_o\right) + \frac{1}{V_\mu}\int_{\Omega_\mu} \mathbf{S}_\mu : \delta\mathbf{E}^w_\mu\left(\mathbf{X}_\mu\right) \; dV$$

Defining the macroscopic stress tensor as the average of the microstructural stress tensor in the RVE domain:

$$\mathbf{S}\left(\mathbf{X}_o, \mathbf{X}_\mu\right) \equiv \frac{1}{V_\mu}\int_{\Omega_\mu} \mathbf{S}_\mu\left(\mathbf{X}_o, \mathbf{X}_\mu\right) \; dV$$

Hill-Mandel principle and RVE Equilibrium

The Hill-Mandel principle will be satisfied if:

$$\int_{\Omega_\mu} \mathbf{S}_\mu : \delta\mathbf{E}_\mu^w(\mathbf{X}_\mu)\ dV = \int_{\Omega_\mu} \mathbf{S}_\mu : \nabla^s \delta\mathbf{w}\ dV = 0$$

RVE variational equilibrium equation

Macroscopic and microscopic stress tensor

The microscopic stress tensor can be obtained as:

$$\begin{aligned}\mathbf{S}_\mu\left(\mathbf{X}_o,\mathbf{X}_\mu\right) &= \mathbf{C}_\mu\left(\mathbf{X}_\mu\right):\mathbf{E}_\mu\left(\mathbf{X}_o,\mathbf{X}_\mu\right)\\ &= \mathbf{C}_\mu\left(\mathbf{X}_\mu\right):\mathbf{E}\left(\mathbf{X}_o\right)+\mathbf{C}_\mu\left(\mathbf{X}_\mu\right):\mathbf{E}_\mu^w\left(\mathbf{X}_\mu\right)\end{aligned}$$

And the macroscopic stress tensor can be calculated as:

$$\mathbf{S}\left(\mathbf{X}_o,\mathbf{X}_\mu\right)=\frac{1}{V_\mu}\int_{\Omega_\mu}\mathbf{S}_\mu\left(\mathbf{X}_o,\mathbf{X}_\mu\right)\ dV$$

$$\mathbf{S}\left(\mathbf{X}_o,\mathbf{X}_\mu\right)=\bar{\mathbf{C}}:\mathbf{E}\left(\mathbf{X}_o\right)+\frac{1}{V_\mu}\int_{\Omega_\mu}\mathbf{C}_\mu:\mathbf{E}_\mu^w\left(\mathbf{X}_\mu\right)\ dV$$

with: $\bar{\mathbf{C}}\equiv\frac{1}{V_\mu}\int_{\Omega_\mu}\mathbf{C}_\mu\ dV$

Macroscopic and microscopic stress tensor

Some remarks regarding the macroscopic stress tensor:

1. It does not depend explicitly on $\mathbf{X}\boldsymbol{\mu}$. Therefore, the stresses provided by the RVE are independent of its size.

   A non-dimensional RVE can be used to characterize the material.

2. The fluctuation strains affect the macro-response of the structure. Depending on the boundary conditions chosen, different macro-stress results will be obtained.

   The Taylor model returns the classical mixing theory results.

IMPLEMENTATION – The Finite Element Method

The Finite Element Method for the analysis of structural problems is based on solving the Principle of Virtual Work:

$$\int_\Omega \delta\mathbf{E}^T \cdot \mathbf{S}\ dV = \int_\Omega \delta\bar{\mathbf{u}}^T \cdot \mathbf{b}\ dV + \int_{\partial\Omega} \delta\bar{\mathbf{u}}^T \cdot \mathbf{q}\ dV + \sum \delta\mathbf{u}_i^T \cdot \mathbf{P}_i$$

Which leads to the solution of the linear system of equations:

$$\mathbf{K} \cdot \bar{\mathbf{u}} = \mathbf{F}$$

being $$\mathbf{K} = \int_\Omega \mathbf{B}^T : \mathbf{C} : \mathbf{B}\ dV$$

And the relation between stresses, strains and displacements:

$$\mathbf{S} = \mathbf{C} : \mathbf{E} = \mathbf{C} : \mathbf{B} \cdot \bar{\mathbf{u}}$$

IN A LINEAR ANALYSIS !

FEM – Flow diagram

In a non-linear analysis, the relation between strains and stresses are different to those predicted by the material stiffness matrix. In an implicit approach the displacements are found with an iterative procedure:

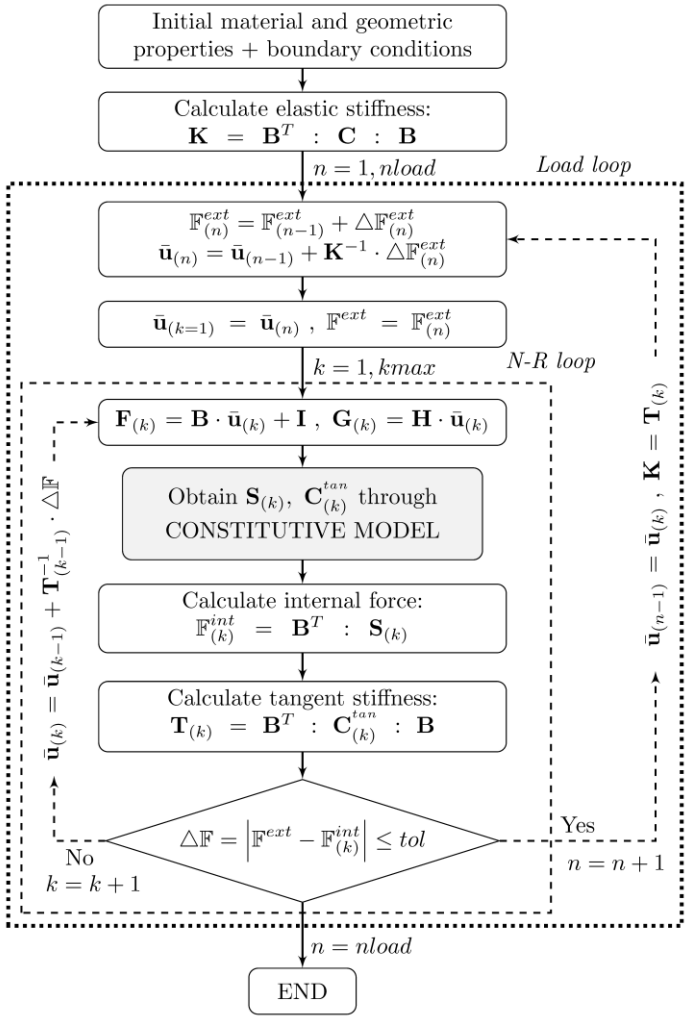

Solution of the MACROSCALE problem

The material stiffness matrix depends on the RVE microstructure

There is no constitutive model. The stress tensor corresponding to the applied stresses is obtained from the RVE solution

IN A LINEAR ANALISYS, THE RVE HAS TO BE SOLVED ONLY ONCE !

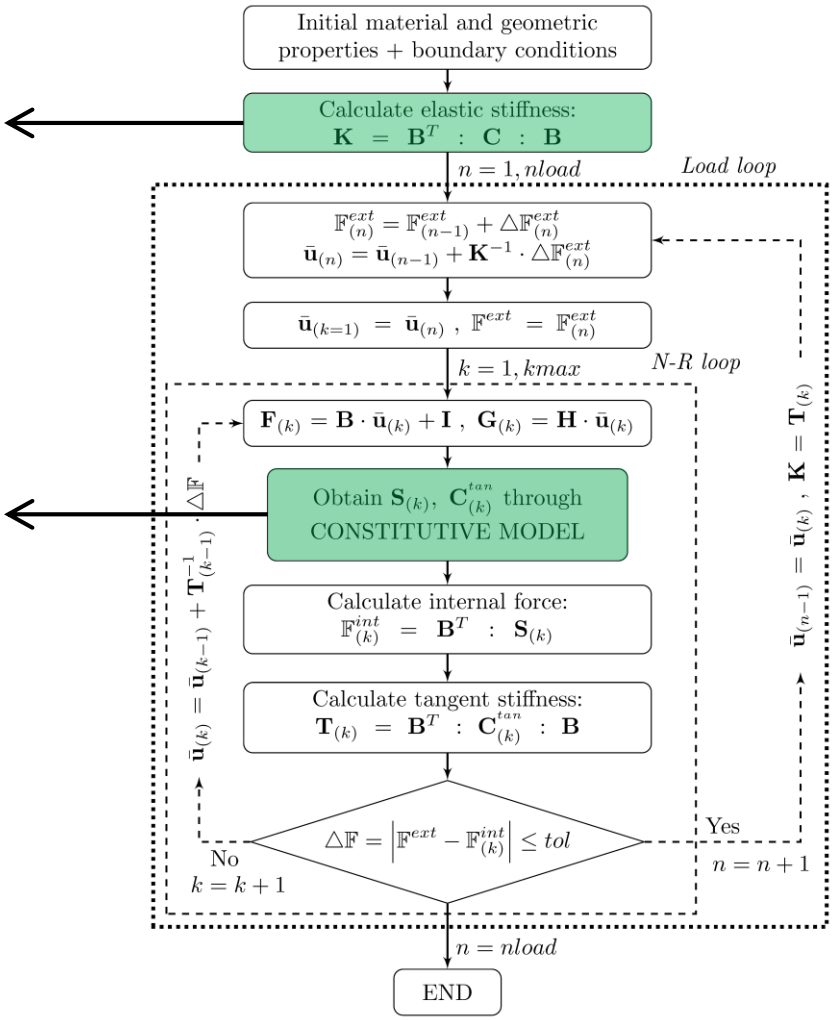

Solution of the MICROSCALE problem

The microscale problem is, by itself, a numerical model that will be solved with the FEM.

The main differences compared to the macroscale problem are:

1. The boundary conditions to be applied to the model are defined by the deformation gradient of the macroscale problem.

2. The result required from the model are the macroscale stresses, which are obtained from the microscale stresses, and the tangent stiffness tensor.

MICRO-STRUCTURE boundary conditions

From the different models that can be applied, the most convenient is the *periodic boundary fluctuations*:

$$\mathbf{w},\ \text{sufficiently regular} \mid \mathbf{w}\left(\mathbf{X}_\mu^+\right) = \mathbf{w}\left(\mathbf{X}_\mu^-\right),\ \forall\ pairs\ \left\{\mathbf{X}_\mu^+, \mathbf{X}_\mu^-\right\} \in \partial\Omega_\mu$$

Which can be rewritten as:

$$\mathbf{u}_\mu(\mathbf{X}_\mu^+) - \mathbf{u}_\mu(\mathbf{X}_\mu^-) = D_1(\mathbf{F}-\mathbf{I})\cdot\mathbf{N}_X^+, \quad in \quad \forall\ pairs\ \left\{\mathbf{X}_\mu^+, \mathbf{X}_\mu^-\right\} \in \partial\Omega_{\mu|\mathbf{N}_X}$$

$$\mathbf{u}_\mu(\mathbf{X}_\mu^+) - \mathbf{u}_\mu(\mathbf{X}_\mu^-) = D_2(\mathbf{F}-\mathbf{I})\cdot\mathbf{N}_Y^+, \quad in \quad \forall\ pairs\ \left\{\mathbf{X}_\mu^+, \mathbf{X}_\mu^-\right\} \in \partial\Omega_{\mu|\mathbf{N}_Y}$$

$$\mathbf{u}_\mu(\mathbf{X}_\mu^+) - \mathbf{u}_\mu(\mathbf{X}_\mu^-) = D_3(\mathbf{F}-\mathbf{I})\cdot\mathbf{N}_Z^+, \quad in \quad \forall\ pairs\ \left\{\mathbf{X}_\mu^+, \mathbf{X}_\mu^-\right\} \in \partial\Omega_{\mu|\mathbf{N}_Z}$$

These boundary conditions are applied by defining master and slave nodes in the RVE model.

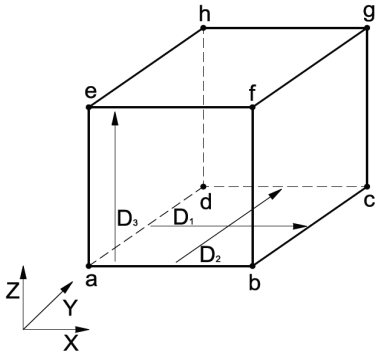

MICRO-STRUCTURE boundary conditions

Master and slave nodes in the RVE:

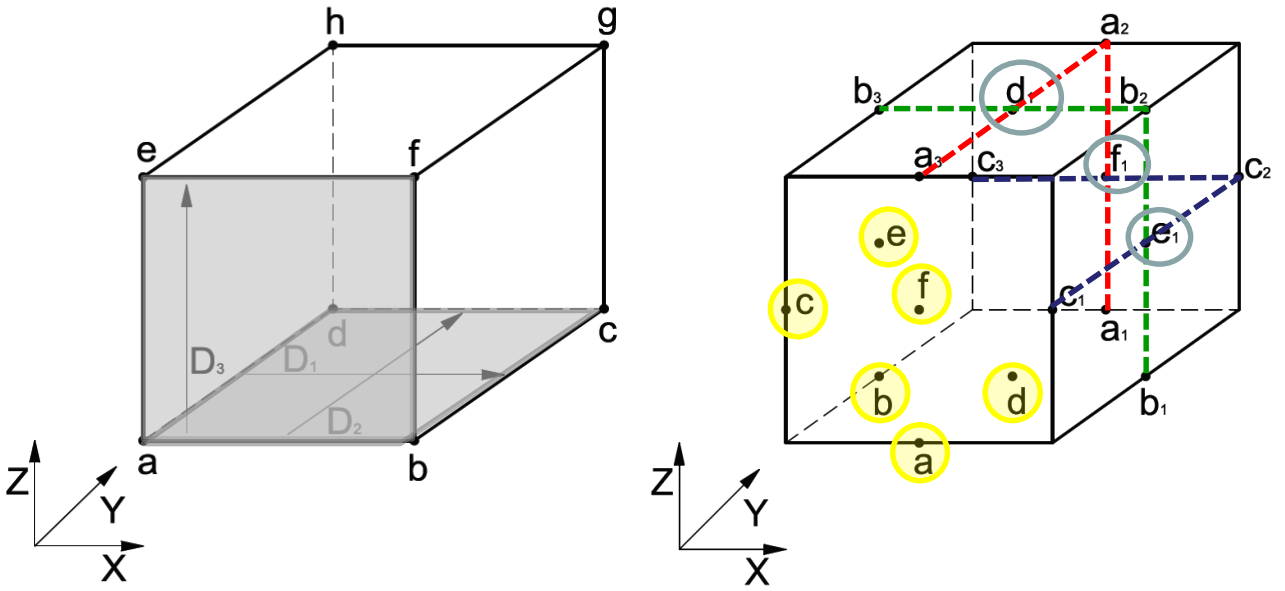

Master nodes	a	b	c	d	e	f
Slave nodes	a_1, a_2, a_3	b_1, b_2, b_3	c_1, c_2, c_3	d_1	e_1	f_1

MICRO-STRUCTURE boundary conditions

Position vector of the different nodes:

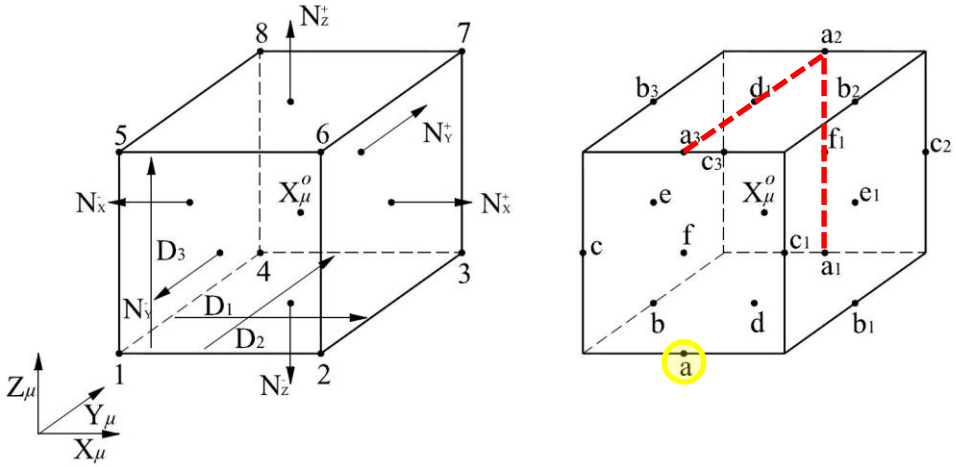

$$\mathbf{X}_{a_1} - \mathbf{X}_a = \left\{ \begin{array}{c} X_\mu \\ D_2/2 \\ -D_3/2 \end{array} \right\} - \left\{ \begin{array}{c} X_\mu \\ -D_2/2 \\ -D_3/2 \end{array} \right\} = \left\{ \begin{array}{c} 0 \\ D_2 \\ 0 \end{array} \right\} = D_2 \mathbf{N}_Y^+$$

$$\mathbf{X}_{a_2} - \mathbf{X}_a = \left\{ \begin{array}{c} X_\mu \\ D_2/2 \\ D_3/2 \end{array} \right\} - \left\{ \begin{array}{c} X_\mu \\ -D_2/2 \\ -D_3/2 \end{array} \right\} = \left\{ \begin{array}{c} 0 \\ D_2 \\ D_3 \end{array} \right\} = D_2 \mathbf{N}_Y^+ + D_3 \mathbf{N}_Z^+$$

$$\mathbf{X}_{a_3} - \mathbf{X}_a = \left\{ \begin{array}{c} X_\mu \\ -D_2/2 \\ D_3/2 \end{array} \right\} - \left\{ \begin{array}{c} X_\mu \\ -D_2/2 \\ -D_3/2 \end{array} \right\} = \left\{ \begin{array}{c} 0 \\ 0 \\ D_3 \end{array} \right\} = D_3 \mathbf{N}_Z^+$$

MICRO-STRUCTURE boundary conditions

Having defined the position vector, the periodic boundary fluctuations condition can be written as:

$$\bar{\mathbf{u}}_{a_1} = \bar{\mathbf{u}}_a + (\mathbf{F} - \mathbf{I}) \cdot (\mathbf{X}_{a_1} - \mathbf{X}_a) = \bar{\mathbf{u}}_a + D_2 (\mathbf{F} - \mathbf{I}) \cdot \mathbf{N}_Y^+$$

defining:

$$\mathbf{sm}_1 = D_1 (\mathbf{F} - \mathbf{I}) \cdot \mathbf{N}_X^+$$
$$\mathbf{sm}_2 = D_2 (\mathbf{F} - \mathbf{I}) \cdot \mathbf{N}_Y^+$$
$$\mathbf{sm}_3 = D_3 (\mathbf{F} - \mathbf{I}) \cdot \mathbf{N}_Z^+$$

the displacement of the slave nodes can be obtained as:

$$\bar{\mathbf{u}}_{a_1} = \bar{\mathbf{u}}_a + \mathbf{sm}_2, \quad \bar{\mathbf{u}}_{a_2} = \bar{\mathbf{u}}_a + \mathbf{sm}_2 + \mathbf{sm}_3, \quad \bar{\mathbf{u}}_{a_3} = \bar{\mathbf{u}}_a + \mathbf{sm}_3,$$
$$\bar{\mathbf{u}}_{b_1} = \bar{\mathbf{u}}_b + \mathbf{sm}_1, \quad \bar{\mathbf{u}}_{b_2} = \bar{\mathbf{u}}_b + \mathbf{sm}_1 + \mathbf{sm}_3, \quad \bar{\mathbf{u}}_{b_3} = \bar{\mathbf{u}}_b + \mathbf{sm}_3,$$
$$\bar{\mathbf{u}}_{c_1} = \bar{\mathbf{u}}_c + \mathbf{sm}_1, \quad \bar{\mathbf{u}}_{c_2} = \bar{\mathbf{u}}_c + \mathbf{sm}_1 + \mathbf{sm}_2, \quad \bar{\mathbf{u}}_{c_3} = \bar{\mathbf{u}}_c + \mathbf{sm}_2,$$
$$\bar{\mathbf{u}}_{d_1} = \bar{\mathbf{u}}_d + \mathbf{sm}_3, \quad \bar{\mathbf{u}}_{e_1} = \bar{\mathbf{u}}_e + \mathbf{sm}_1, \quad \bar{\mathbf{u}}_{f_1} = \bar{\mathbf{u}}_f + \mathbf{sm}_2.$$

Solution of the FEM problem with the given BC

The micro-structural problem to be solved consists on a RVE in which are known the displacement relations between its parallel faces.

This problem can be solved with two different approaches:

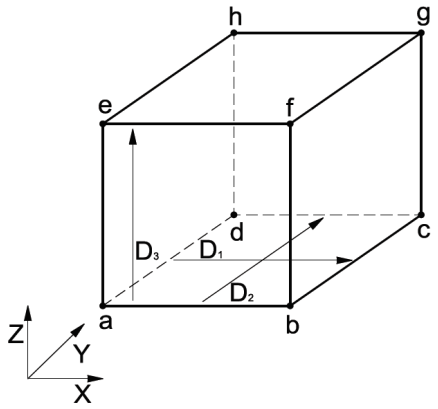

1. Definition of Lagrange Multipliers that relate the displacement relation between master and slave nodes.

$$\begin{bmatrix} \mathbf{K} & \mathbf{k}_p^T & \mathbf{k}_p^T \\ \mathbf{k}_p & \mathbf{I} & -\mathbf{I} \\ \mathbf{k}_p & -\mathbf{I} & \mathbf{I} \end{bmatrix} \cdot \begin{bmatrix} \mathbf{u} \\ \boldsymbol{\lambda}_1 \\ \boldsymbol{\lambda}_2 \end{bmatrix} = \begin{bmatrix} \mathbf{F} \\ \Delta\mathbf{D} \\ \Delta\mathbf{D} \end{bmatrix}$$

2. Removing the slave degrees of freedom from the linear system of equations.

Elimination of slave degrees of freedom

The linear system of equations to be solved can be rewritten differentiating internal (u), master (m) and slave (s) nodes:

$$\left[\begin{array}{c|c|c} K_{uu} & K_{um} & K_{us} \\ \hline K_{mu} & K_{mm} & K_{ms} \\ \hline K_{su} & K_{sm} & K_{ss} \end{array}\right] \left\{\begin{array}{c} d_u \\ \hline d_m \\ \hline d_s \end{array}\right\} = \left\{\begin{array}{c} F_u \\ \hline F_m \\ \hline F_s \end{array}\right\}$$

$$\Downarrow$$

$$\left[\begin{array}{c} K_{uu} \\ \hline K_{mu} \\ \hline K_{su} \end{array}\right] \{d_u\} + \left[\begin{array}{c} K_{um} \\ \hline K_{mm} \\ \hline K_{sm} \end{array}\right] \{d_m\} + \left[\begin{array}{c} K_{us} \\ \hline K_{ms} \\ \hline K_{ss} \end{array}\right] \{d_s\} = \left\{\begin{array}{c} F_u \\ \hline F_m \\ \hline F_s \end{array}\right\}$$

The displacement of the slave nodes can be written as a function of the master nodes:

$$\{d_s\} = [S_{sm}]\{d_m\} + \{\triangle_d\}$$

Elimination of slave degrees of freedom

Therefore:

$$\left[\begin{array}{c} K_{uu} \\ \hline K_{mu} \\ \hline K_{su} \end{array}\right]\{d_u\} + \left[\begin{array}{c} K_{um} \\ \hline K_{mm} \\ \hline K_{sm} \end{array}\right]\{d_m\} + \left[\begin{array}{c} K_{us} \\ \hline K_{ms} \\ \hline K_{ss} \end{array}\right][S_{sm}]\{d_m\} + \left[\begin{array}{c} K_{us} \\ \hline K_{ms} \\ \hline K_{ss} \end{array}\right]\{\triangle_d\} = \left\{\begin{array}{c} F_u \\ \hline F_m \\ \hline F_s \end{array}\right\}$$

$$\Downarrow$$

$$\left[\begin{array}{c} K_{uu} \\ \hline K_{mu} \\ \hline K_{su} \end{array}\right]\{d_u\} + \left[\begin{array}{c} K_{um} + K_{us}S_{sm} \\ \hline K_{mm} + K_{ms}S_{sm} \\ \hline K_{sm} + K_{ss}S_{sm} \end{array}\right]\{d_m\} + \left[\begin{array}{c} K_{us} \\ \hline K_{ms} \\ \hline K_{ss} \end{array}\right]\{\triangle_d\} = \left\{\begin{array}{c} F_u \\ \hline F_m \\ \hline F_s \end{array}\right\}$$

The periodic boundary fluctuation condition requires that the sum of forces in the master and slave nodes to be zero:

$$\{F_m\} + [S_{ms}]\{F_s\} = 0$$

Elimination of slave degrees of freedom

The linear system of equation can be rewritten as:

$$\left[\frac{K_{uu}}{K_{mu}+S_{ms}K_{su}}\right]\{d_u\}+\left[\frac{K_{um}+K_{us}S_{sm}}{K_{mm}+K_{ms}S_{sm}+S_{ms}K_{sm}+S_{ms}K_{ss}S_{sm}}\right]\{d_m\}+$$

$$+\left[\frac{K_{us}}{K_{ms}+S_{ms}K_{ss}}\right]\{\triangle_d\}=\left\{\frac{F_u}{F_m+S_{ms}F_s}\right\}$$

$$\Downarrow$$

$$\left[\frac{K_{uu}}{K_{mu}+S_{ms}K_{su}}\middle|\frac{K_{um}+K_{us}S_{sm}}{K_{mm}+K_{ms}S_{sm}+S_{ms}K_{sm}+S_{ms}K_{ss}S_{sm}}\right]\left\{\frac{d_u}{d_m}\right\}=\left\{\frac{F_u-K_{us}\{\triangle_d\}}{(K_{ms}+S_{ms}K_{ss})\{\triangle_d\}}\right\}$$

$$\Downarrow$$

$$\mathbf{K}_r\cdot\mathbf{d}_r=\mathbf{F}_r$$

Solution of the MICROSCALE problem

Input data provided by the macroproblem.

Each gauss point provides a different input data.

Output result are the macro-stress and the material tangent stiffness tensor

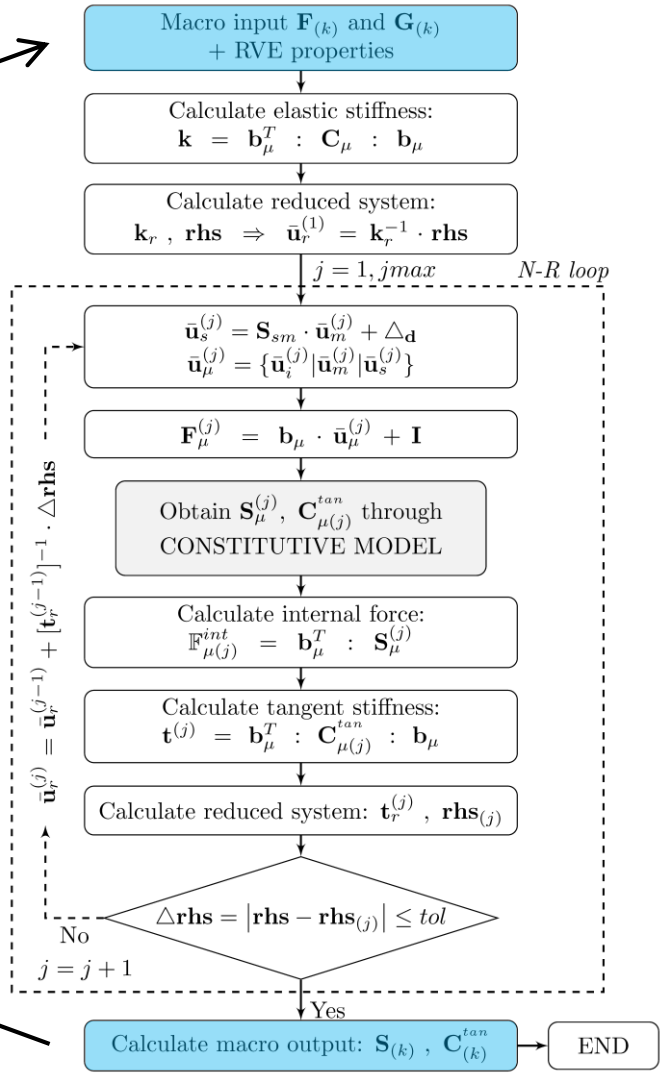

Macro stress and tangent constitutive tensor

The expression that provides the macro-stress tensor as been shown when describing the formulation behind the FOCH:

$$\mathbf{S}\left(\mathbf{X}_o, \mathbf{X}_\mu\right) = \frac{1}{V_\mu} \int_{\Omega_\mu} \mathbf{S}_\mu\left(\mathbf{X}_o, \mathbf{X}_\mu\right)\ dV$$

$$\mathbf{S}\left(\mathbf{X}_o, \mathbf{X}_\mu\right) = \bar{\mathbf{C}} : \mathbf{E}\left(\mathbf{X}_o\right) + \frac{1}{V_\mu} \int_{\Omega_\mu} \mathbf{C}_\mu : \mathbf{E}_\mu^w\left(\mathbf{X}_\mu\right)\ dV$$

$$\bar{\mathbf{C}} = \frac{1}{V_\mu} \int_{\Omega_\mu} \mathbf{C}_\mu\ dV$$

The stiffness matrix of the RVE material cannot be obtained from the average of the micro-stiffness matrices, as the effect of the fluctuations would not be considered.

Tangent constitutive tensor

The RVE constitutive tensor (elastic and tangent) is obtained with a numerical derivation by perturbations.

The relation between strains and stresses can be written, in matrix form:

$$\begin{bmatrix} \dot{\mathrm{S}}_1 \\ \vdots \\ \dot{\mathrm{S}}_n \end{bmatrix} = \begin{bmatrix} \mathrm{C}_{11}^{tan} & \cdots & \mathrm{C}_{1n}^{tan} \\ \vdots & \ddots & \vdots \\ \mathrm{C}_{n1}^{tan} & \cdots & \mathrm{C}_{nn}^{tan} \end{bmatrix} \begin{bmatrix} \dot{\mathrm{E}}_1 \\ \vdots \\ \dot{\mathrm{E}}_n \end{bmatrix}$$

The stress tensor can be also obtained as the sum of n partial stress tensors, which are defined as:

$$\dot{\mathbf{S}} \equiv \sum_{j=1}^{n} \delta^j \mathbf{S} = \sum_{j=1}^{n} \mathbf{C}_j^{tan} . \delta \mathrm{E}_j$$

with $$\mathbf{C}_j^{tan} = \begin{bmatrix} \mathrm{C}_{1j}^{tan} & \mathrm{C}_{2j}^{tan} & \cdots & \mathrm{C}_{nj}^{tan} \end{bmatrix}^T$$

Tangent constitutive tensor

The calculation of each one of these columns is obtained by defining a perturbed strain value in the different space directions:

$$\mathbf{C}_j^{tan} = \frac{{}^j\dot{\mathbf{S}}}{\dot{\mathbf{E}}_j} \equiv \frac{\delta^j \mathbf{S}}{\delta \mathbf{E}_j}$$

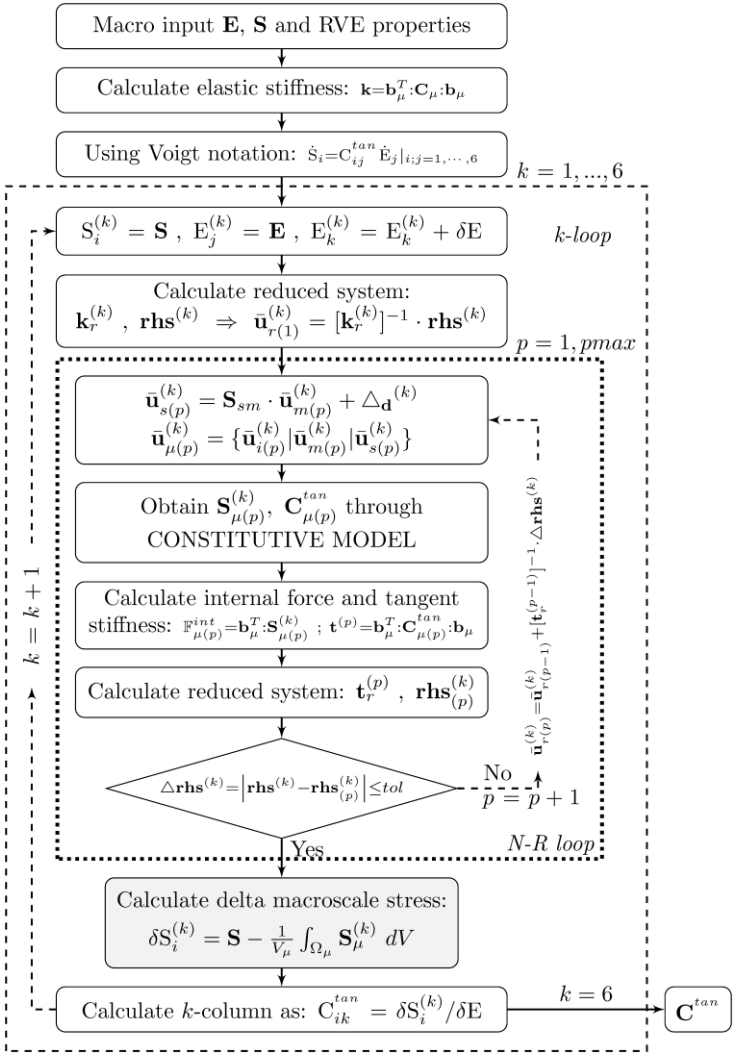

Summary

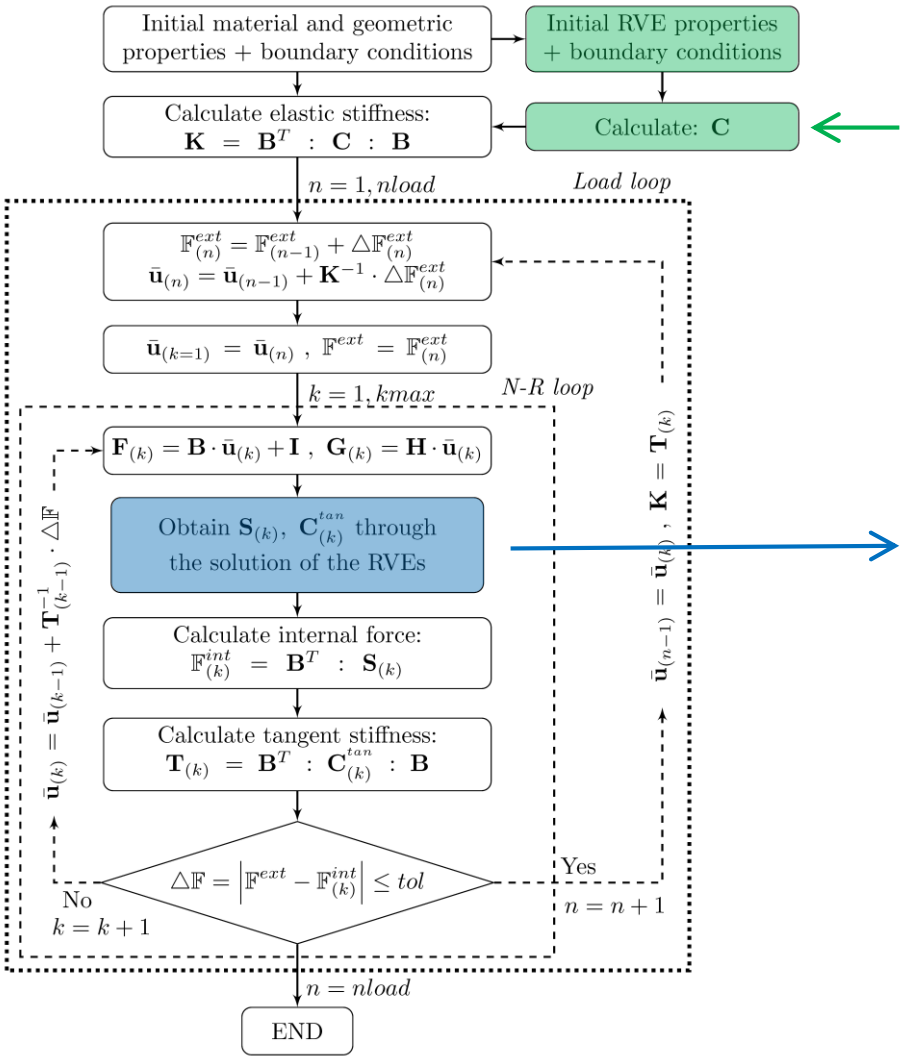

Applying six initial perturbations along the normal and shear directions of the RVE

In a LINEAR PROBLEM this step is not required. The stresses are obtained with the RVE stiffness matrix.

In a FE^2 problem, the RVE has to be solved at each load step in order to obtain the updated stresses.

The tangent constitutive tensor has to be recalculated if materials inside the RVE become non-linear.

The boundary conditions applied at the RVE are defined by the deformation gradient tensor.

NUMERICAL EXAMPLES

In the following section three different numerical examples will be described and studied.

1. **Quasi-isotropic material.**
2. **Long fiber composite.**

   These examples will be used to show the basic performance of a multiscale procedure in a linear regime.

3. **Laminated composite.**

   This example will be used to show the performance of the formulation if non-linear effects are considered. It also compares the results obtained with a multiscale procedure and other approaches such as a micro-model and a model using the serial/parallel mixing theory.

Quasi-homogeneous mat. – Problem description

Problem description

Simulation of a structure with a heterogeneous material composite. The macrostructure is a rectangle of 20x20 cm section and length 80 cm and the microstructure is a matrix with spherical inclusions.

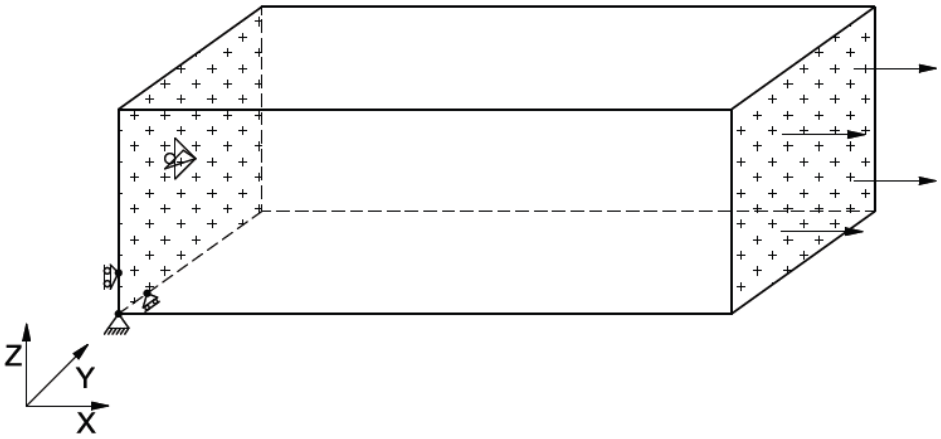

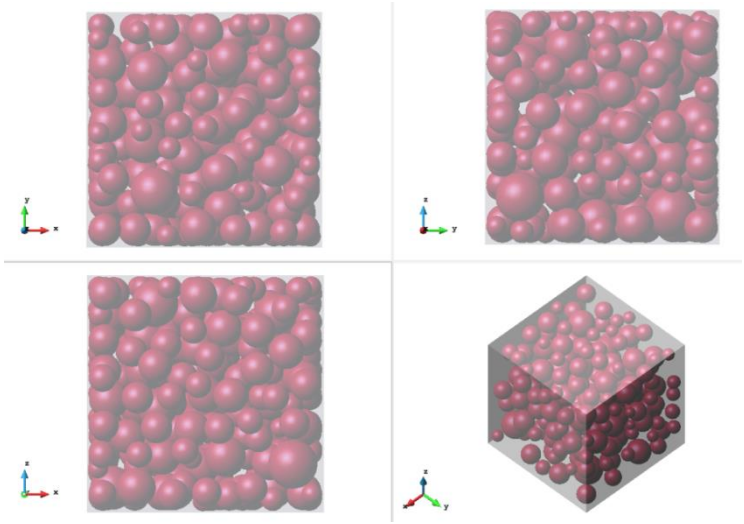

Macro Model

The macro FE mesh has 256 second order hexahedral element (20 nodes) and 1505 nodes.

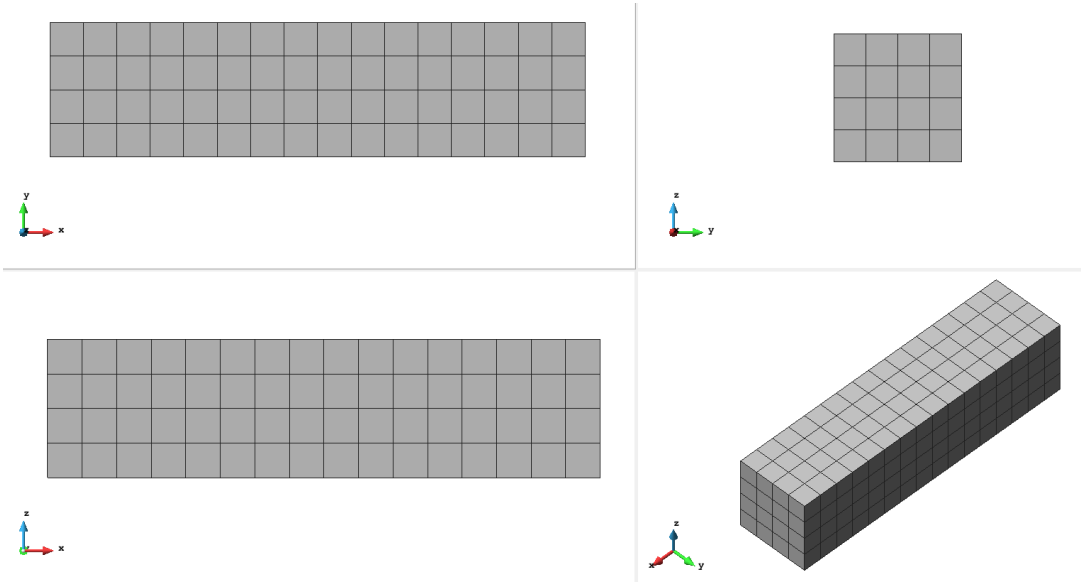

It is completely fixed in one end and it has an “x” displacement applied to the other end.

Micro Model

The micromodel is a cube with a length of 10 containing 252 spheres from d = 0,7 to d = 2,2. The spheres are randomly distributed.

The FE mesh has 87405 first order tetrahedral elements and 15946 nodes. The spheres represent 27% of the total volume.

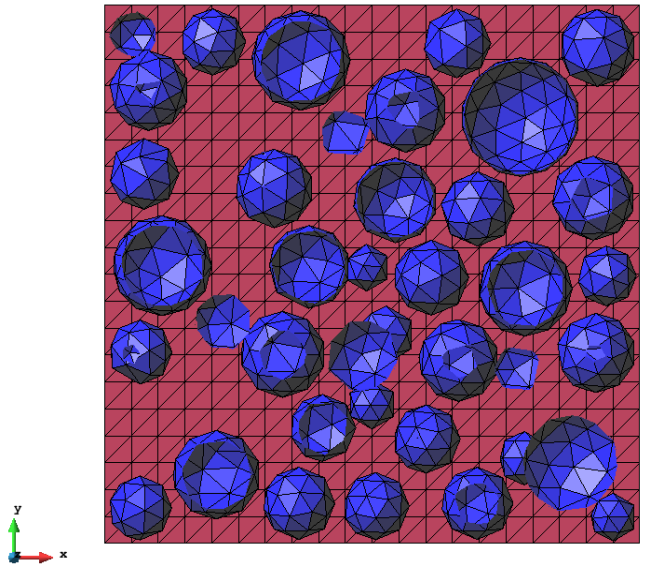

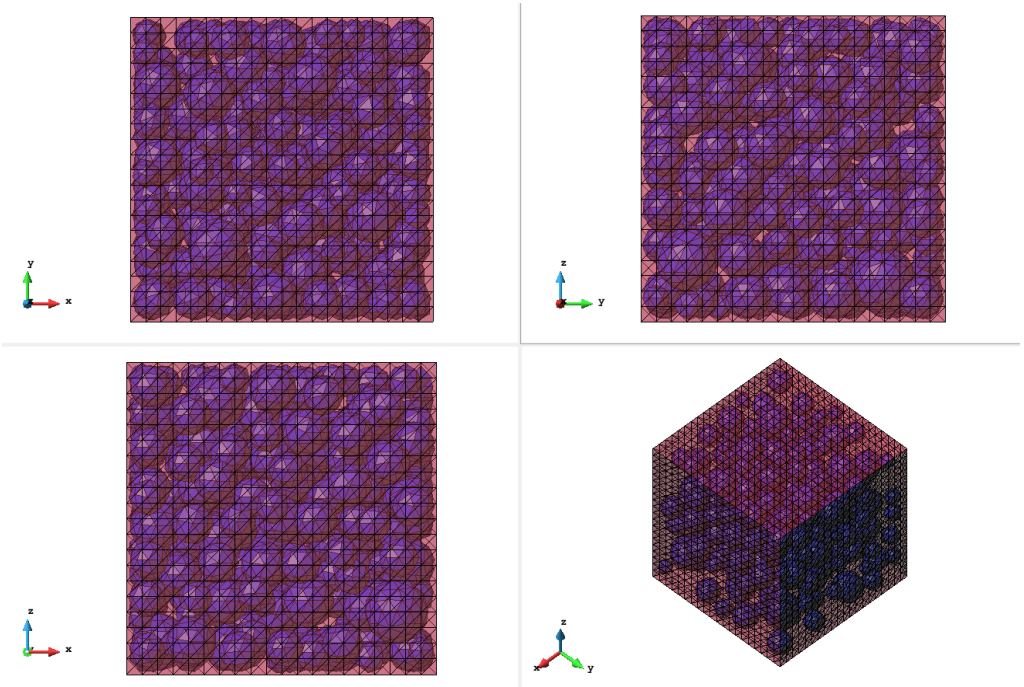

Materials and models considered

Two different isotropic materials have been considered in the simulation. Each one is defined with its Young and Poisson Modulus. The shear modulus is obtained from these two.

Material ID	E [GPa]	ν
1	3.5	0.2
2	210	0.3

These two materials have been combined to create four different RVE models:

Model	Matrix	Spheres
RVE 1	1	1
RVE 2	1	2
RVE 3	2	1
RVE 3	1	-

Stiffness matrix comparison

The multiscale procedures provides the stiffness matrix of the RVE considered. These are:

Model	Matrix	Spheres
RVE 1	1	1
RVE 2	1	2
RVE 3	2	1
RVE 3	1	-

RVE 1

3.89	0.97	0.97	0	0	0
0.97	3.89	0.97	0	0	0
0.97	0.97	3.89	0	0	0
0	0	0	1.46	0	0
0	0	0	0	1.46	0
0	0	0	0	0	1.46

RVE 2

8.17	1.66	1.65	0	-0.03	0
1.66	8.15	1.65	-0.02	0	0
1.65	1.65	8.07	0	-0.02	0
0	-0.02	0	3.15	0	-0.01
-0.03	0	-0.02	0	3.10	-0.01
0	0	0	-0.01	-0.01	3.12

RVE 3

170.21	64.99	64.80	-0.03	-0.13	0.04
64.99	170.10	64.87	-0.13	-0.04	-0.06
64.80	64.87	169.48	-0.01	-0.06	0.05
-0.03	-0.13	-0.01	52.00	0.03	-0.04
-0.13	-0.04	-0.06	0.03	51.81	0
0.04	-0.06	0.05	-0.04	0	51.89

RVE 4

2.42	0.57	0.57	0	-0.02	0.01
0.57	2.42	0.57	-0.02	0	-0.01
0.57	0.57	2.41	0	-0.01	0.01
0	-0.02	0	0.91	0.01	-0.01
-0.02	0	-0.01	0.01	0.91	0
0.01	-0.01	0.01	-0.01	0	0.91

Macro structural performance

DISPLACEMENT IN ALL RVEs

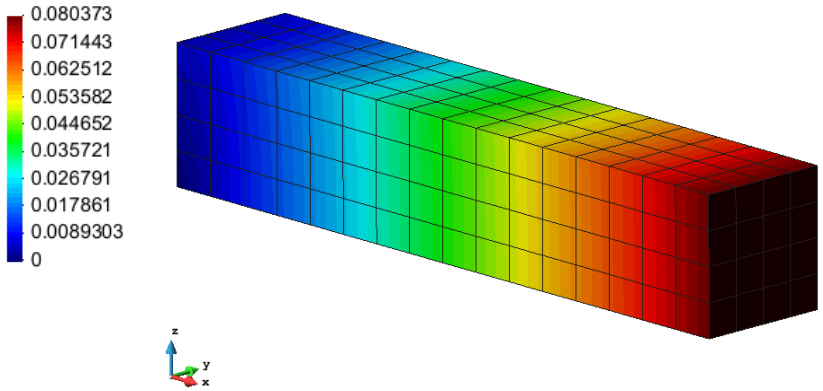

Model	Matrix	Spheres
RVE 1	1	1
RVE 2	1	2
RVE 3	2	1
RVE 3	1	-

All macro results are very similar, varying only the stress values due to the different stiffness provided by the RVE model

STRESS IN RVE 1

σ = 0.35GPa

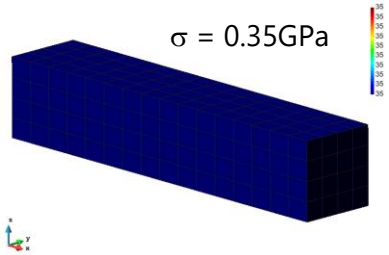

STRESS IN RVE 2

σ = 0.76GPa

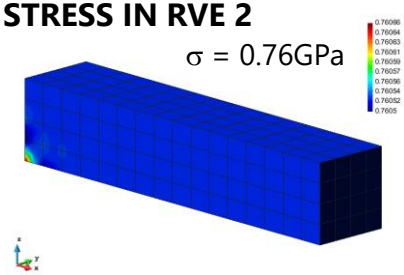

STRESS IN RVE 3

σ = 13GPa

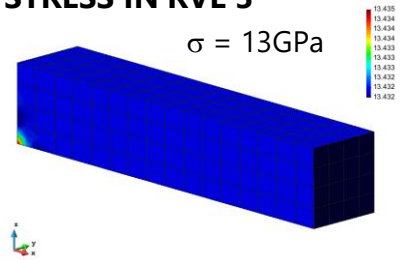

STRESS IN RVE 4

σ = 0.22GPa

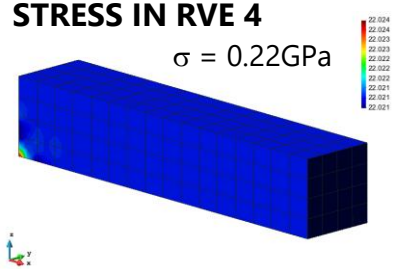

Micro structural performance – RVE 1

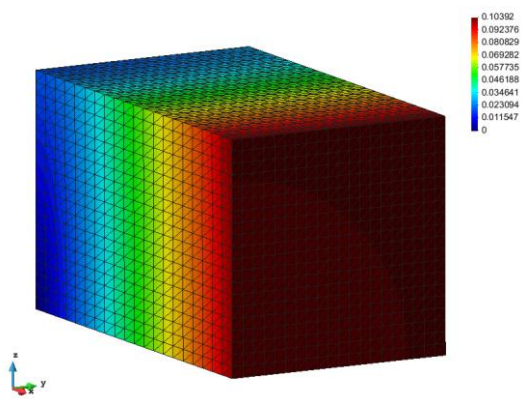

Displacements

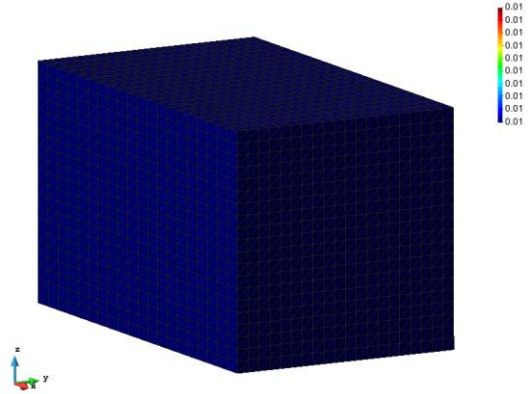

x strains

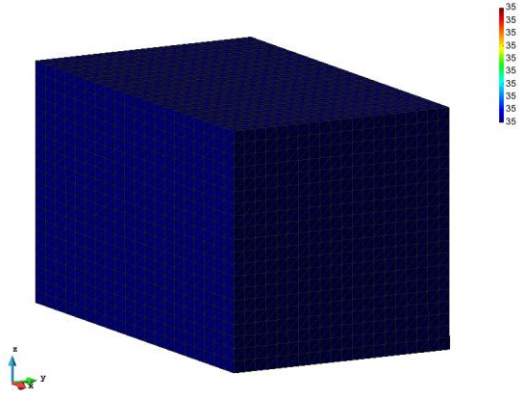

x stresses

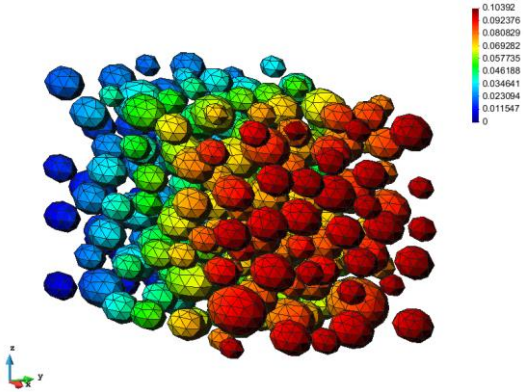

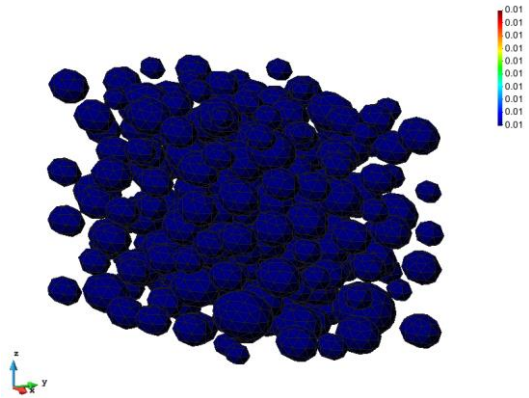

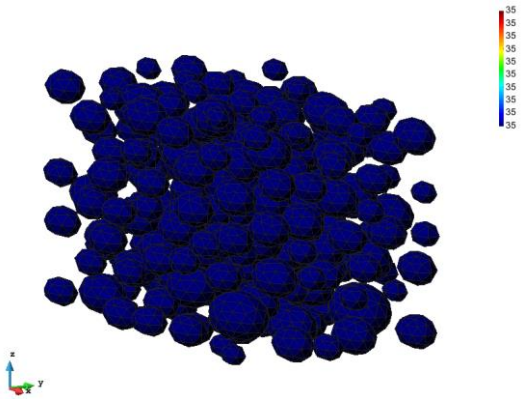

Micro structural performance – RVE 4

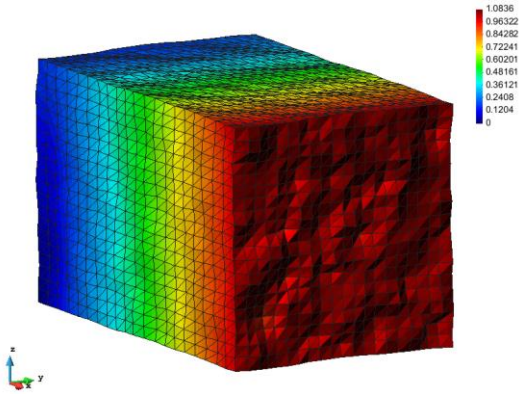

Displacements

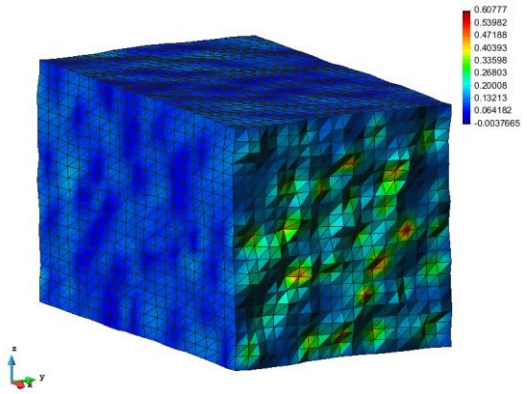

x strains

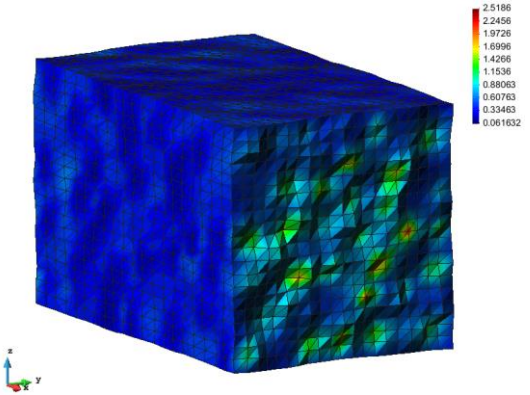

x stresses

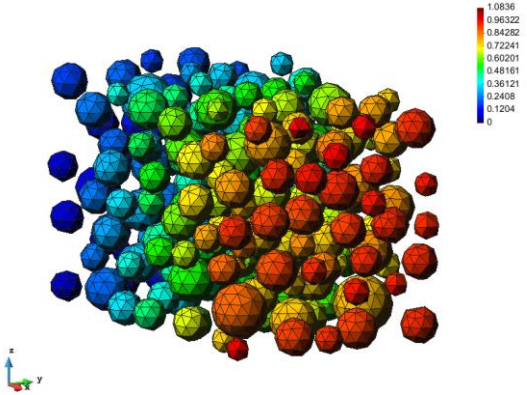

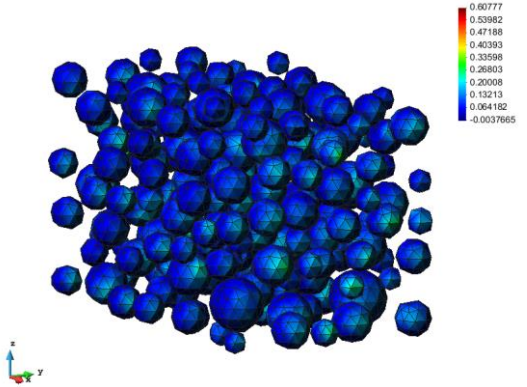

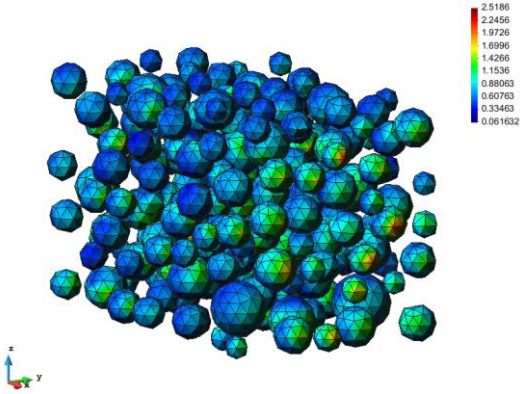

LONG FIBER COMPOSITE – Model

This example analyzes a clamped beam with a vertical displacement in its free edge. The micro-structure corresponds to a long fibre composite.

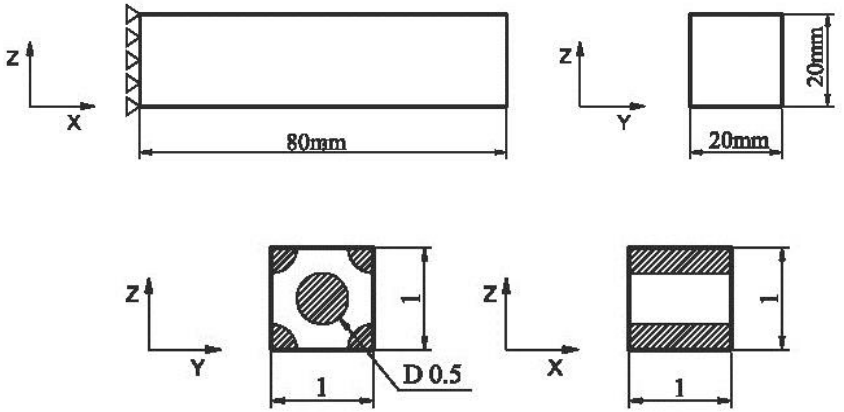

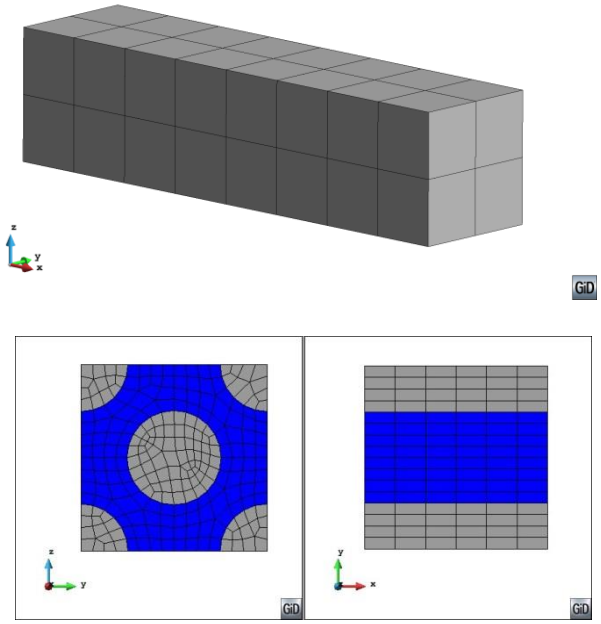

Material	E [GPa]	ν
Matrix	3.1	0.38
Fibre	24.1	0.20

LONG FIBER COMPOSITE – Results

Macro and micro results

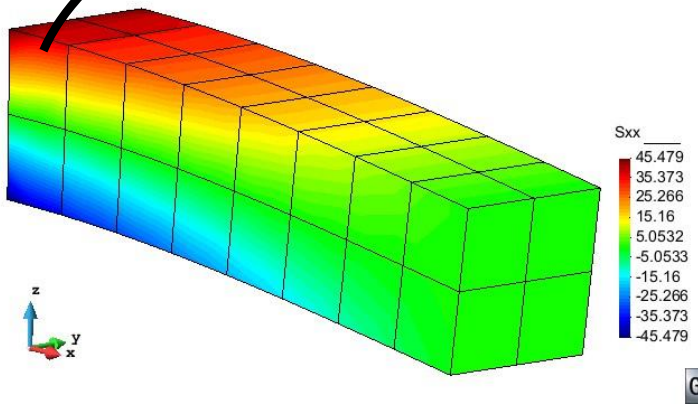

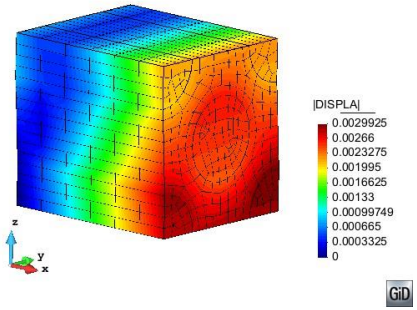

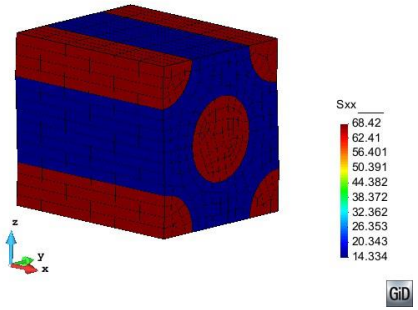

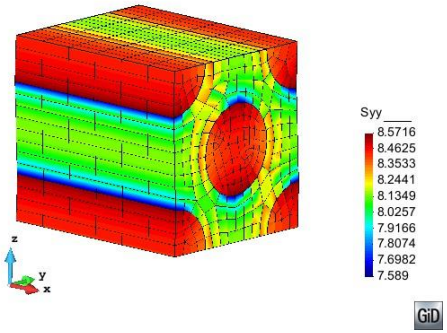

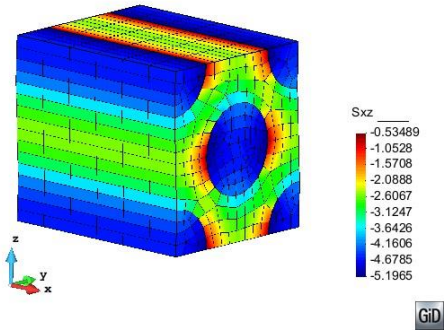

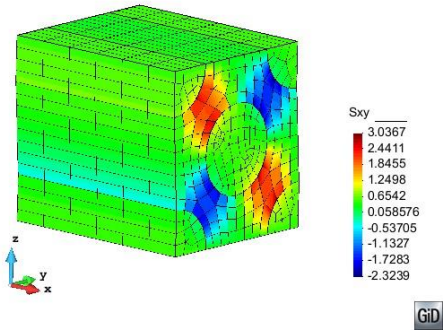

LAMINATED COMPOSITE – Problem description

In this example the results provided by different theories will be compared in order to assess the improvements provided by the multiscale method, as well as its possible drawbacks and costs.

The problem to study is a double clamped beam made of a laminated structure

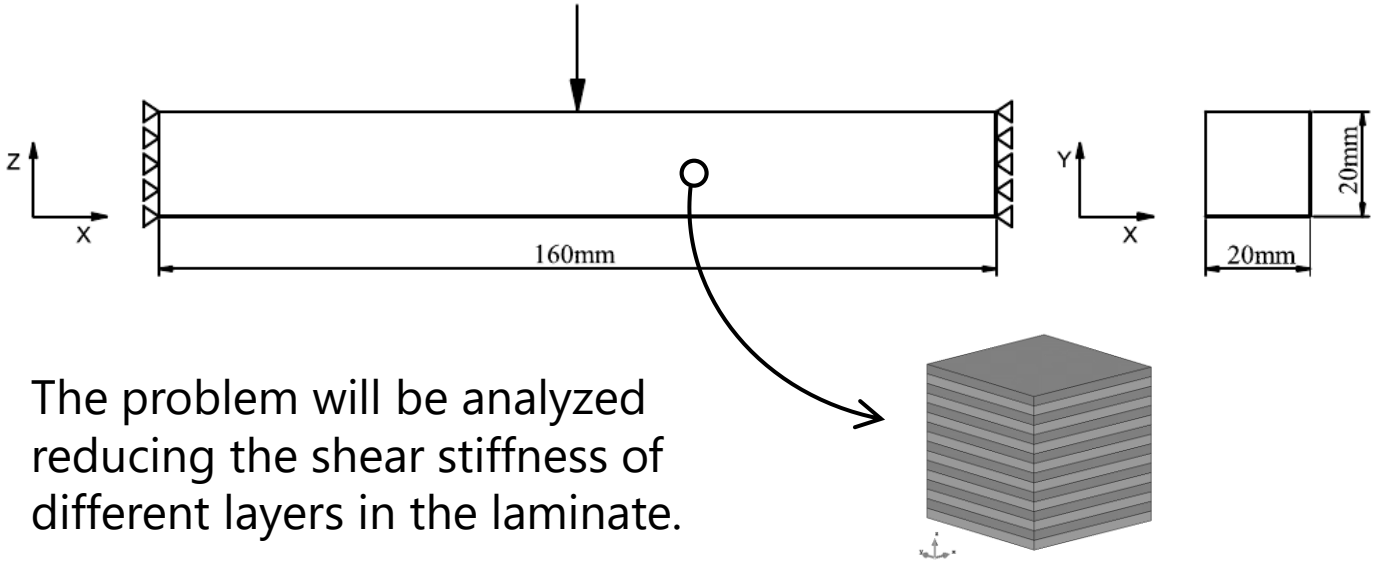

The problem will be analyzed reducing the shear stiffness of different layers in the laminate.

Formulations to be tested

The proposed problem will be analyzed with three different approaches:

1. **Micro model**. In which all layers are discretized.
2. **Serial-Parallel mixing theory.**
3. **First Order Computational Homogenization.**

The interest lays on comparing the **accuracy** of the solution provided by the different formulations, as well as the **computational cost** required to conduct the analysis.

Numerical models

Macro-model:

Only half of the beam has been simulated using the existing symmetry.

The macro FE mesh has 2048 first order hexahedral elements (8 nodes) and 2673 nodes.

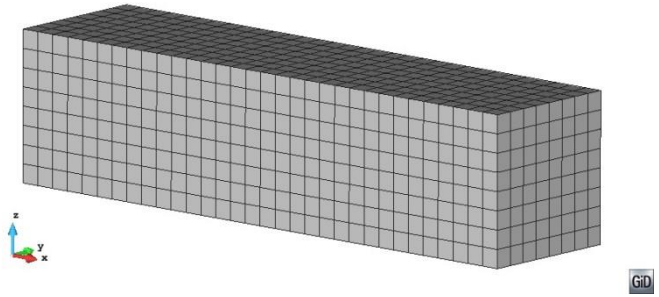

Micro-model:

Different RVE micro-models have been defined to account for different number of layers with reduced shear stiffness (damaged layers).

The material properties defined are those shown in the table.

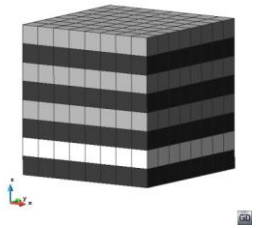

Material	Color	E [GPa]	G [GPa]	ν
Lamina 1	Black	210	80.76	0.38
Lamina 2	Grey	3.5	1.46	0.20
Lamina 3	White	3.5	0.146	0.20

Global damage case – Comparison FOCH vs SP RoM

The first analysis made has been over a laminate in which all layers have the same "damage" value. This comparison has made between the FOCH and the SP RoM approaches.

Completely undamaged results:

Different macro-model meshes have been analyzed to study the convergence of the problem.

Material	Color	E [GPa]	G [GPa]	ν
Lamina 1	Black	210	80.76	0.38
Lamina 2	Grey	3.5	1.46	0.20

Micro-model:

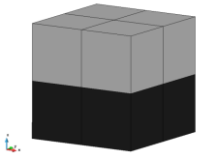

SP RoM model:

Parallel directions: *X* and *Y*

Serial directions: *Z* and *shear*

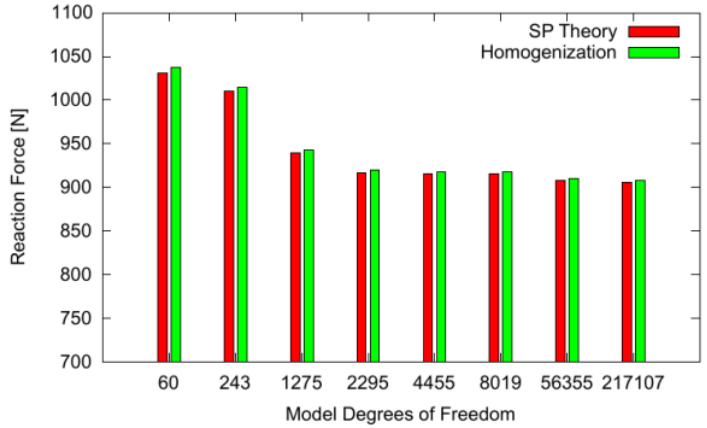

Global damage case – Comparison FOCH vs SP RoM

Damage evolution:

The weakest lamina has been analyzed with different values of shear stiffness in order to asses the effect of this value on the results.

Material	Color	E [GPa]	G [GPa]	ν
Lamina 1	Black	210	80.76	0.38
Lamina 2	Grey	3.5	varing	0.20

Model	0%	12.5%	25%	50%	100%
G [GPa]	1.46	1.295	1.131	0.803	0.146

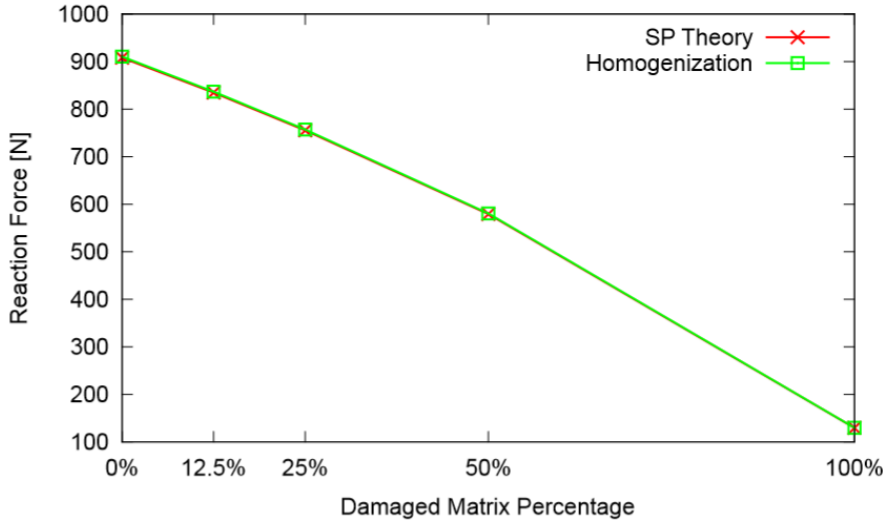

As expected, results are identical for both theories

Local damage case – All approaches comparison

In this case, the performance of the structure is analyzed when different proportions of layers have a reduced stiffness.

These analyses is made with all three approaches: micro-models, Serial/Parallel RoM and FOCH.

Cases considered:

Five different cases are considered: 0, 12.5, 25, 50 and 100%

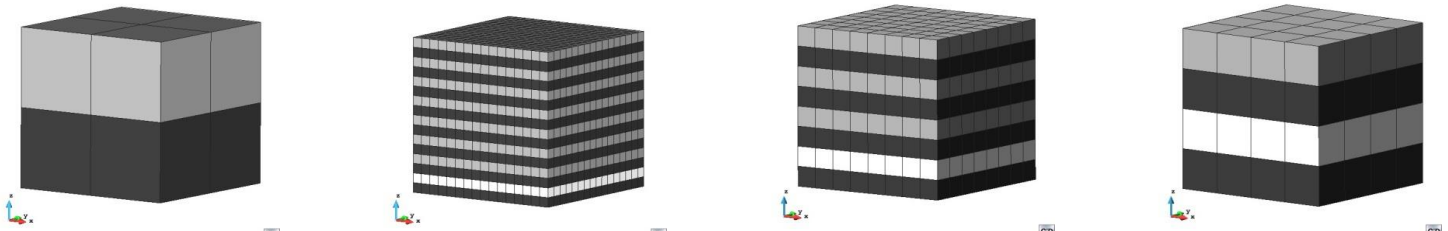

0% 12,5% 25% 50%

Local damage case – All approaches comparison

Results obtained:

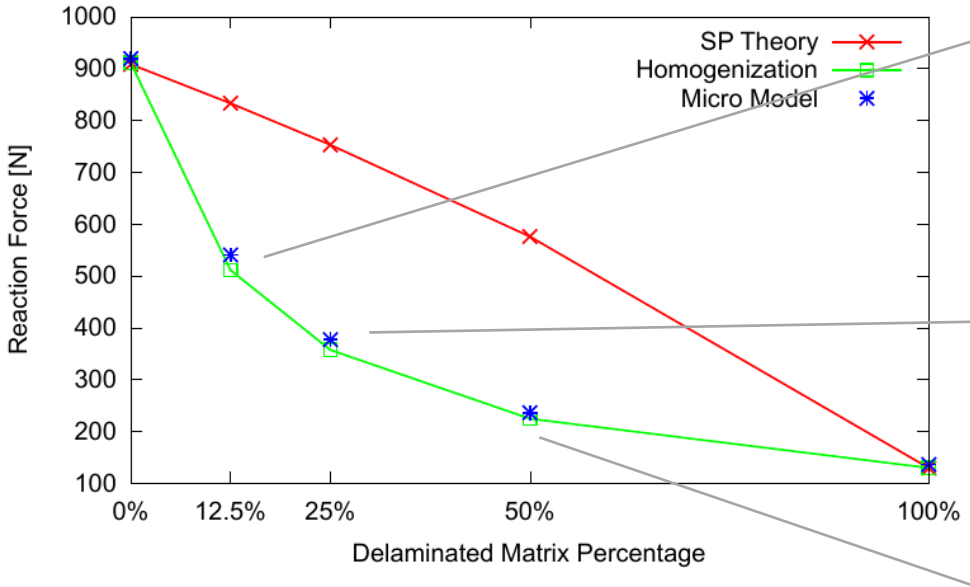

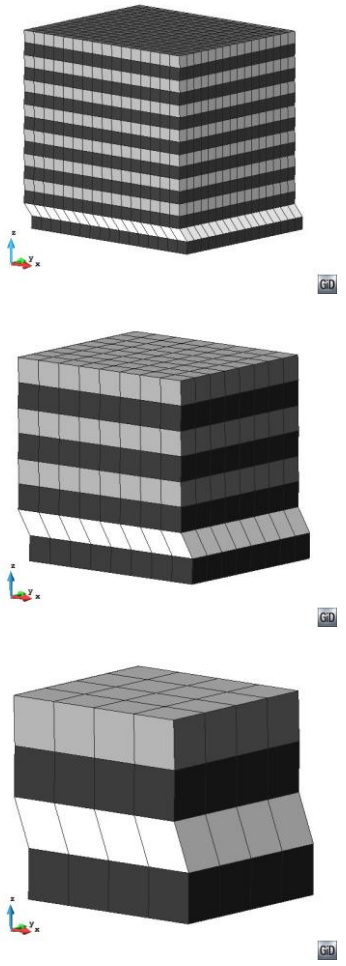

The serial parallel mixing theory, as it assumes a parallel behavior of the different layers of the composite, cannot capture the abrupt variation of stiffness produced by damage in one layer.

Local damage case – All approaches comparison

However, if a global damage is applied to the RVEs of some macro-model elements, the results provided by both theories are very similar

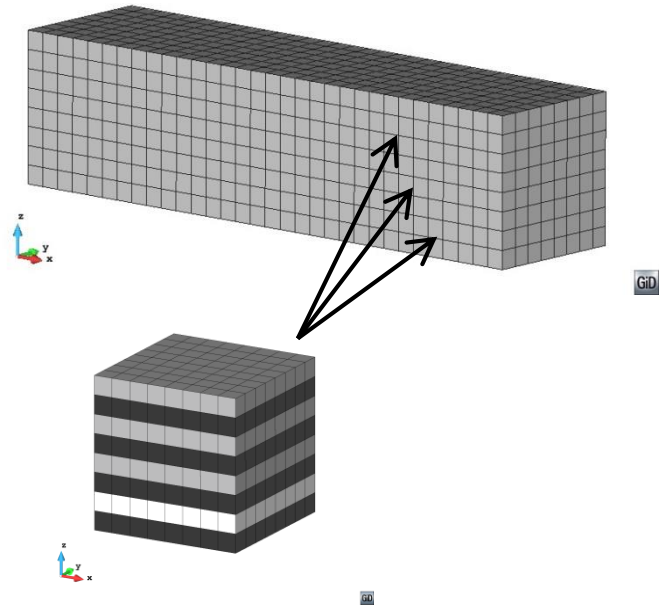

Approach	Reaction
FOCH	357.4 N
SP RoM	752.8 N

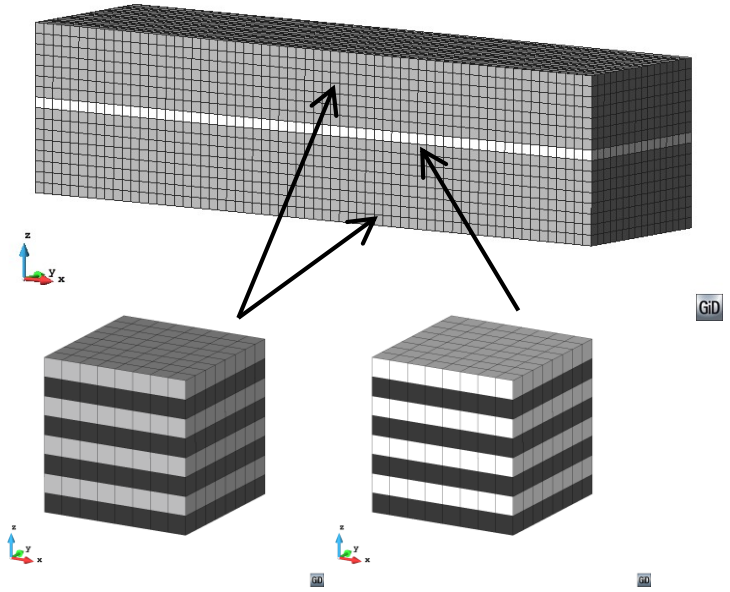

Approach	Reaction
FOCH	666.4 N
SP RoM	663.9 N

Computational cost – Time & Memory

In the following table is shown the computational cost required to perform the analysis of 50% local damage, by the different approaches considered:

Item	Micro-model	FE^2	Linear FOCH	SP RoM
Real Time (Min:Seg)	6:46	2:27	0:01	0:02
CPU Time (Min:Seg)	8:44	9:31	0:03	0:17
Memory (Mbytes)	2690,00	7,45	7,45	15,82
Reaction Force (N)	236,1	224,7	224,7	576,7

- Micro-model: Excessive CPU time and memory requirements
- FE^2 model: Excessive time with a substantial reduction of CPU
- Linear FOCH & SP RoM: The most efficient

3. Enhanced First Order Computational Homogenization

Enhanced first order computational homogen.

3. Enhanced First Order Computational Homogenization (EFOCH)
    - 3.1. Introduction
    - 3.2. Formulation
    - 3.3. Numerical example – Comparison FOCH vs. EFOCH
    - 3.4. Discussion

Need to account for 2nd order effects

2nd order elements provide a better approximation of the displacement, strain and stress fields:

Shape Functions:

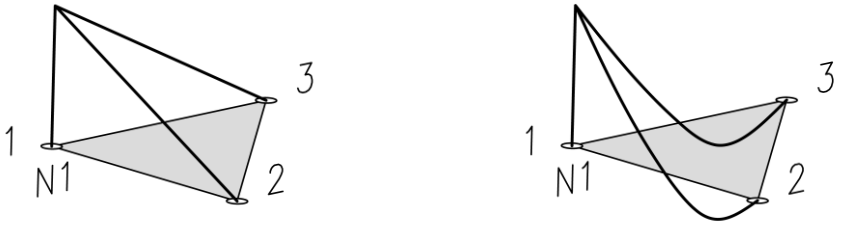

Beam displacements:

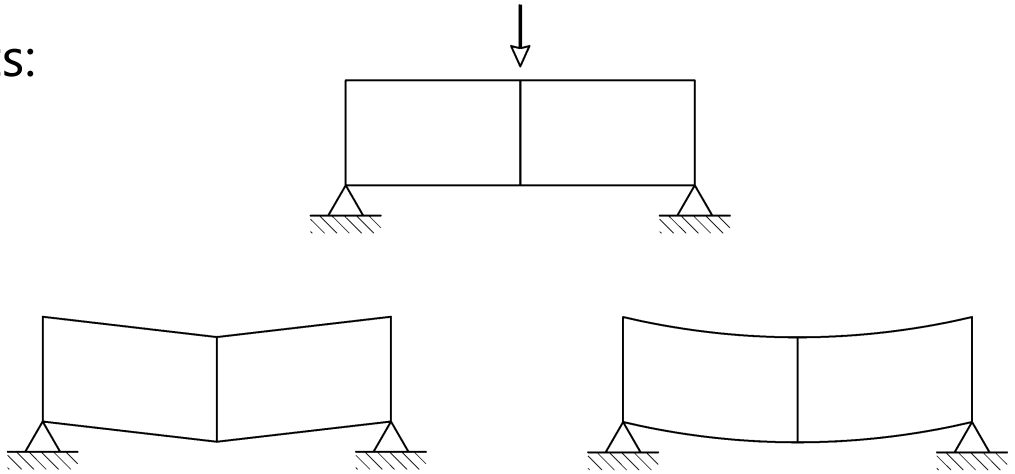

Need to account for 2nd order effects

If second order elements are used, the displacement field in the macrostructure uses the gradient of the deformation gradient

$$\triangle \mathbf{x} = \mathbf{F}\left(\mathbf{X}_o\right) \cdot \triangle \mathbf{X} + \frac{1}{2}\mathbf{G}\left(\mathbf{X}_o\right) : \triangle \mathbf{X} \otimes \triangle \mathbf{X} + \mathcal{O}\left(\triangle \mathbf{X}_o^3\right)$$

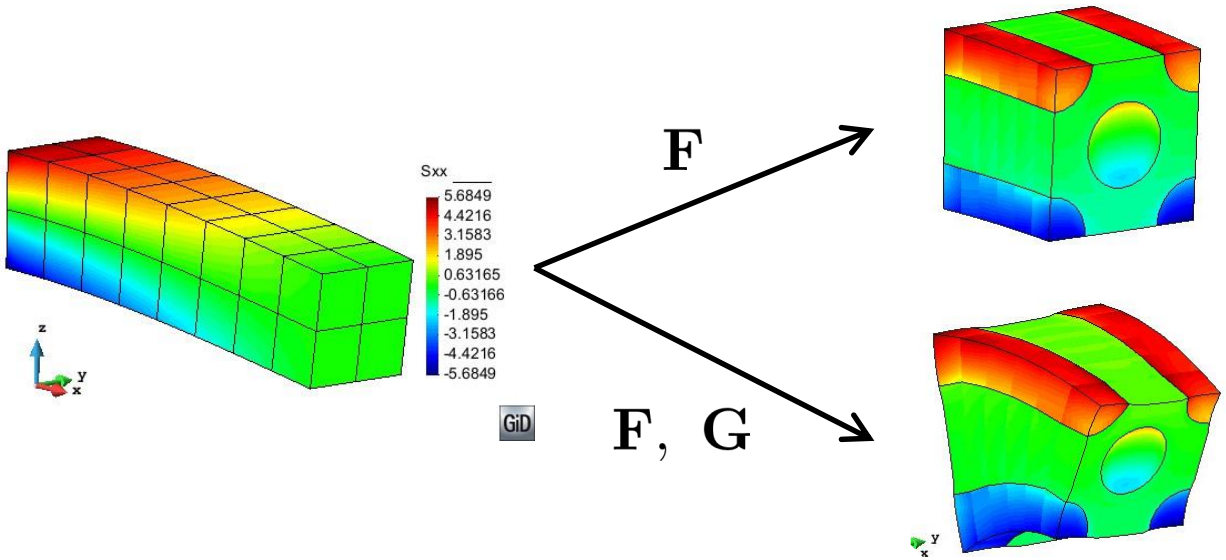

Micro Displacement

The Enhanced First Order Computational Homogenization (EFOCH) uses the first two terms of the macro displacement field

$$\mathbf{x}_\mu\left(\mathbf{X}_o,\mathbf{X}_\mu\right)\cong\mathbf{x}_\mu^o+\mathbf{F}\left(\mathbf{X}_o\right)\cdot\triangle\mathbf{X}_\mu+\frac{1}{2}\mathbf{G}\left(\mathbf{X}_o\right):\triangle\mathbf{X}_\mu\otimes\triangle\mathbf{X}_\mu+\mathbf{w}\left(\mathbf{X}_\mu\right)$$

$$\triangle\mathbf{x}=\mathbf{F}\left(\mathbf{X}_o\right)\cdot\triangle\mathbf{X}+\frac{1}{2}\mathbf{G}\left(\mathbf{X}_o\right):\triangle\mathbf{X}\otimes\triangle\mathbf{X}+\mathcal{O}\left(\triangle\mathbf{X}_o^3\right)$$

Defining the origin of coordinates at the center of the RVE, the displacements can be written as:

$$\mathbf{u}_\mu\left(\mathbf{X}_o,\mathbf{X}_\mu\right)\cong\left[\mathbf{F}\left(\mathbf{X}_o\right)-\mathbf{I}\right]\cdot\mathbf{X}_\mu+\frac{1}{2}\mathbf{G}\left(\mathbf{X}_o\right):\mathbf{X}_\mu\otimes\mathbf{X}_\mu+\mathbf{w}\left(\mathbf{X}_\mu\right)$$

Boundary Conditions in the RVE

The second order terms are also present in the expression of the microstructural deformation gradient:

$$\mathbf{F}_\mu\left(\mathbf{X}_o,\mathbf{X}_\mu\right)=\nabla\mathbf{x}_\mu\left(\mathbf{X}_o,\mathbf{X}_\mu\right)\cong\mathbf{F}\left(\mathbf{X}_o\right)+\mathbf{G}\left(\mathbf{X}_o\right)\cdot\mathbf{X}_\mu+\nabla\mathbf{w}\left(\mathbf{X}_\mu\right)$$

And the volume average theorem over the deformation gradient becomes:

$$\frac{1}{V_\mu}\int_{\Omega_\mu}\mathbf{F}_\mu\left(\mathbf{X}_o,\mathbf{X}_\mu\right)\;dV=\mathbf{F}\left(\mathbf{X}_o\right)+\mathbf{G}\left(\mathbf{X}_o\right)\cdot\frac{1}{V_\mu}\int_{\Omega_\mu}\mathbf{X}_\mu\;dV+\frac{1}{V_\mu}\int_{\Omega_\mu}\nabla\mathbf{w}\left(\mathbf{X}_\mu\right)\;dV$$

Having defined the origin of the RVE in its center, the first moment of volume is zero:

$$\int_{\Omega_\mu}\mathbf{X}_\mu\;dV=0$$

And the BC defined for the FOCH is recovered: $$\int_{\partial\Omega_\mu}\mathbf{w}\left(\mathbf{X}_\mu\right)\otimes\mathbf{N}\;dA=\mathbf{0}$$

Boundary Conditions in the RVE

However, in the EFOCH it is necessary to apply the average theorem also to the gradient of the deformation gradient:

$$\mathbf{G}\left(\mathbf{X}_o\right) = \frac{1}{V_\mu}\int_{\Omega_\mu} \mathbf{G}_\mu\left(\mathbf{X}_o, \mathbf{X}_\mu\right)\ dV$$

Defining the gradient of the deformation gradient in the microstructure as:

$$\mathbf{G}_\mu\left(\mathbf{X}_o, \mathbf{X}_\mu\right) = \nabla\left(\nabla \mathbf{x}_\mu\left(\mathbf{X}_o, \mathbf{X}_\mu\right)\right) \cong \mathbf{G}\left(\mathbf{X}_o\right) + \nabla\left(\nabla \mathbf{w}\left(\mathbf{X}_\mu\right)\right)$$

The new boundary condition that has to be applied to the RVE becomes:

$$\int_{\partial\Omega_\mu} \nabla \mathbf{w}\left(\mathbf{X}_\mu\right) \otimes \mathbf{N}\ dA = \mathbf{0}$$

Boundary Conditions in the RVE

Considering an hexahedral RVE, these last conditions can be rewritten as:

$$\left(\int_{\mathbf{N}_X^+} \nabla \mathbf{w}\ dA_{yz} - \int_{\mathbf{N}_X^-} \nabla \mathbf{w}\ dA_{yz}\right) \otimes \mathbf{N}_X^+$$
$$+ \left(\int_{\mathbf{N}_Y^+} \nabla \mathbf{w}\ dA_{xz} - \int_{\mathbf{N}_Y^-} \nabla \mathbf{w}\ dA_{xz}\right) \otimes \mathbf{N}_Y^+$$
$$+ \left(\int_{\mathbf{N}_Z^+} \nabla \mathbf{w}\ dA_{xy} - \int_{\mathbf{N}_Z^-} \nabla \mathbf{w}\ dA_{xy}\right) \otimes \mathbf{N}_Z^+ = \mathbf{0}$$

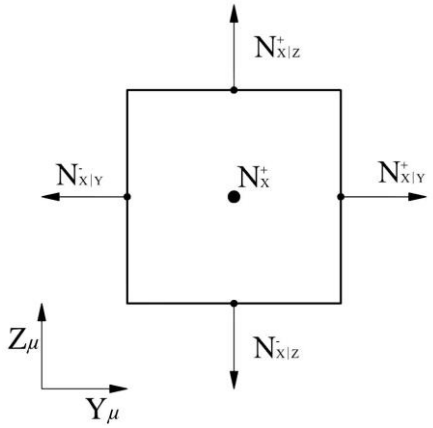

And, a set of fluctuations that satisfy this last expression is:

$$\int_{\mathbf{N}_X^+} \nabla_X \mathbf{w}\ dA_{yz} = \int_{\mathbf{N}_X^-} \nabla_X \mathbf{w}\ dA_{yz},$$
$$\int_{\mathbf{N}_Y^+} \nabla_Y \mathbf{w}\ dA_{xz} = \int_{\mathbf{N}_Y^-} \nabla_Y \mathbf{w}\ dA_{xz},$$
$$\int_{\mathbf{N}_Z^+} \nabla_Z \mathbf{w}\ dA_{xy} = \int_{\mathbf{N}_Z^-} \nabla_Z \mathbf{w}\ dA_{xy}$$

Micro strain tensor

The expression that defines the microscopic strain tensor is:

$$\mathbf{E}_\mu\left(\mathbf{X}_o,\mathbf{X}_\mu\right)=\mathbf{E}\left(\mathbf{X}_o\right)+\mathbf{E}_\mu^G\left(\mathbf{X}_o,\mathbf{X}_\mu\right)+\mathbf{E}_\mu^w\left(\mathbf{X}_\mu\right)$$

with,

$$\mathbf{E}_\mu^w=\frac{1}{2}\left(\nabla\mathbf{w}+\left(\nabla\mathbf{w}\right)^T\right)=\nabla^s\mathbf{w}$$

$$\mathbf{E}_\mu^G=\frac{1}{2}\left(\mathbf{G}\cdot\mathbf{X}_\mu+\left(\mathbf{G}\cdot\mathbf{X}_\mu\right)^T\right)$$

Now, the microscopic strain depends on the size of the RVE!

Hill-Mandel principle and RVE Equilibrium

The Hill-Mandel energy condition states that the virtual work of the point $\mathbf{X_0}$ must be equal to the volume average of the virtual work in the RVE for any kinematically admissible displacement field.

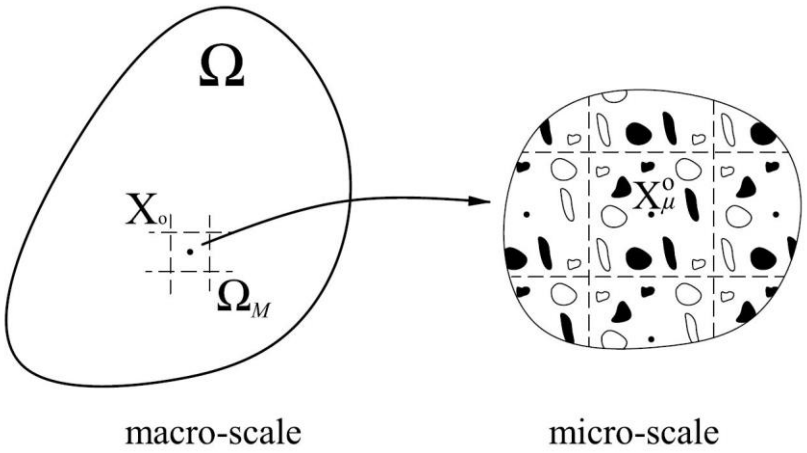

When using a second order theory to describe the displacement field in the macro model, it is assumed that there is a virtual work of the point corresponds to an average of a macro-volume Ω_M around the point. Therefore,

$$\frac{1}{V_M}\int_{\Omega_M} \mathbf{S} : \delta\mathbf{E}\; dV = \frac{1}{V_\mu}\int_{\Omega_\mu} \mathbf{S}_\mu : \delta\mathbf{E}_\mu\; dV$$

Hill-Mandel principle and RVE Equilibrium

Operating over the last expression and defining the homogenized stress tensor as:

$$\hat{\mathbf{S}} \equiv \frac{1}{V_M} \int_{\Omega_M} \mathbf{S} \; dV \equiv \frac{1}{V_\mu} \int_{\Omega_\mu} \mathbf{S}_\mu \; dV$$

And the homogenized second order stress tensor as:

$$\hat{\mathbf{Q}} \equiv \frac{1}{V_M} \int_{\Omega_M} \mathbf{S} \otimes \triangle \mathbf{X} \; dV \equiv \frac{1}{V_\mu} \int_{\Omega_\mu} \mathbf{S}_\mu \otimes \mathbf{X}_\mu \; dV$$

The final variational equilibrium equation becomes:

$$\int_{\Omega_\mu} \mathbf{S}_\mu : \nabla^s \delta \mathbf{w} \; dV = 0$$

Which is the same that was obtained for the FOCH

Macroscopic and microscopic stress tensor

Microscopic Stress Tensor:

The microscopic stress tensor is calculated as:

$$\mathbf{S}_\mu = \mathbf{C}_\mu : \mathbf{E}\left(\mathbf{X}_o\right) + \mathbf{C}_\mu : \mathbf{E}_\mu^G\left(\mathbf{X}_o, \mathbf{X}_\mu\right) + \mathbf{C}_\mu : \mathbf{E}_\mu^w\left(\mathbf{X}_\mu\right),$$

It has to be noted that now, the stresses on the different elements of the RVE depends on the position of these elements in the RVE!

Macroscopic Stress Tensor:

The macroscopic stress tensor is obtained using the expression:

$$\hat{\mathbf{S}} \equiv \frac{1}{V_M}\int_{\Omega_M} \mathbf{S}\; dV \equiv \frac{1}{V_\mu}\int_{\Omega_\mu} \mathbf{S}_\mu\; dV$$

Macroscopic and microscopic stress tensor

Which leads to:

$$\hat{\mathbf{S}} = \bar{\mathbf{C}} : \mathbf{E}(\mathbf{X}_o) + \bar{\mathbf{B}} : \mathbf{G}(\mathbf{X}_o) + \frac{1}{V_\mu}\int_{\Omega_\mu} \mathbf{C}_\mu : \mathbf{E}^w_\mu(\mathbf{X}_\mu)\ dV \qquad \bar{\mathbf{B}} \equiv \frac{1}{V_\mu}\int_{\Omega_\mu} \mathbf{C}_\mu \otimes \mathbf{X}_\mu\, dV$$

$\bar{\mathbf{B}}$ is equivalent to the bending-extension coupling matrix in shells and beam elements. In order to use it, it is necessary to have these sort of elements.

To simplify this formulation in solid elements, it is necessary to have a RVE with symmetry in the material distribution around its center.

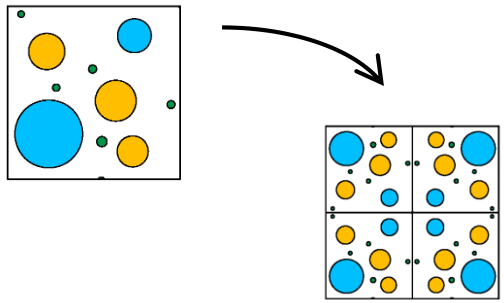

With this RVE, $\bar{\mathbf{B}} = \mathbf{0}$, and therefore:

$$\mathbf{S}(\mathbf{X}_o, \mathbf{X}_\mu) = \bar{\mathbf{C}} : \mathbf{E}(\mathbf{X}_o) + \frac{1}{V_\mu}\int_{\Omega_\mu} \mathbf{C}_\mu : \mathbf{E}^w_\mu(\mathbf{X}_\mu)\ dV$$

Numerical Example – Cantilever Beam

- 3. Numerical example

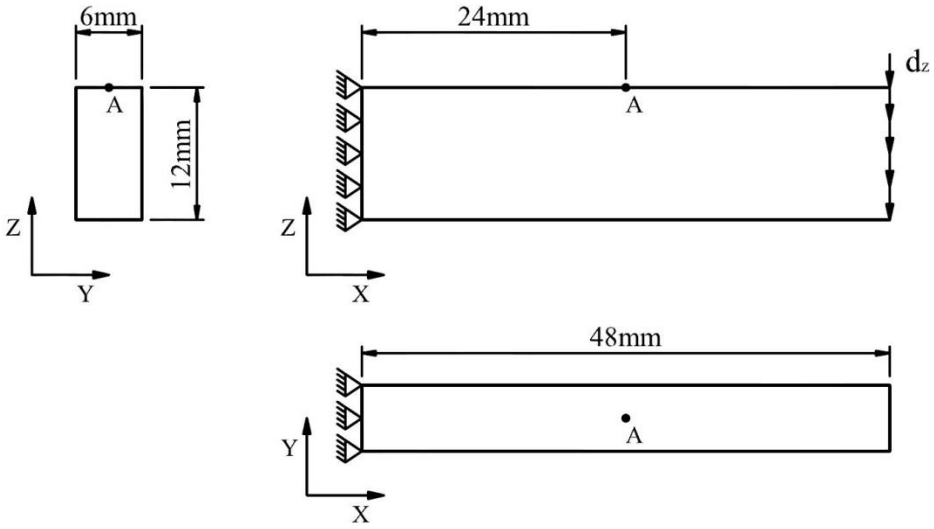

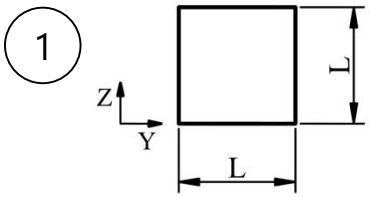

Properties	E (GPa)
Homg mat.	26.56

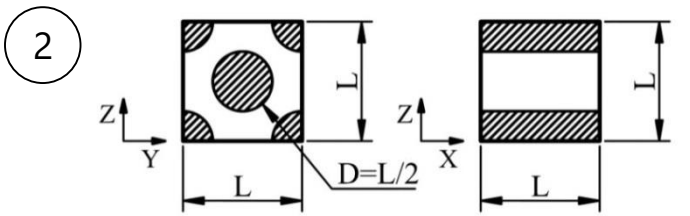

Properties	E (GPa)	v
Matrix	4,52	0,36
Long. Fiber (40%)	235	0,21

Model	Elements	Theory
LE&FO	Linear	First-order
QE&FO	Quadratic	First-order
QE&EFO	Quadratic	Enhanced-first-order

Mesh	Elements	L (mm)
Macro1	8x1x2	1,3525
Macro2	16x2x4	0,6762
Macro3	32x4x8	0,3381
Macro4	64x8x16	0,1691

Cantilever beam – Homogeneous material

Microstructure Results

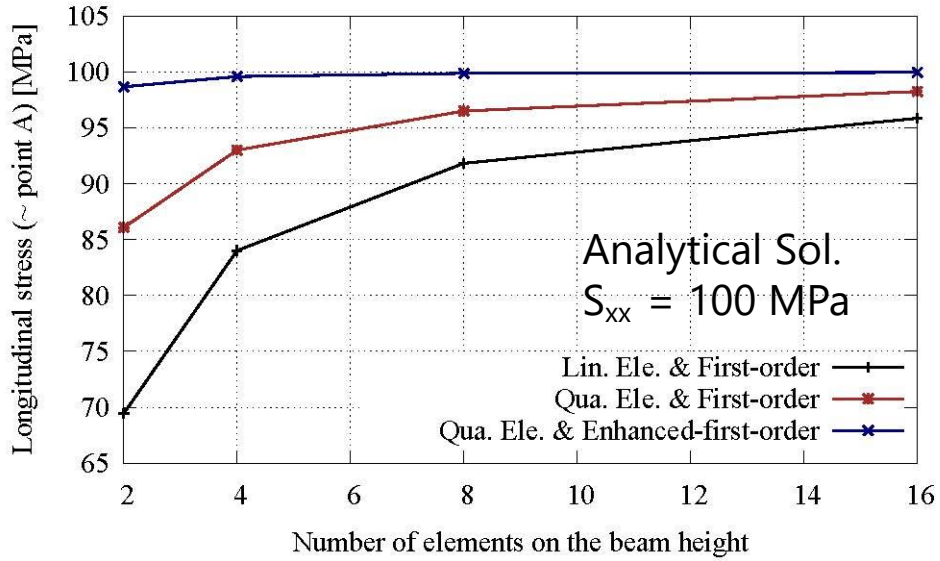

Sxx (MPa)	LE&FO	%	QE&FO	%	QE&EFO	%
Macro1	69,43	30,57	86,08	13,92	98,66	1,34
Macro2	84,02	15,98	93,00	7,00	99,59	0,41
Macro3	91,82	8,18	96,50	3,50	99,87	0,14
Macro4	95,86	4,14	98,25	1,75	99,96	0,04

LE&FO

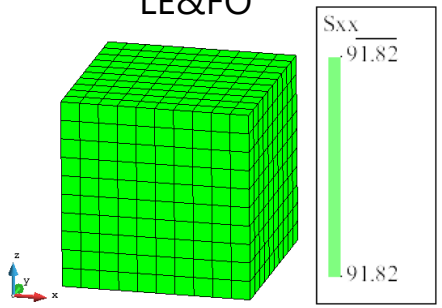

QE&FO

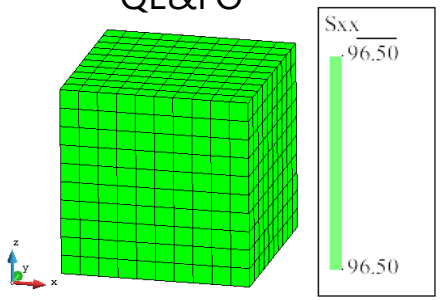

QE&EFO

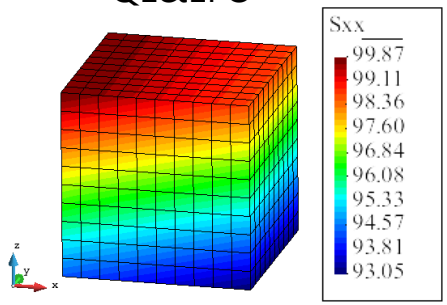

Cantilever beam – Homogeneous material

Macrostructure Results

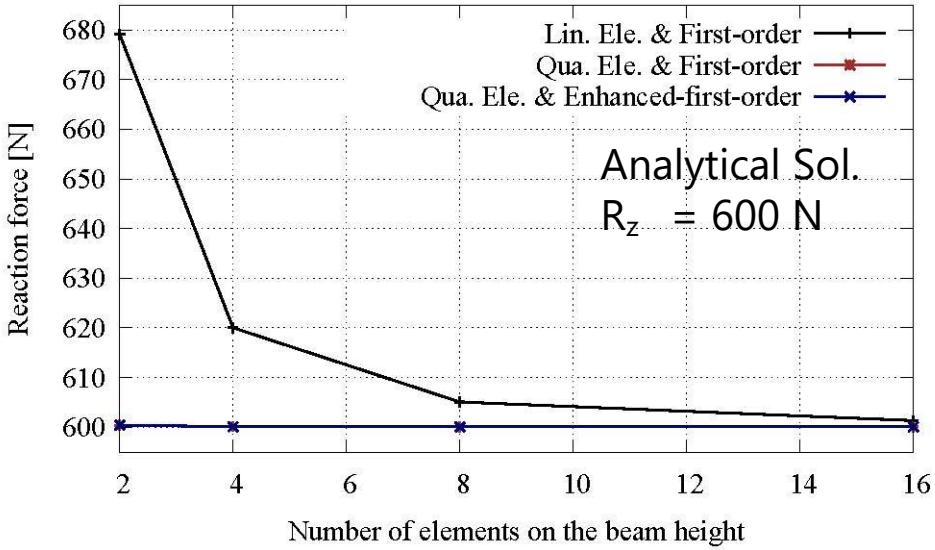

Rz (N)	LE&FO	%	QE&FO	%	QE&EFO	%
Macro1	679,09	13,18	600,43	0,07	600,43	0,07
Macro2	620,03	3,34	600,12	0,02	600,12	0,02
Macro3	605,09	0,85	600,09	0,01	600,09	0,01
Macro4	601,34	0,22	600,08	0,01	600,08	0,01

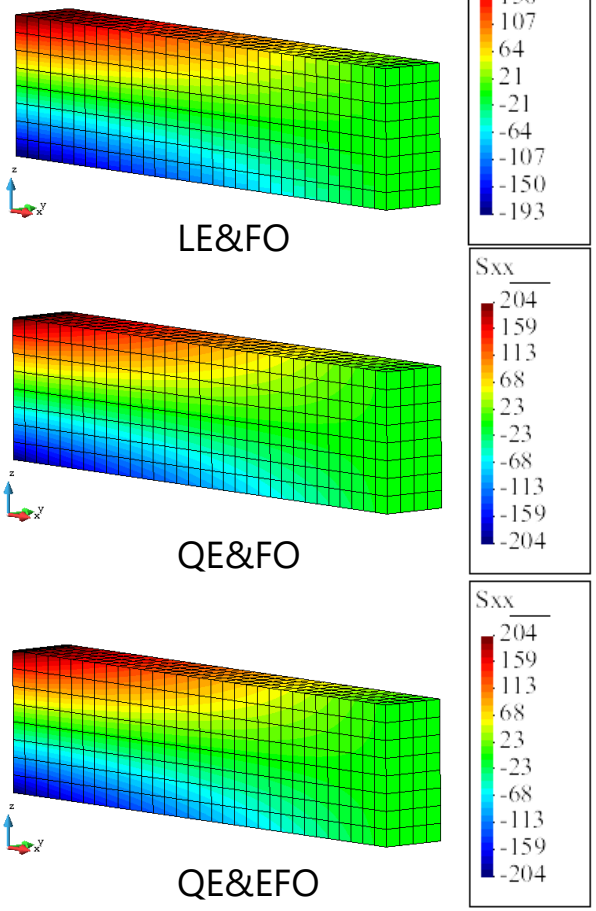

Cantilever meam – Composite material

Microstructure Results

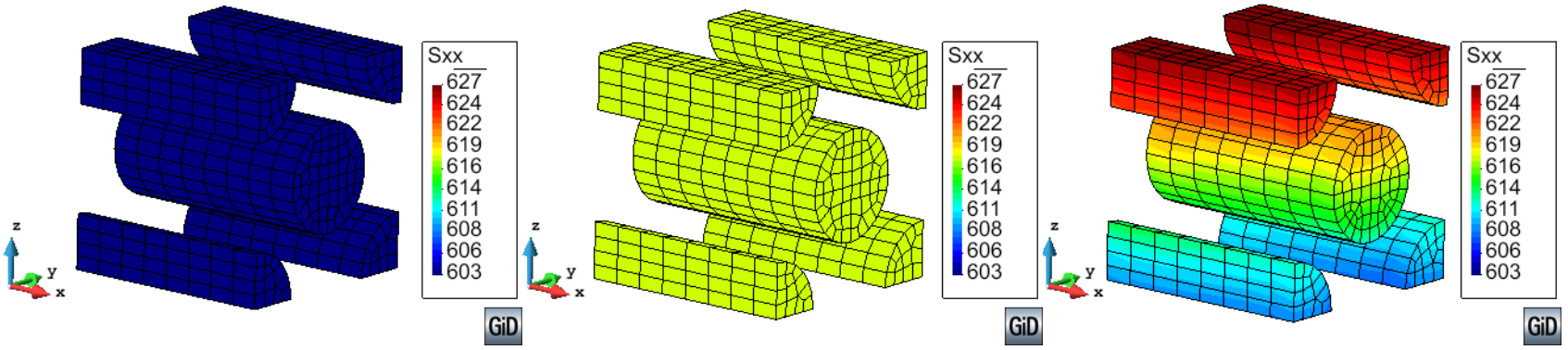

LE&FO QE&FO QE&EFO

Sxx (MPa)	Fiber			Matrix		
	LE&FO	QE&FO	QE&EFO	LE&FO	QE&FO	QE&EFO
Macro1	454,56	543,31	616,13	11,11	11,18	14,10
Macro2	534,71	584,90	622,41	11,69	12,01	13,67
Macro3	578,97	606,60	625,56	12,23	12,46	13,25
Macro4	603,02	617,54	627,07	12,53	12,68	12,98

DISCUSSION. Are second order terms needed?

Homogenization methods are an improved procedure to characterize the material response.

- Do we need to know the failure mechanism of the material?
- Do we need to characterize the material non-linear behavior of the structure?

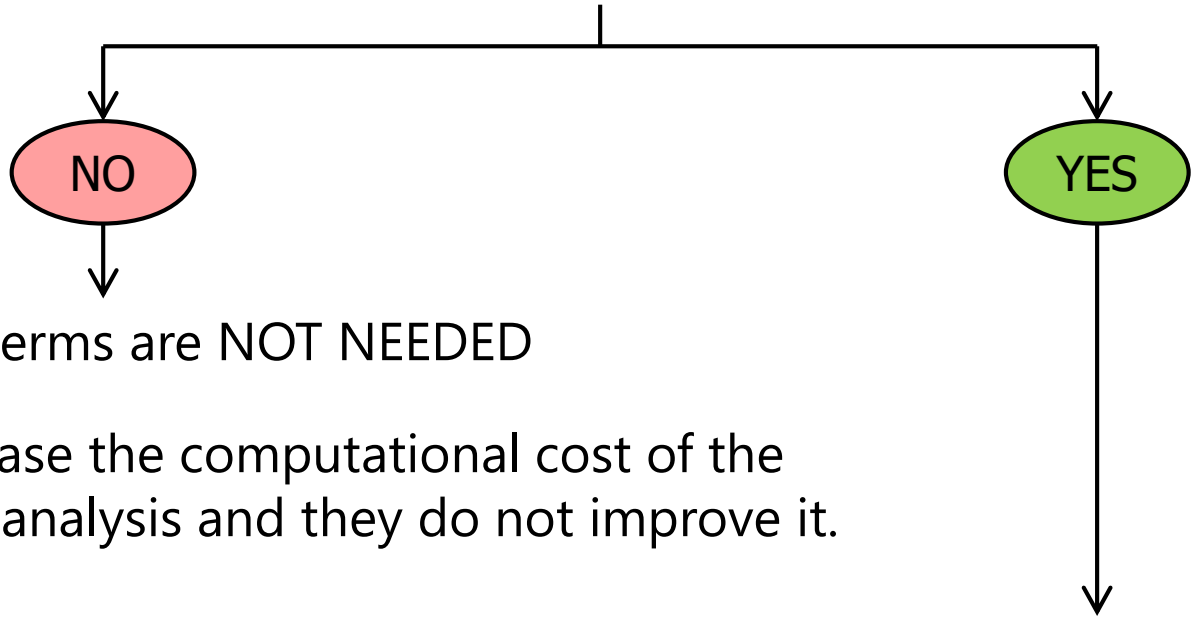

2nd order terms are NOT NEEDED

They increase the computational cost of the numerical analysis and they do not improve it.

Are second order terms really needed?

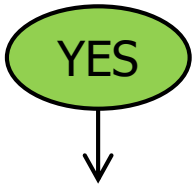

Is the main aim of the simulation to characterize the micro-structure or the macro-structure?

Including 2nd order terms will provide a better characterization of the material failure mode, however, not always this improved characterization is required.

In most cases, it is more useful to improve the discretization of the macro-structure than to have a detailed prediction of the material performance.

Are second order terms really needed?

micro-structure

In this case the 2nd order terms can become a requirement for the correct prediction of material failure.

Taking into account 2nd order terms allows considering loading cases that cannot be taken into account with a first order approach (i.e. bending modes).

Therefore, there will be some failure modes that will not be characterized unless these terms are used.

There are some drawbacks

- Non-linear analysis using multi-scale methods are really expensive.
- Including 2nd order terms:
  - Increases also the computational cost of the analysis.
  - Makes necessary to account for the size of the microstructure Representative Volume Element.
  - Requires a RVE with a symmetric material distribution around its center.

4. Non-Linear Analyses Using Multiscale Methods

UNIVERSITAT POLITÈCNICA DE CATALUNYA BARCELONATECH
CIMNE International Center for Numerical Methods in Engineering
PLCd

Non-linear analyses using multiscale methods

4. Non-Linear Analyses Using Multiscale Methods
    - 4.1. Different approaches to conduct non-linear analyses
    - 4.2. Proposal of a Non-Linear Strategy (NLS + SFS)
    - 4.3. Numerical Examples

Need for non-linear analyses

As engineers, when analyzing a structure, we want to know its mechanical response and its safety factor.

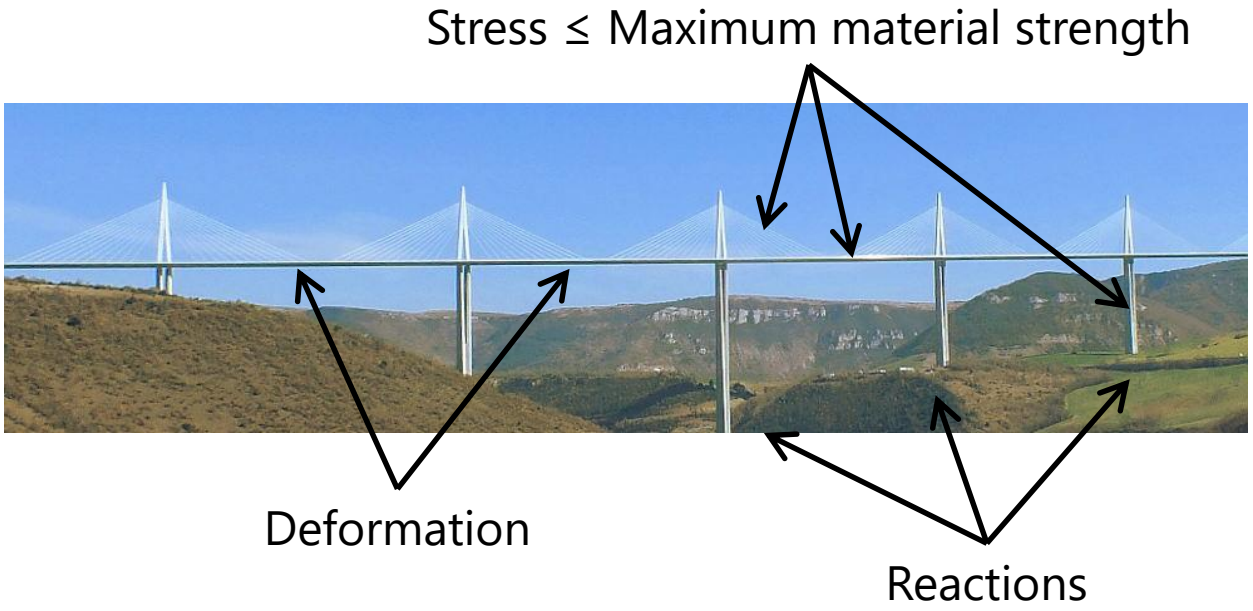

If a multiscale method wants to be useful, it must provide the same information.

Need for non-linear analyses

A linear procedure is capable of providing the structural performance. This is, the forces and displacements on the macro-structure.

But it does not provide the safety factor.

This loop is not done and the component stresses are unknown

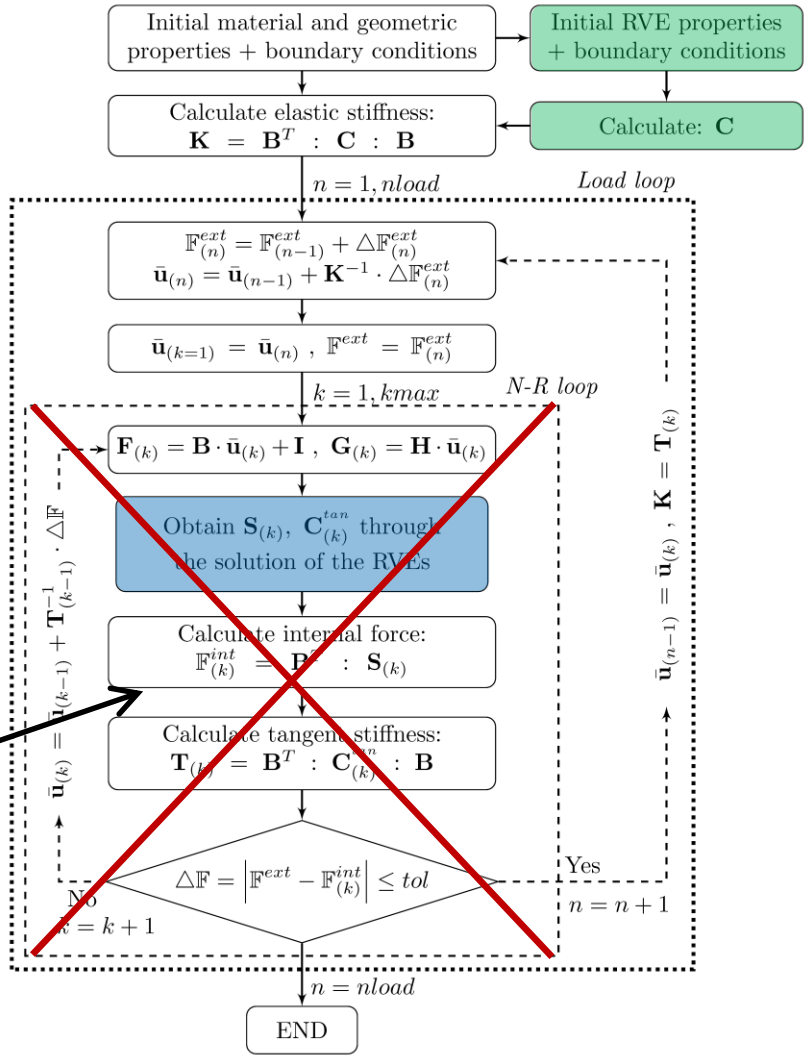

DIFFERENT APPROACHES: 1. FE^2

A FE2 consists on using the RVE as a constitutive equation, therefore it is solved at each load step, for each gauss point.

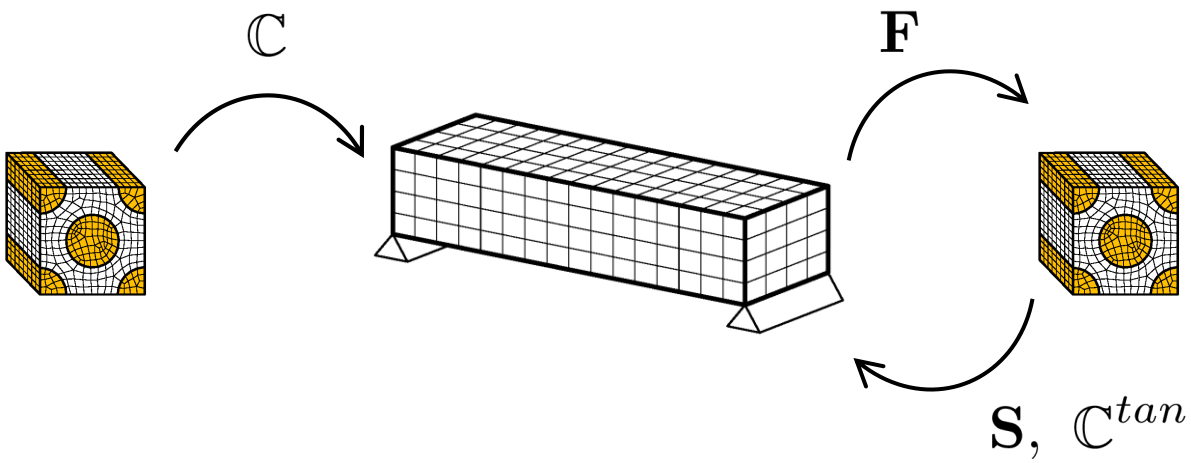

Advantage: It is the most accurate method

Drawback: Humongous computational cost

2. Failure Characterization

A failure characterization procedure consist on analyzing, after completing the macro-analysis, the most critical RVEs with the exact strain values obtained from the macro-analysis, increasing them until failure.

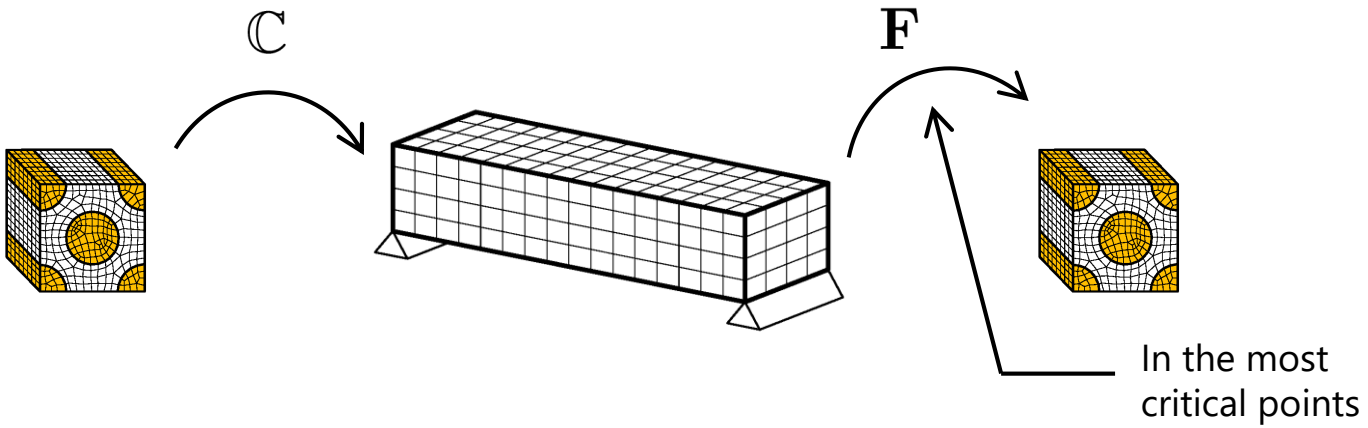

Advantage: With an affordable computational cost it is possible to know the SF in the macro-structure and the material failure of the RVE.

Drawback: Difficult to know with certainty which is the most critical RVE

3. Micro-constitutive equation

The RVE can be used as an experimental sample and it can be tested to obtain the parameters required by a given constitutive equation.

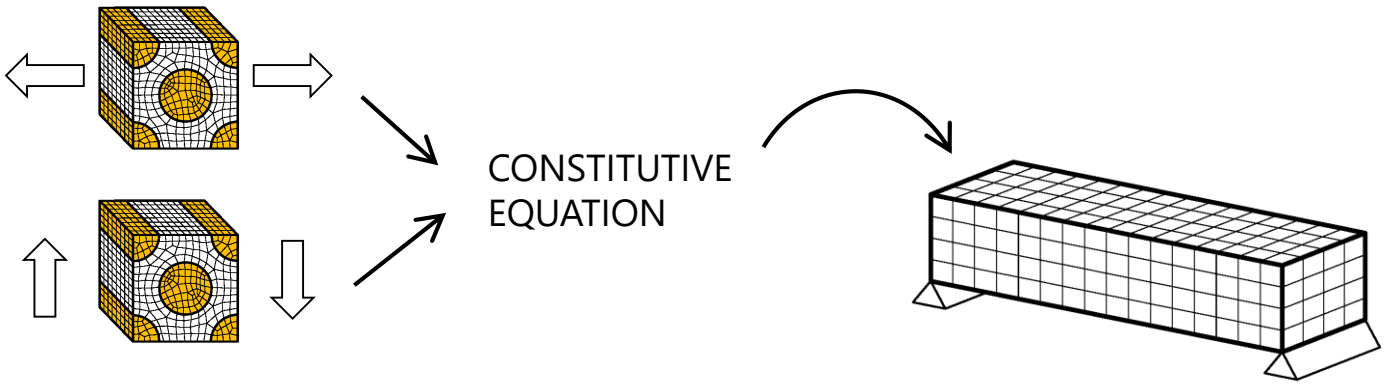

The constitutive equation can be either an existing one (i.e. damage with a Von-Mises yield surface) or can be defined explicitly.

3. Micro-constitutive equation

An explicit constitute equation is obtained by loading the RVE in different characteristic directions and recording its damage evolution and stress-strain in that direction.

The macro-model will use the stress-strain curve recorded in the direction given and, if it does not exist, it will interpolate it from the closest ones.

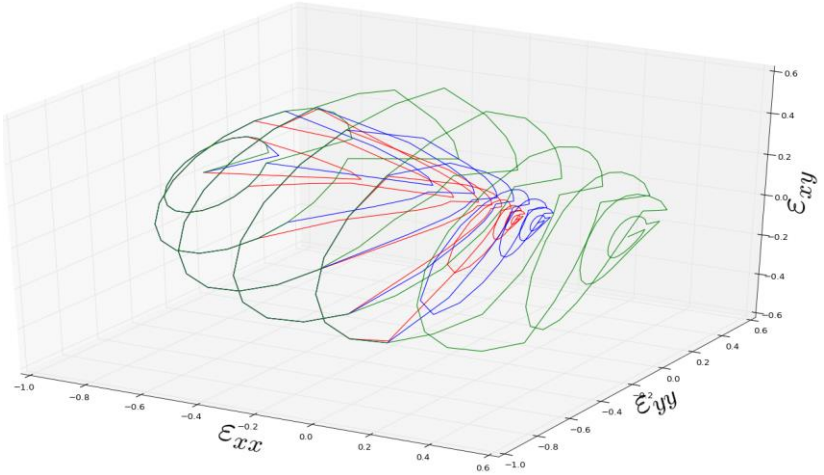

Advantage: It is possible to create a material library and, with it, the solution of the macro-structure is very cheap.

Drawback: It is not a proven method and it is possible to lose some failure modes.

4. Non-Linear Strategy

A non-linear strategy has been developed to analyze, only the RVEs that are close to failure.

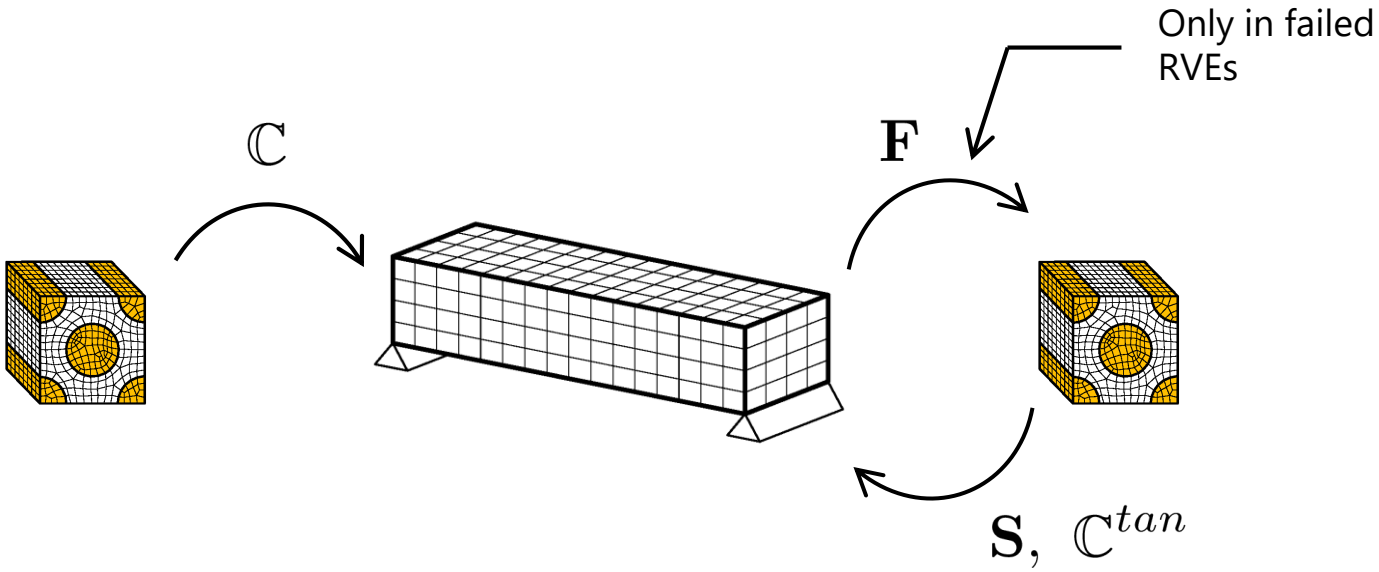

Advantage: It reduces enormously the computational cost compared to a FE^2 method.

Drawback: It is still expensive, specially when failure occurs.

Non-Linear Strategy (NLS)

The NLS defined aims reducing the computational cost of analyzing a large structure, with an double scale homogenization method, taking into account material non-linearities.

This is achieved with two different procedures:

1. Definition of a **Non-Linear Activation Function (NLAF)**
2. Definition of a **Smart First Step (SFS)** algorithm

It is important to remark that NLS does not try to reduce the computational cost by extrapolating some non-linear results (as reduction models do). Instead, it is designed to solve the minimum number of RVEs (those that have a non-linear performance)

NLS – NON-LINEAR ACTIVATION FUNCTION

The objective of the NLAF is to have a threshold in the macro-model that tells when the micro-model will become non-linear. And, therefore, if it is necessary to calculate it.

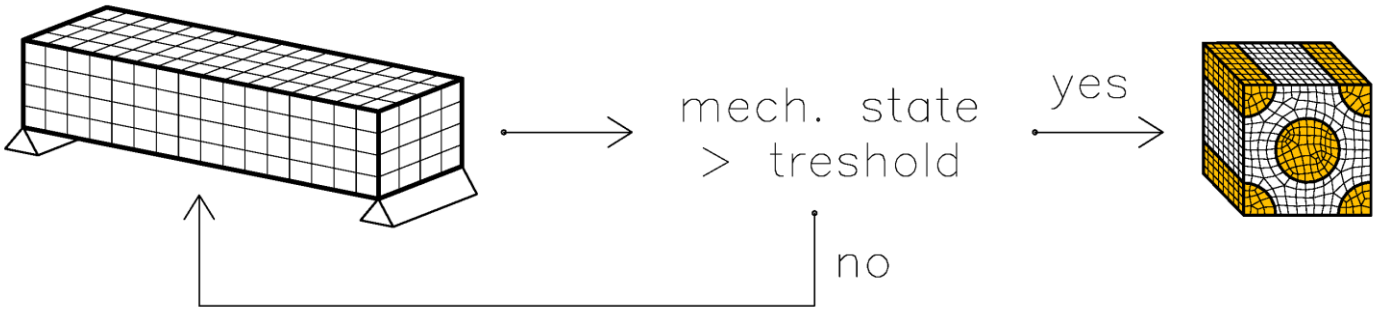

NLAF must be calculated in the macro-model and must depend on damage activation of the micro-model.

NLS – NON-LINEAR ACTIVATION FUNCTION

The NLAF is defined using the elastic energy density of the material:

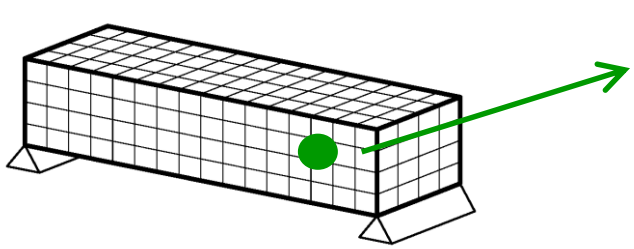

For each integration point, we can calculate: $\Psi_e = \frac{1}{2}\sigma : \varepsilon$

Each integration point is represented by an RVE, which has a maximum elastic energy density of: Ψ_e^{Lim}

The threshold function is defined as: $\Psi_e - \Psi_e^{Lim} \leq 0$

In order to calculate the limit elastic energy density in the macro model, Ψ_e^{Lim}, the following assumption is made:

NLS – NON-LINEAR ACTIVATION FUNCTION

The material becomes no-linear when the first material point of the RVE becomes non-linear.

For a given strain-stress state we can calculate, in the RVE, for each integration point (k):

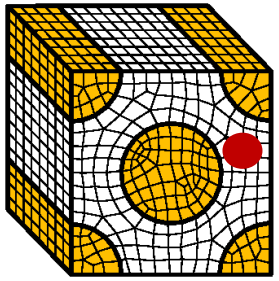

$$\Psi_{e_k} = \frac{1}{2}\sigma_k : \varepsilon_k$$

$$\Psi_e^{Lim}{}_k = \frac{1}{2}\sigma^{Lim}{}_k : \varepsilon^{Lim}{}_k$$

We can define a function f that relates how close is any integration point of the RVE to its elastic energy threshold:

$$f_k = \frac{\Psi_{e_k}}{\Psi_e^{Lim}{}_k} \xrightarrow{\text{Extrapolation to macro-model}} f = \max\{ f_k \}$$

Therefore: $\Psi_e^{Lim} = \frac{\Psi_e}{f}$

NLS – NON-LINEAR ACTIVATION FUNCTION

The elastic energy density limit calculated defines the amount of energy in the material before its failure, for a given strain state.

If the strain state changes, the elastic energy density limit will also change.

It makes necessary to verify, at each load step, $\varepsilon_n \sim \varepsilon_0$, and recalculate Ψ_e^{Lim} if the proportionality is not verified

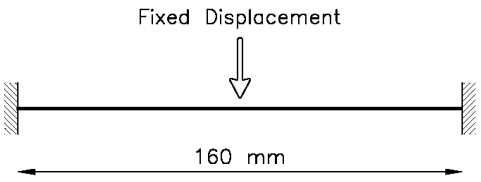

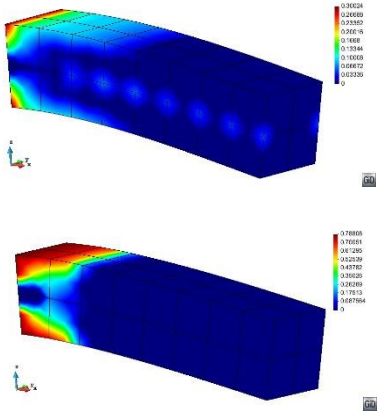

Result if proportionality is not verified

Result verifying proportionality

NLS – NON-LINEAR ACTIVATION FUNCTION

The final flow diagram of the Non-Linear Activation Function is:

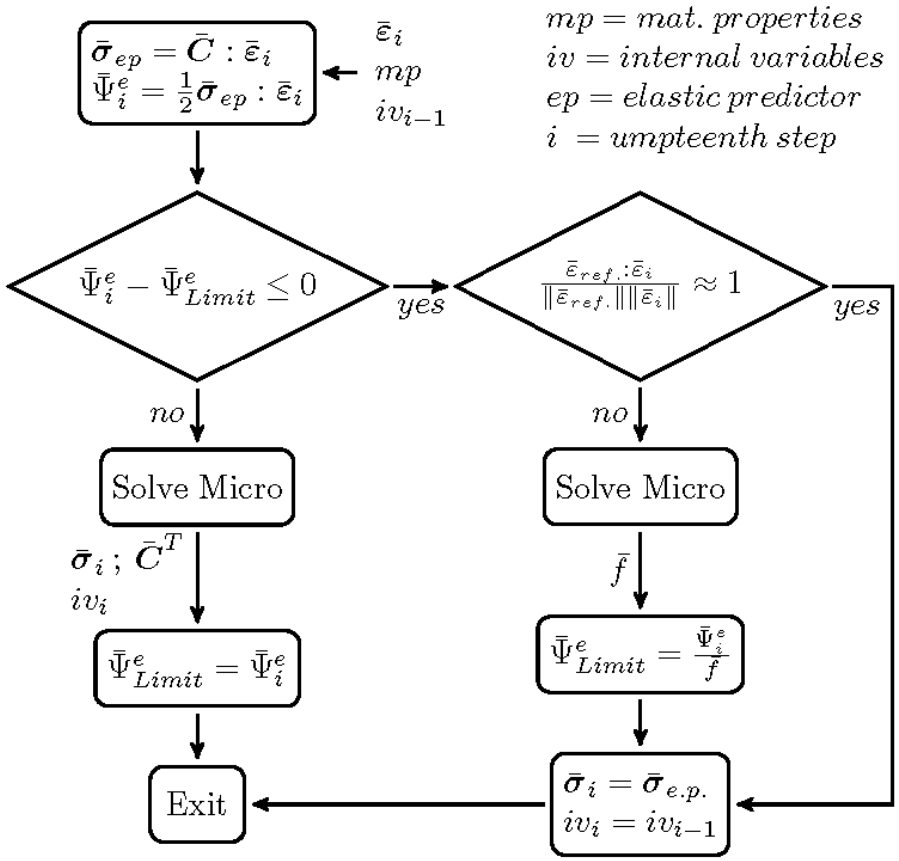

NLS – SMART FIRST STEP

The proposed procedure requires analyzing the RVE of each integration point in the first load step, in order to calculate Ψ_e^{Lim}

However, in many simulations, there are many strain-stress states that are proportional from the very beginning:

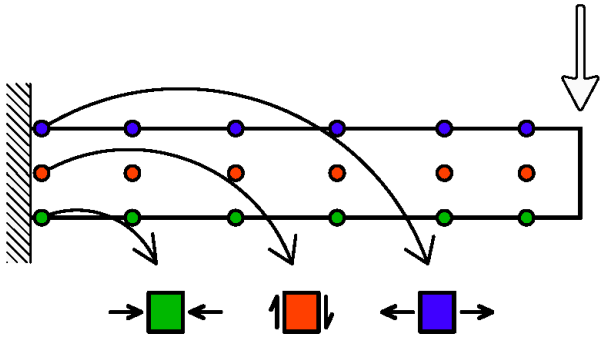

It is possible to define a *Smart First Step* that minimizes the number of RVEs that must be analyzed to obtain the elastic energy limit of all integration points.

NLS – SMART FIRST STEP

The flow diagram of the Smart First Step is:

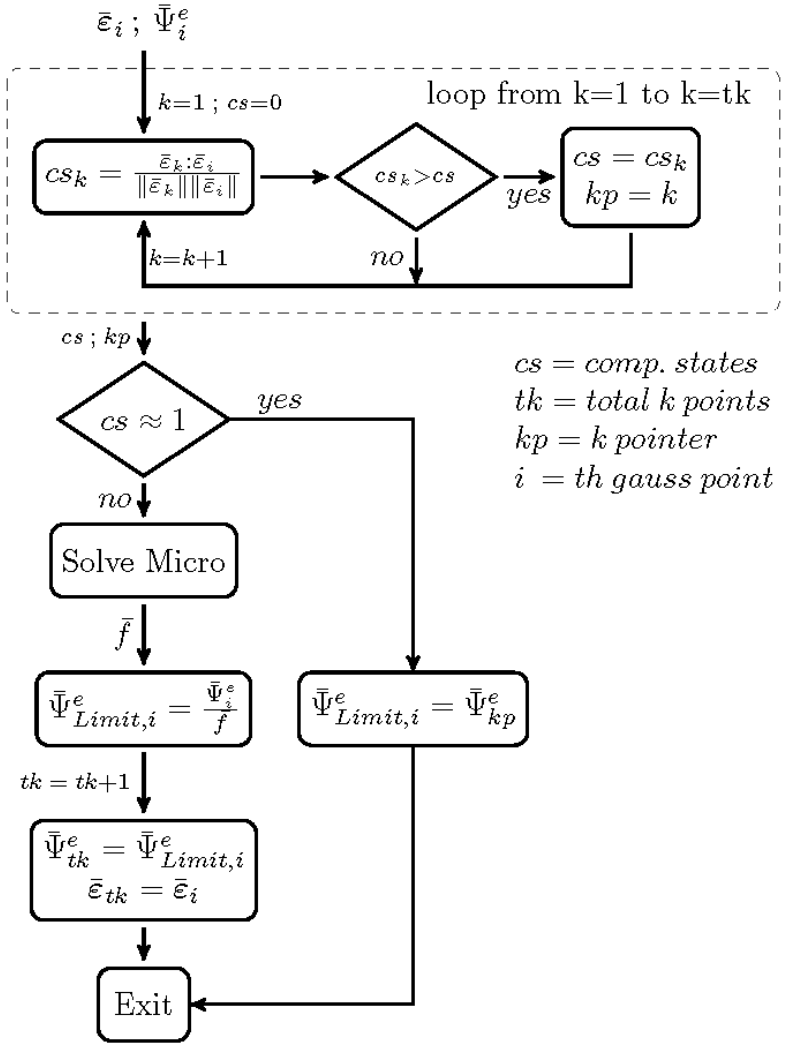

NLS – FINAL REMARKS

1. Once an integration point becomes non-linear, it will remain non-linear. The RVE has to be solved at each load step from then on.

2. A material non-linear analysis requires a good approximation of the tangent stiffness tensor. In an homogenization procedure, this is calculated by numerical derivation. This requires analyzing the RVE 6 more times after convergence, with the consequent increase of computational cost.

Concluding: **A non-linear analysis is expensive, independently of the strategy used.**

NUMERICAL EXAMPLE – PLATE WITH A HOLE

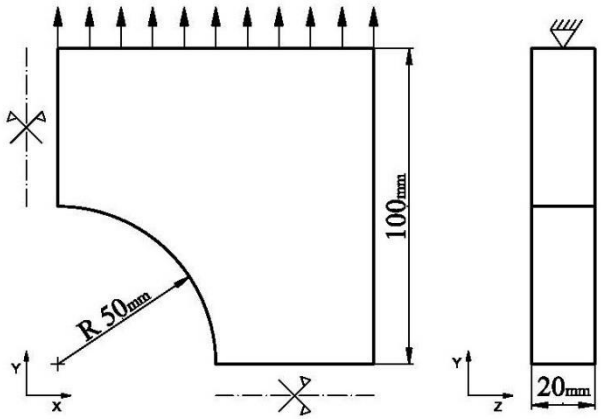

Property	Grey mat.	Blue mat.
E [GPa]	100	100
ν	0.15	0.15
σ_{lim} [MPa]	102	100
Gf [kJ/m^2]	10	10

Both materials are characterized with an explicit scalar damage model

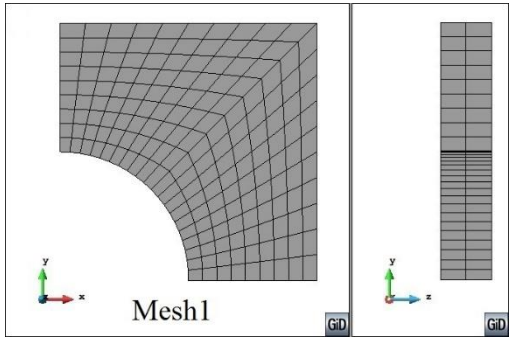

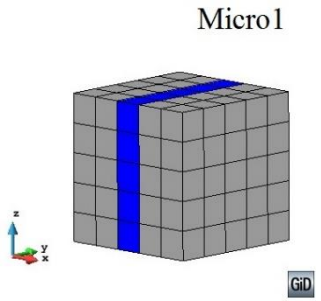

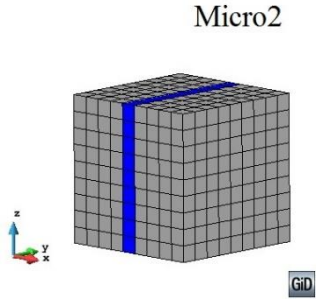

NUMERICAL EXAMPLE – PLATE WITH A HOLE

Results obtained. Damage parameter

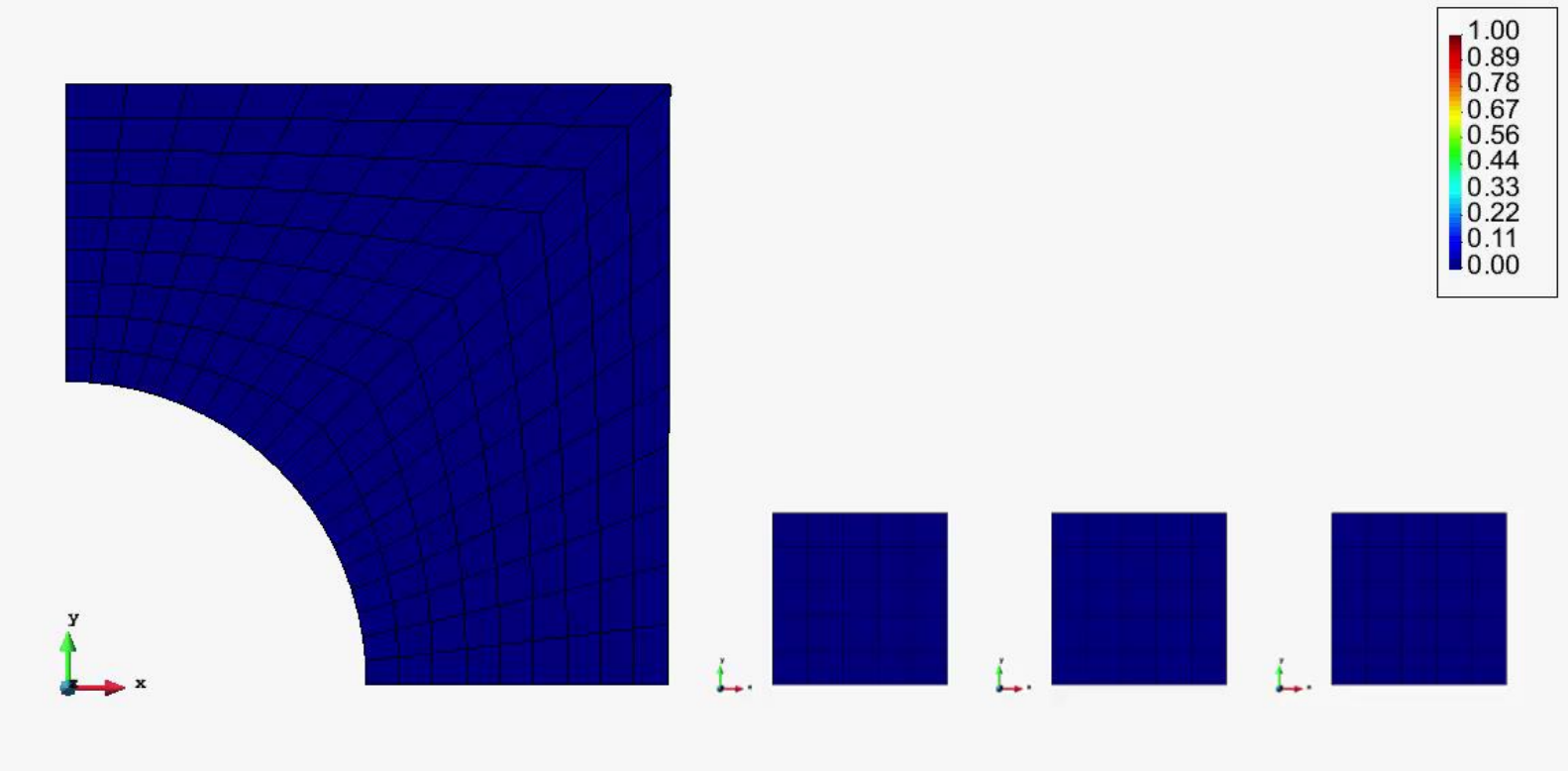

NUMERICAL EXAMPLE – PLATE WITH A HOLE

Force-Displacement graphs for the different models analyzed.

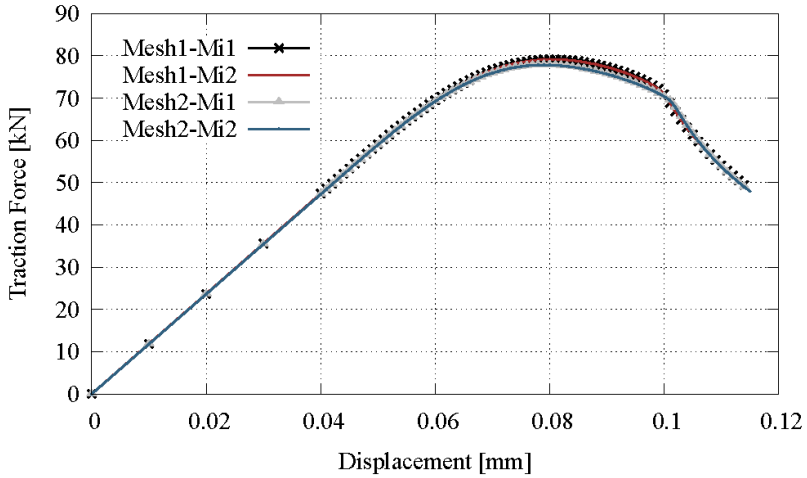

Computational cost:

If this simulation stops at Displ = 0.08mm, the speed ratio is 7.0

Model	FE^2	NLS	Speed ratio
Mesh1-Micro1	1h 21′ 53″	28′ 19″	2.89
Mesh1-Micro2	8h 41′ 19″	3h 10′ 44″	2.73
Mesh2-Micro1	11h 19′ 49″	2h 29′ 28″	4.55
Mesh2-Micro2	76h 40′ 33″	18h 39′ 33″	4.11

NUMERICAL EXAMPLE – PLATE WITH A HOLE

Improvement of the computational cost thanks to the Smart First Step strategy

Model	Without SFS		With SFS		Speed ratio
	Time	RVE solved	Time	RVE solved	
Mesh1-Micro1	18″	2,880	1″	151	17.9
Mesh1-Micro2	1′ 48″	2,880	6″	151	16.7
Mesh2-Micro1	2′ 12″	23,040	3″	303	50.8
Mesh2-Micro2	14′ 06″	23,040	12″	303	67.7

NUMERICAL EXAMPLE – INDUSTRIAL COMPONENT

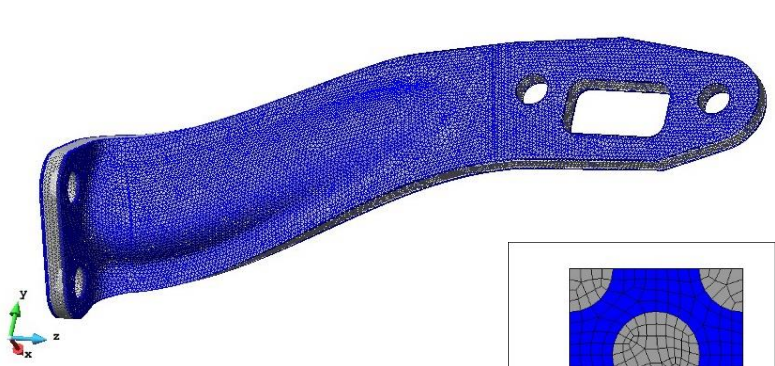

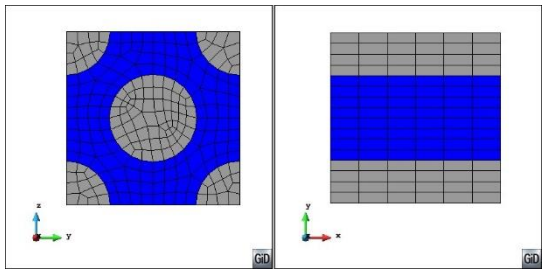

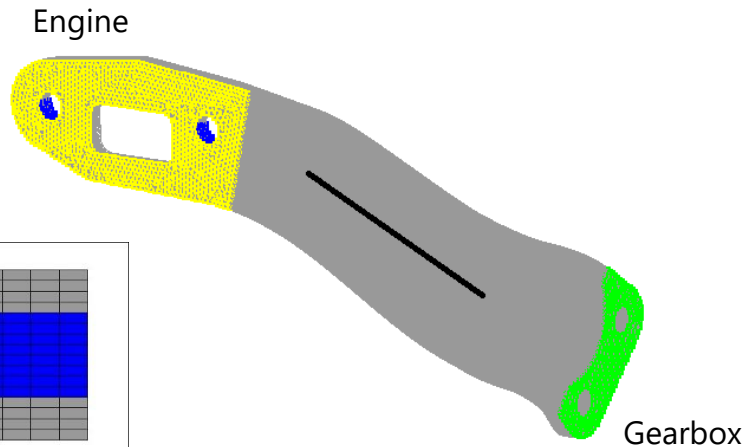

Material	Model	E [GPa]	ν	σ_{lim} [MPa]	Gf [kJ/m^2]
Fibre (Carbon)	Elastic	235	0.21	4410	-
Matrix (Epoxy)	Damage	4.52	0.36	68	780

Material	Model	E1 [GPa]	E2 [GPa]	G [MPa]
TenCate core	Elastic	56.1	55.6	4.5

NUMERICAL EXAMPLE – Industrial component

Results obtained. Damage parameter

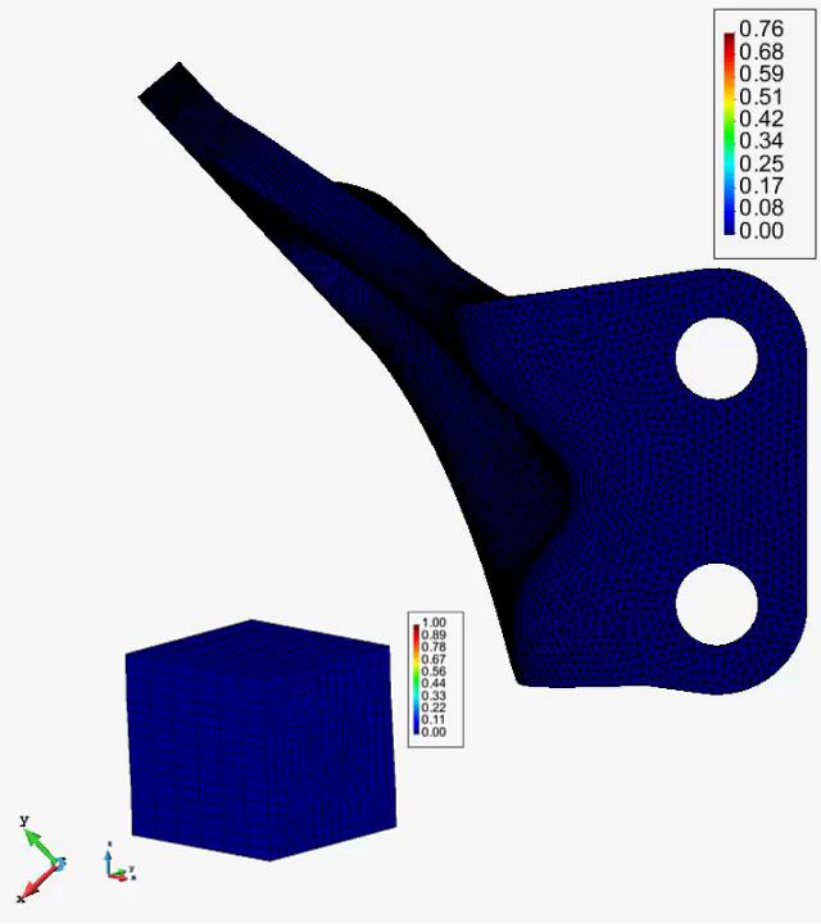

Note: Damage parameter in the macro-model is calculated based on the lost of stiffness of the whole RVE, and not as the integral of the damage over the RVE volume.

NUMERICAL EXAMPLE – INDUSTRIAL COMPONENT

Expected failure regions:

Higher value means lower elastic energy available. Value equal to 1.0 means that all elastic energy has been consumed.

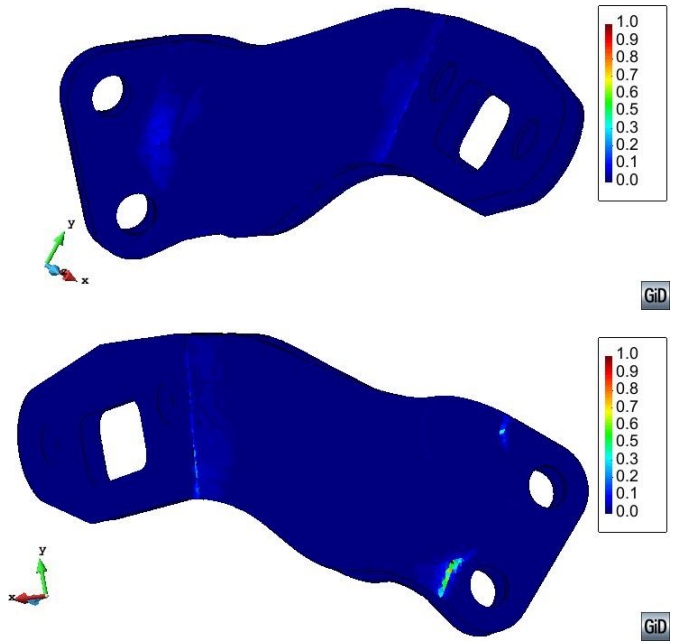

Computational cost:

Model	FE^2	NLS	Speed ratio
Mesh1-Micro1	32d 14h 46’	11h 36’	67.4

98.5 % reduction of the computational cost !

Conclusions

This work presents a Non-Linear Strategy procedure that makes possible the analysis of structures using homogenization procedures.

The NLS is based on reducing the number of times in which the RVE has to be solved. In other words, in solving the RVE only when it is strictly necessary.

Validation examples have shown the excellent performance provided by the NLS, which in large problems can reduce the computational cost in a 98.5%

These sort of strategies are a must in order to use homogenization procedures in non-linear analysis of structures.

Acknowledgements

This work has been supported by the European Community under Grant: NMP-2009-2.5-1 246067M_RECT "*Multiscale Reinforcement of Semi-crystalline Thermoplastic Sheets and Honeycombs*", by European Research Council through of Advanced Grant: ERC-2012-AdG 320815 COMP-DES-MAT "*Advanced tools for computational design of engineering materials*", by Dirección General de Investigación Científica y Técnica: MAT2014-60647-R OMMC "*Optimización multi-escala y multi-objetivo de estructuras de laminados compuestos*", by Abengoa Research, and by Universitat Politècnica de Catalunya (UPC).

All this support is gratefully acknowledged.